

Oil-acrylic hybrid latexes

Citation for published version (APA):

Hamersveld, E. M. S. (1999). *Oil-acrylic hybrid latexes*. [Phd Thesis 2 (Research NOT TU/e / Graduation TU/e), Chemical Engineering and Chemistry]. Technische Universiteit Eindhoven. <https://doi.org/10.6100/IR527261>

DOI:

[10.6100/IR527261](https://doi.org/10.6100/IR527261)

Document status and date:

Published: 01/01/1999

Document Version:

Publisher's PDF, also known as Version of Record (includes final page, issue and volume numbers)

Please check the document version of this publication:

- A submitted manuscript is the version of the article upon submission and before peer-review. There can be important differences between the submitted version and the official published version of record. People interested in the research are advised to contact the author for the final version of the publication, or visit the DOI to the publisher's website.
- The final author version and the galley proof are versions of the publication after peer review.
- The final published version features the final layout of the paper including the volume, issue and page numbers.

[Link to publication](#)

General rights

Copyright and moral rights for the publications made accessible in the public portal are retained by the authors and/or other copyright owners and it is a condition of accessing publications that users recognise and abide by the legal requirements associated with these rights.

- Users may download and print one copy of any publication from the public portal for the purpose of private study or research.
- You may not further distribute the material or use it for any profit-making activity or commercial gain
- You may freely distribute the URL identifying the publication in the public portal.

If the publication is distributed under the terms of Article 25fa of the Dutch Copyright Act, indicated by the "Taverne" license above, please follow below link for the End User Agreement:

www.tue.nl/taverne

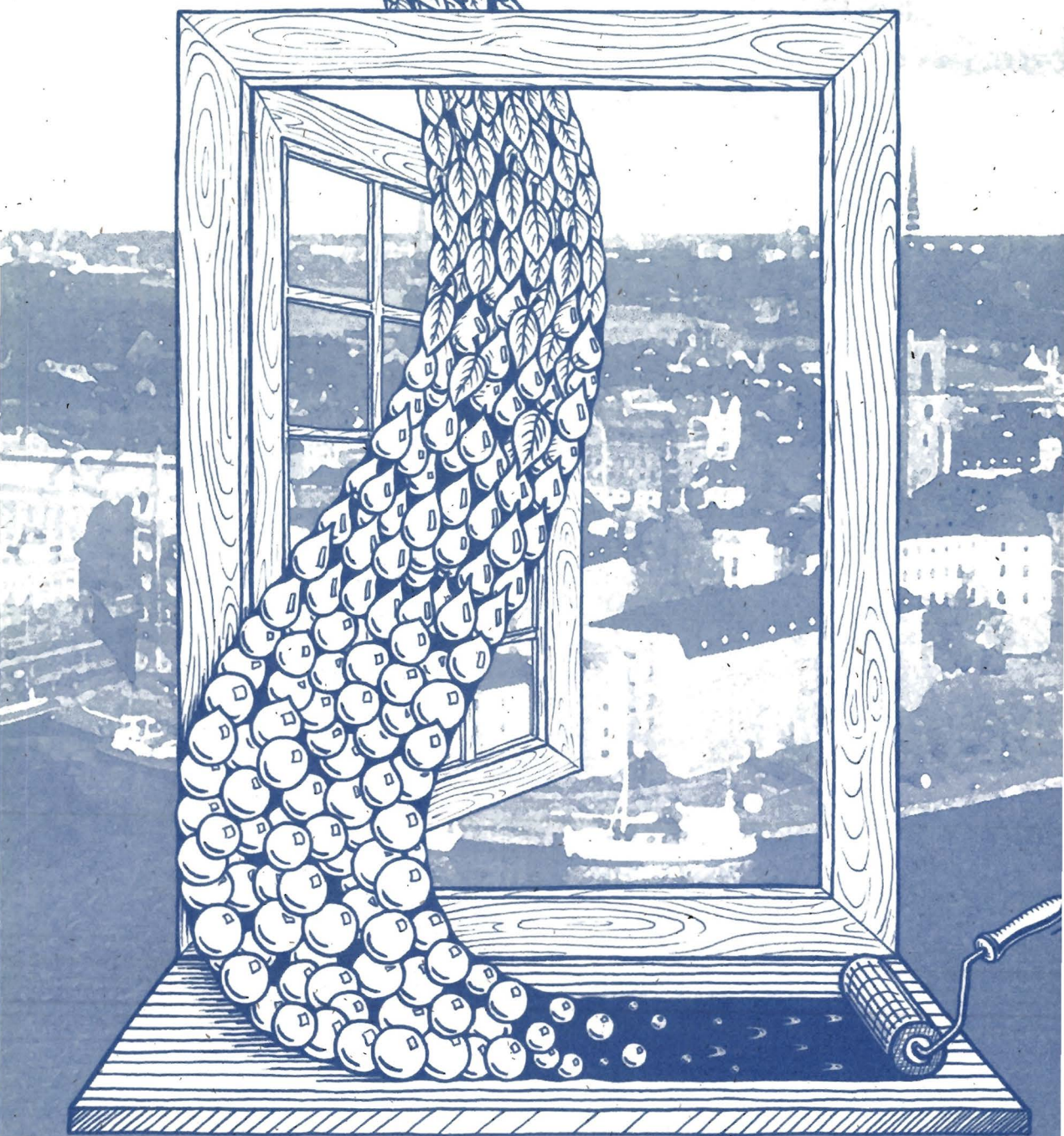
Take down policy

If you believe that this document breaches copyright please contact us at:

openaccess@tue.nl

providing details and we will investigate your claim.

Oil - Acrylic Hybrid Latexes



E.M.S. van Hamersveld

Oil-Acrylic Hybrid Latexes

CIP-DATA LIBRARY TECHNISCHE UNIVERSITEIT EINDHOVEN

Hamersveld, Eelco M.S.

Oil-Acrylic Hybrid Latexes / by Eelco M.S. van Hamersveld. – Eindhoven :
Technische Universiteit Eindhoven, 1999.

Proefschrift. – ISBN 90-386-2661-4

NUGI 813

Trefwoorden: emulsiepolymerisatie / mini-emulsiepolymerisatie /
polymeerstructuur / composietpolymeren

Subject headings: emulsion polymerization / mini-emulsion polymerization / latex
/ polymer morphology / polymer composites

© Copyright 1999, E.M.S. van Hamersveld

Omslagontwerp: Sander A. Pul

Druk: Universiteitsdrukkerij, TUE

Oil-Acrylic Hybrid Latexes

PROEFSCHRIFT

ter verkrijging van de graad van doctor aan de
Technische Universiteit Eindhoven, op gezag van
de Rector Magnificus, prof.dr. M. Rem, voor een
commissie aangewezen door het College voor
Promoties in het openbaar te verdedigen op
dinsdag 19 oktober 1999 om 16.00 uur

door

Eelco Michiel Sebastiaan van Hamersveld

geboren te Hoogland

Dit proefschrift is goedgekeurd door de promotoren:

Prof.dr.ir. A.L. German

en

Prof. K. Holmberg

Copromotor:

Dr. J.J.G.S. van Es

The author is indebted to I.O.P. (Innovative Research Program) Coatings for financial support of the work described in this thesis.

*"There are many ways of going forward,
but only one way of standing still"*

(Franklin D. Roosevelt)

aan mijn ouders
en Yvette

TABLE OF CONTENTS

CHAPTER 1

Historical Background and Scope of the Thesis

| | |
|--------------------------------------|----|
| 1.1 Introduction | 2 |
| 1.2 Historical Background | 3 |
| 1.3 Oil/Alkyd-Acrylic Hybrid Systems | 7 |
| 1.4 Object and Survey of the Thesis | 14 |
| 1.5 References | 16 |

CHAPTER 2

Preparation of Emulsions of Oxidized Vegetable Oils

| | |
|--|----|
| 2.1 Introduction | 20 |
| 2.2 Autoxidative Drying | 22 |
| 2.3 Experimental | 25 |
| 2.3.1 Materials | 25 |
| 2.3.2 Oxidation Procedures | 26 |
| 2.3.3 Analysis | 27 |
| 2.4 Results and Discussion | 30 |
| 2.4.1 Oxidation of Emulsions | 30 |
| 2.4.1.1 Emulsification of Vegetable Oils | 30 |
| 2.4.1.2 High Pressure Oxidation of Vegetable Oil Emulsions | 31 |
| 2.4.2 Bulk Oxidation of Sunflower Oil | 39 |
| 2.5 Conclusions | 42 |
| 2.6 References | 43 |

CHAPTER 3

Fatty-Acid Hydroperoxide-Initiated Mini-Emulsion Polymerization of MMA

| | |
|--|----|
| 3.1 Introduction | 46 |
| 3.2 Experimental | 48 |
| 3.2.1 Materials | 48 |
| 3.2.2 Sunflower Oil Oxidation | 48 |
| 3.2.3 Mini-Emulsion Preparation and Polymerization | 48 |
| 3.2.4 Analysis | 49 |
| 3.3 Results and Discussion | 50 |
| 3.3.1 Sunflower Oil Oxidation | 50 |
| 3.3.2 Mini-Emulsion Polymerization | 51 |

| | |
|--|----|
| 3.3.2.1 Monomer Droplet Formation | 51 |
| 3.3.2.2 Particle Morphology | 53 |
| 3.3.2.3 Mini-Emulsion Polymerization of MMA Initiated by Fatty-Acid Hydroperoxide Groups | 55 |
| 3.4 Conclusions | 59 |
| 3.5 References | 59 |

CHAPTER 4

Morphology Development of Films Prepared from Alkyd-Acrylic Hybrid Latexes: Surface Properties

| | |
|--|----|
| 4.1 Introduction | 62 |
| 4.2 Film Formation | 63 |
| 4.2.1 Film Formation of Polymer Latexes | 63 |
| 4.2.2 Film Formation of Alkyd Emulsions | 66 |
| 4.3 Experimental | 68 |
| 4.3.1 Materials | 68 |
| 4.3.2 Oil/Alkyd-Acrylic Hybrid Preparation | 68 |
| 4.3.3 Analysis | 69 |
| 4.3.4 Surface Properties | 71 |
| 4.3.4.1 Atomic Force Microscopy (AFM) | 71 |
| 4.3.4.2 Static Contact Angle Measurements | 72 |
| 4.3.4.3 Electron Spectroscopy for Chemical Analysis (ESCA) | 73 |
| 4.4 Results and Discussion | 74 |
| 4.4.1 Oil/Alkyd-Acrylic Hybrid Latexes | 74 |
| 4.4.2 Surface Properties | 79 |
| 4.4.2.1 Atomic Force Microscopy | 79 |
| 4.4.2.2 Surface Properties of Films | 87 |
| 4.5 Conclusions | 91 |
| 4.6 References | 92 |

CHAPTER 5

Morphology Development of Films Prepared from Alkyd-Acrylic Hybrid Latexes: Time Resolved Fluorescence Measurements

| | |
|--|-----|
| 5.1 Introduction | 98 |
| 5.2 Experimental | 101 |
| 5.2.1 Materials | 101 |
| 5.2.2 Labeled Alkyd-Acrylic Hybrid Preparation | 101 |
| 5.2.3 Analysis | 104 |
| 5.3 Results and Discussion | 107 |

| | |
|---|-----|
| 5.3.1 Determination of the Optimum Excitation and Detection Wavelengths | 107 |
| 5.3.2 Hybrid Latex Characteristics | 110 |
| 5.3.3 Fluorescence Resonance Energy Transfer Measurements | 111 |
| 5.4 Conclusions | 117 |
| 5.5 References | 118 |

CHAPTER 6

Preliminary Investigations on the Performance of Oil/Alkyd-Acrylic Hybrid Coatings

| | |
|---|-----|
| 6.1 Introduction | 120 |
| 6.2 Experimental | 121 |
| 6.2.1 Materials | 121 |
| 6.2.2 Preparation and Formulation of the Systems | 121 |
| 6.2.3 Analysis | 123 |
| 6.3 Results and Discussion | 125 |
| 6.3.1 Morphology of Films Prepared from Blend Systems | 125 |
| 6.3.2 Coating Performance of Hybrids vs. Blends | 130 |
| 6.4 Conclusions | 135 |
| 6.5 References | 135 |

CHAPTER 7

General Discussion & Prospects for Further Research

| | |
|--|-----|
| 7.1 Introduction | 137 |
| 7.2 Oil-Acrylic Hybrid Latexes by Mini-Emulsion Polymerization | 138 |
| 7.3 Experimental Techniques | 139 |
| 7.4 References | 141 |

| | |
|----------------|------------|
| Summary | 143 |
|----------------|------------|

| | |
|---------------------|------------|
| Samenvatting | 147 |
|---------------------|------------|

| | |
|----------------------------------|------------|
| Dankwoord/Acknowledgement | 151 |
|----------------------------------|------------|

| | |
|-------------------------|------------|
| Curriculum Vitae | 153 |
|-------------------------|------------|

CHAPTER 1: HISTORICAL BACKGROUND AND SCOPE OF THE THESIS

Summary

This chapter provides an introduction to the research described in this thesis. The developments of coatings in the past and the use of vegetable oils as binders for paints and coatings are reviewed in general. The development of binders prepared from mineral oil derivatives, e.g., alkyd resins and latexes is elaborated upon, and the different approaches used in the development of oil/alkyd-acrylic hybrids are discussed. The chapter concludes with the objective of the thesis and a survey of the research described in the other chapters of the thesis.

1.1 Introduction

The use of paints and coatings dates back to at least the times of the old Egyptians (2000 B.C.). The protection and decoration of objects were, and still are, the major reasons for the use of paints and coatings. Surprisingly, in this large time frame the general composition of paints remained relatively unchanged. Paints are still composed of binder, pigment and solvent. The binder material forms the polymeric matrix, in which the pigments are dispersed, ensures adhesion to the substrate and provides for protection from external influences like air, water, chemicals, UV-radiation and/or scratches. The pigments account for the decorative properties of a paint system. Organic solvent or water is added to the paint system for processing and application purposes and to ensure flow and leveling during film formation. Special additives, e.g., UV-absorbents, fungicides and gloss promoters [1], are added to the paint for their specific properties.

In modern society there are many new requirements for a coating system. The shape and material of objects that need protection are diverse and many different ways of application are requested. On the other hand, the demands regarding the environment and performance by the users are high. As a result, coating formulation and application have developed over the last decades from a craftsmanship, which was passed on from generation to generation, to a true technology [2] that combines different fields of science, e.g., organic-polymer chemistry, polymer physics, surface chemistry and colloidal chemistry.

The increased fundamental knowledge in chemistry and physics, and the development of advanced techniques for the analysis of the composition and the morphology of coatings, e.g., Atomic Force Microscopy (AFM) and Time-of-Flight Secondary Ion Mass Spectroscopy (TOF-SIMS), have increased the understanding of the structure-property relationships of the binders that determine the chemistry and properties of coatings. Modern coating developers are using this knowledge and have started to design binders with controlled chemical reactivity and morphology that result in high performance coatings with specific properties upon film formation. Over the last ten years this has resulted in the development of paint systems that apply novel cross-linking technologies, *i.e.*, reactive latexes and UV-curing systems [3,4]. Also, new application technologies, like powder spraying are used [5,6] and hybrid systems containing different types of polymers have been developed [7-9]. The latter combination of two, or more, components in one hybrid system creates the opportunity to combine specific properties of each of the components, or to reduce the need for

additives. The design and characterization of such a hybrid system has been the objective of this thesis.

The developments in new chemistry and technology have not lessened the interest in conventional systems, like drying oils and alkyds. Moreover, awareness that the supply of mineral oil is limited, and the increased fundamental understanding in coating-technology have resulted in an increased interest in and research of the use of renewable resources, like vegetable oils, for coating applications in the past years. This has, for instance, resulted in the development of a powder coating binder with a cross-linker based on epoxidized vegetable oil [10].

The research described in this thesis was aimed at the development of a waterborne hybrid binder system composed of a vegetable oil resin, or a long oil alkyd resin, and an acrylic polymer. Vegetable oil-based systems and acrylic latexes have been successfully used separately as binders for coating applications in the past. Various studies have shown that hybrid systems give unique combinations of properties. Since a number of the properties of vegetable oil resins and acrylic polymer are complementary it may be expected that a hybrid composed of vegetable oil and acrylic polymer results in a system with enhanced properties.

In this chapter a historical background on the use of vegetable oils in coatings and the development of mineral oil-based binders is presented. The different approaches used in the past for the synthesis of oil/alkyd-acrylic hybrid systems and the strategy of the work of this thesis are discussed. A survey of its contents is given at the end of the chapter.

1.2 Historical Background

Agricultural raw materials preceded petrochemicals by millennia in non-food applications. Vegetable oils, for instance, have been used for lubricating purposes as well as for coatings and paints for many centuries before an abundant and cheap supply of mineral oil became available. Vegetable oils are obtained from plant seeds [11] and consist mainly of mixtures of triglycerides. The characteristic property of highly unsaturated oils that makes them suitable as a paint binder, is the ability to dry by polymerization upon exposure to air. Typical examples of such oils are linseed oil, safflower oil and tung oil. A three-dimensional structure is formed by a series of reactions of atmospheric oxygen and the fatty acid chains of the triglycerides in a process known as autoxidative

drying [12]. A detailed review of the process of autoxidative drying is given in Chapter 2 of this thesis. The reactivity of the fatty acid chains towards autoxidative polymerization is related to the number of conjugated and/or 1,4-unsaturated double bonds. In general, the best effect is obtained with the utilization of oils with the highest number of double bonds and with the use of oils that contain the more efficient conjugated double bonds. With reference to the films that are obtained after autoxidative drying vegetable oils are classified as [13]:

- non-drying oils: do not form a cross-linked structure,
- semi-drying oils: form sticky films,
- drying oils: form solid films.

Typical fatty acid compositions of selected oils frequently used in paints are presented in Table 1.1.

Since distant past man has tried to improve the characteristics of oils for paint purposes. In the beginning of the century vegetable oils were often pre-polymerized to a certain extent. In the presence of drier and air oils were heated to form 'blown', or 'boiled' oils, or in the absence of drier and air 'stand' oils were prepared. Due to increased demand for fast drying paints and coatings in this century there have been many developments in the synthesis of binders from vegetable oils.

Table 1.1. Typical Fatty Acid Composition of Selected Vegetable Oils, (%) [14]

| Oil | Fatty Acids | | | | |
|-------------------|-------------|-------|----------|-----------|-----------------|
| | Saturated | Oleic | Linoleic | Linolenic | Other |
| Linseed | 10 | 22 | 16 | 52 | |
| Soybean | 15 | 25 | 51 | 9 | |
| Sunflower | 13 | 26 | 61 | | |
| Safflower | 11 | 13 | 75 | | 1 |
| Tung | 5 | 8 | 4 | 3 | 80 ^a |
| Castor | 3 | 7 | 3 | | 87 ^b |
| Dehydrated Castor | 3 | 8 | 62 | | 27 ^c |
| Tall ^d | 8 | 46 | 41 | 3 | 2 ^e |

a) α -Elaeostearic acid (18:3 conjugated)

b) Ricinoleic acid (hydroxy fatty-acid)

c) Conjugated diene

d) By-product of kraft pulping

e) Rosin

From the 1940s, the developments in the prepolymerization of vegetable oils could not meet the increasing demand for fast drying paints with a low degree of yellowing. This has resulted in the partial replacement of vegetable oils as binders for paints by mineral oil-based binders with specific properties: alkyd resins and acrylic latexes.

Alkyd Resins

Alkyd resins are based on polymeric resins developed in the 1920s [15]. They are synthesized by the polycondensation reaction between polyols and polybasic acids [16]. The name alkyd (bastardization of 'alcid') was derived from the chemicals from which the polymer was prepared, namely 'alcohol' and 'acid'. Unsaturated fatty acids are incorporated in alkyd resins for chemical drying by polymerization induced by oxygen. The most frequently used polyols for alkyd resin synthesis are glycerol and pentaerythritol, whereas phthalic anhydride is most often used as dibasic acid (Figure 1.1).

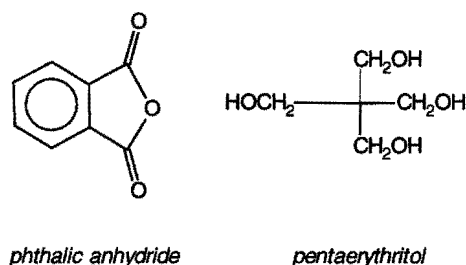


Figure 1.1. Dibasic acid and polyol most often used for alkyd synthesis.

The amount and the nature of fatty acids used in the alkyd resin synthesis largely determine the resin properties and application possibilities of alkyd resins. Therefore, alkyd resins are often classified by their fatty acid type and their 'oil length' [17]. The oil length of an alkyd resin is defined as the weight percent of fatty acids in the resins.

$$\text{Oil length} = \frac{\text{weight of oil or fatty acid}}{\text{theoretical weight of resin}} \times 100 \quad (1.1)$$

Alkyd resins are classified into four groups by oil length (Table 1.2):

Table 1.2. Definition of Oil Length of Alkyd Resins

| Oil length | % Oil or fatty acids |
|---------------------|----------------------|
| Very long oil alkyd | > 70 |
| Long oil alkyd | 56-70 |
| Medium oil alkyd | 46-55 |
| Short oil alkyd | 35-45 |

The fast drying and low yellowing characteristics of alkyd-based paints are mainly the result of physical drying by solvent evaporation and the use of semi-drying low yellowing oils, e.g. soybean oil and tall oil.

From the above it follows that alkyds, especially long-oil alkyds, resemble prepolymerized oils and that their properties are similar. However, beside modification with fatty acids, alkyd resins can also be modified with a wide variety of reactive chemicals and other polymers like silicones, phenolic resins, or vinyl resins [16], giving them extra features. This has made them very popular. Combination with other chemical groups has resulted in a versatile binder system with a wide spectrum of properties.

Latexes

Latex systems are a serious alternative for the conventional solvent-borne oil-based systems. Latex paints consist of dispersions of polymer particles in water. A film is formed from the latex polymer particles upon evaporation of water followed by the process of coagulation and coalescence. A detailed review on the film formation process of polymer latexes is given in Chapter 4 of this thesis. Often, co-solvent is added to the system to ensure good film formation. Latex coatings were introduced in the 1950s and show short drying-time, low odor and easy clean up with water. The polymer particles are often synthesized from mineral oil-based vinyl monomers, like e.g. styrene, vinyl acetate and acrylic esters, using free radical emulsion polymerization [18].

New Developments

The development and increased use of alkyd resins followed by the replacement of oil-based solvent-borne systems by waterborne latexes has resulted in a decline in the use of vegetable oils for coating applications.

By the end of the 1960s it was recognized that materials used in paints, especially the solvents, contributed substantially to the pollution of the environment. Therefore, regulations were proposed [19], forcing the coating industry to search for new paint systems. Reduction of emissions of volatile

organic components (VOC) and of hazardous air pollutants (HAP) [20] became a main topic. This resulted, amongst others, in the development of high-solids and waterborne alkyd-based paints [21]. However, these systems still contained a certain amount of organic solvents and did not always yield the application and film properties of the conventional alkyd paints. Progress in research on latex systems resulted in a reduction of the use of coalescing agents while drying became more oriented towards chemical drying [3]. Other systems that should meet the new standards are based on novel application techniques such as radiation curable binders and powder systems. These do not involve the use of solvents.

The overview presented above shows that there have been several trends in the development of high performance, low VOC binders in recent years. First, new alkyd systems with increased reactivity have been developed for high solids alkyds and alkyd emulsions. Second, interest in the use of renewable resources has been growing. Finally, incorporation of chemical drying in latexes has gained increasing interest. This has resulted in the research and development of hybrid latexes composed of alkyd resin and acrylic polymer as reviewed in the next section.

1.3 Oil/Alkyd-Acrylic Hybrid Systems

Although traditional solvent-borne alkyd resins and waterborne latex systems can be used for similar applications, they are usually considered as two opposite systems. This is mainly the result of the differences in physico-chemical properties and in the drying process of the two systems. Acrylic latexes are composed of high molecular weight polymer particles dispersed in water. These form a film by a process of particle coagulation and coalescence upon evaporation of the water (the physical drying process) [22]. Vegetable oils and alkyds, on the other hand, are low molecular weight resins dissolved in organic solvent, or in case of alkyd emulsions, dispersed in water. After evaporation of the solvent the alkyd resins dry chemically by autoxidative drying, which is a comparatively slow process. Because of these differences coatings from alkyd resins and acrylic latexes have different properties. In Table 1.3 some of the properties of traditional alkyd resins and acrylic latexes are compared.

Table 1.3 suggests that an ideal binder system may be generated when synergy is obtained in a combined system of alkyd resin and acrylic polymer. This system would combine the autoxidative drying, high gloss and penetration properties of

Table 1.3. Properties of Alkyd Resins and Acrylic Latexes

| | Alkyd resin | Acrylic latex |
|---|---------------------|---------------------|
| Molecular weight (M_w) | 4000 – 6000 | $10^5 - 10^6$ |
| Drying process | chemically | physically |
| Minimum appl. temperature | > - 20 °C | > 0 °C ^a |
| Use of organic solvent | 23-80% ^b | 1-10% ^c |
| Drying time | 4-20 h | 0.5-6 h |
| Penetration in porous substr. (wood [23]) | 20-60 μm | < 5 μm |
| Adhesion | good | fair |
| Gloss | good | fair ^c |
| Corrosion resistance | good | fair |
| Color retention | troublesome | fair |
| Chemical resistance | fair ^d | good |

a) The result of water being used as solvent

b) In case of solvent-borne system

c) Depends on amount of coalescing agent added

d) Poor alkali resistance

alkyd resins in a waterborne system with the fast drying, color retention and chemical stability properties of acrylic latexes.

The combination of these properties, for waterborne as well as for solvent-borne systems, has been the objective of several studies in the past. In these studies, four different approaches have been used (Figure 1.2): (a) synthesis of alkyd followed by copolymerization of vinyl, or acrylic, monomer with the alkyd resin, (b) modification of alkyd building blocks with vinyl, or acrylic, polymer followed by synthesis of alkyd, (c) modification of acrylic monomer with fatty-acid chain followed by free radical polymerization, and (d) mechanical blending. A brief discussion on the four approaches is given below.

Copolymerization of Vinyl or Acrylic Monomer with Alkyd Resin

The polymerization of vinyl or acrylic monomer in the presence of a drying oil, or alkyd resin, has been the approach that has been applied most often for the synthesis of hybrid binders. This approach has been used for the preparation of solvent-borne, waterborne, and ultra high solids [24-26] systems. One of the first reports of reacting a vinyl monomer with a drying oil, or alkyd, resin was published in 1931 and comprised the polymerization in an aqueous emulsion of

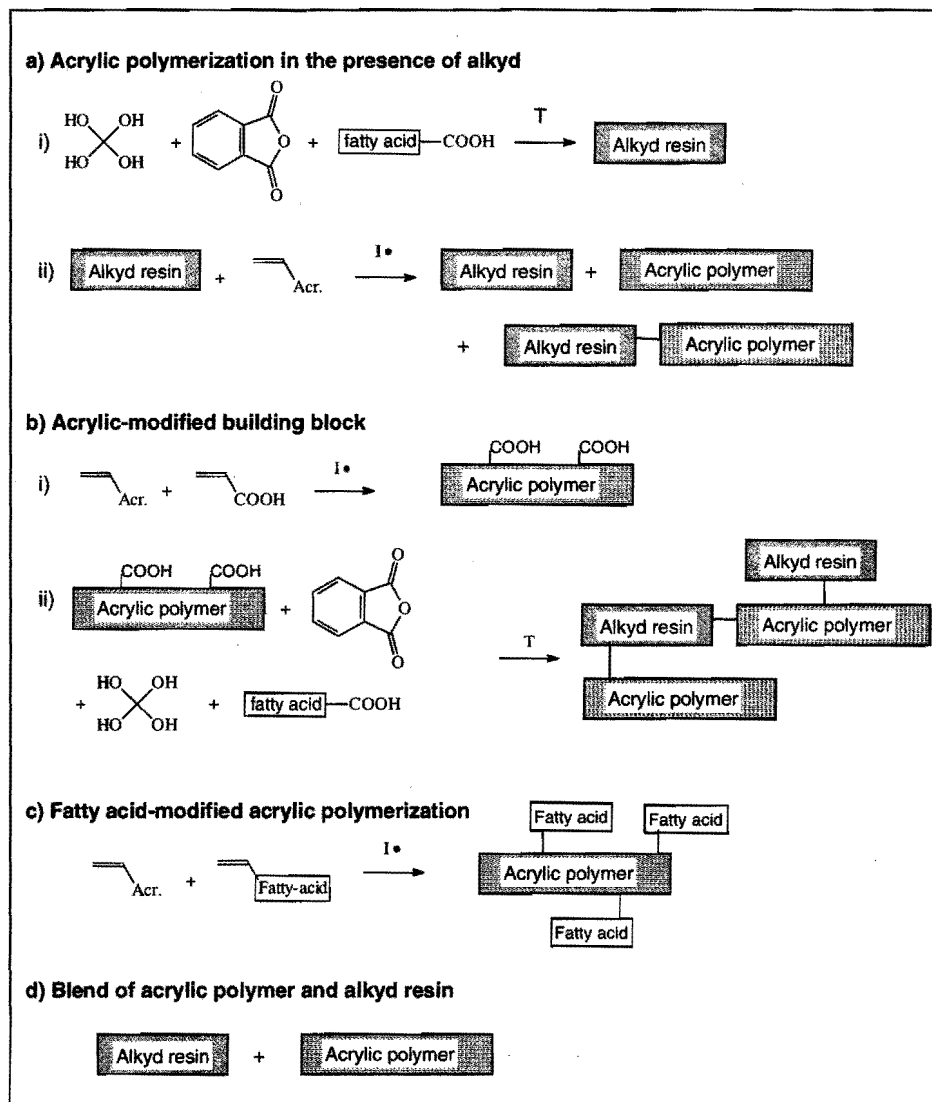


Figure 1.2. Schematic representation of the different approaches that have been used in the past for the preparation of oil/alkyd-acrylic hybrid systems.

styrene and tung oil using hydrogen peroxide as initiator [27]. The polymerization of acrylic monomer in the presence of alkyd resin can result in different ratios of acrylic homopolymer and alkyd resin to copolymer of alkyd resin and acrylic polymer as illustrated in Figure 1.2a. The presence of a copolymer as a

compatibilizer is essential because the acrylic homopolymer and alkyd resin are incompatible [28,29]. From the early work on polymerization of styrene and acrylic monomers in the presence of drying oils or alkyd resins [30-34], two mechanisms for the reaction of a growing polymer chain with an unsaturated fatty acid have been proposed. The nature of the fatty acids present in the system during polymerization determines the amount and the chemical structure of the copolymer of alkyd resin and acrylic polymer.

Hewitt and Armitage [35] have proposed a chain-transfer mechanism in the reaction with non-conjugated oils (Figure 1.3). According to this chain-transfer mechanism a pentadienylic radical at the fatty-acid chain with low reactivity is formed. Since re-initiation by this radical is unlikely, this results in a decrease in the rate of polymerization and in a decrease in the overall degree of polymerization. Termination by radical combination of pentadienyl radicals results in the formation of oil dimers [36].

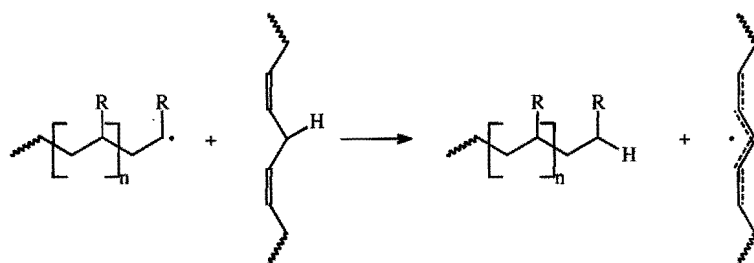


Figure 1.3. Chain-transfer reaction of growing polymer chain and non-conjugated fatty acid.

Hewitt and Armitage also suggested that with conjugated fatty acids copolymerization takes place involving (1,2)- or (1,4)-addition across the conjugated linkages as illustrated in Figure 1.4. This mechanism is similar to that observed in styrene-butadiene copolymerization. Others have also suggested this reaction mechanism [37]. Propagation of polymer chains across conjugated double bonds enables the incorporation of oil or alkyd resin into the polymer chain.

In general, it is believed that the propagation of polymer chains across conjugated fatty acids results in the formation of copolymer of alkyd resin and acrylic polymer. Therefore, a certain amount of alkyd with conjugated fatty acid

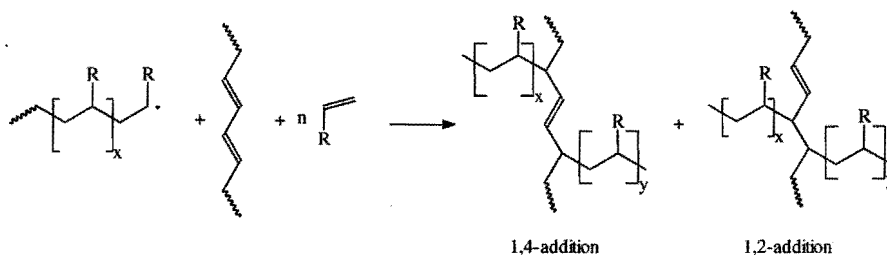


Figure 1.4. Propagation of growing polymer by 1,4- or 1,2-addition across a conjugated diene present in oil, or alkyd, resin.

chains is often added to the system when a homogeneous oil/alkyd-acrylic hybrid is synthesized [38,39].

In our laboratories, the use of emulsion polymerization for the synthesis of alkyd-acrylic hybrid emulsions and the morphology development in these particles was studied [9,40]. An alkyd emulsion was formed by high-pressure homogenization. The alkyd emulsion was used as a 'seed' for batch- and semi-batch emulsion polymerization of acrylics. It was shown that the formation of a secondary generation of all acrylic particles could be a problem. The formation of a secondary generation of particles could be avoided when alkyd emulsions with build-in surfactant were used. Also, it was shown that phase separation between the alkyd resin and the acrylic polymer in the particles occurred. The use of hydroperoxide-functionalized alkyd resins as initiators for the polymerization of the acrylic was introduced as an alternative to increase the amount of grafting between the alkyd resin and the acrylic polymer. In 1996 Wang *et al.* [41] showed that the formation of a secondary generation of all acrylic particles can be avoided by performing the polymerization in mini-emulsion. However, they did not discuss the morphology of the hybrid particles synthesized by mini-emulsion polymerization.

Acrylic-Modified Alkyd

The second approach for the development of alkyd-acrylic hybrid binders involves the incorporation of a functionalized acrylic polymer during alkyd synthesis. This approach consists of (i) preparing a reactive acrylic solution polymer with a functional group by free radical co-polymerization, and (ii) conventional processing of the synthesized acrylate with alkyd components. The

product is a copolymer of acrylic polymer and alkyd resin as illustrated in Figure 1.2b. Using this method, solvent-borne alkyd-acrylic hybrids have been made by Solomon *et al.* [42-45]. They synthesized acrylic polymers functionalized with anhydride, epoxy, or carboxyl groups. The solvent-borne alkyd-acrylic hybrid systems thus developed showed fast drying and resulted in homogeneous films. For the synthesis of waterborne hybrids, acrylic polymers with hydroxyl or carboxyl functionality have been used by others [46-48]. Because of the high viscosity of the alkyd-acrylic copolymer, emulsification of the hybrid resin to form a surfactant-stabilized emulsion is very difficult. Therefore, this approach has mainly been used for the synthesis of self-emulsifying resins using methacrylic acid copolymers. This resulted in particles with the alkyd resin in the core and methacrylic acid copolymer in the shell [46,47] (Figure 1.5).

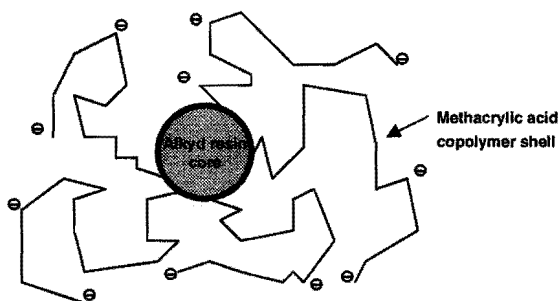


Figure 1.5. Schematic representation of self-emulsifying alkyd-acrylic hybrid particle.

Polymerization of Alkyd-Functionalized Acrylic Monomer

The polymerization of fatty alcohol-functionalized acrylic monomer is the third approach for the synthesis of oil/alkyd-acrylic hybrid systems. This approach involves the modification of vinyl monomer with fatty alcohol groups followed by free radical polymerization (Figure 1.2c). The product of this approach has an acrylic polymer backbone and can be described as an air drying-, or fatty acid modified-, acrylic (Figure 1.6) [49]. Joshi and Chatterjee [50,51] have used this approach for the development of a waterborne hybrid system. They observed that the mechanism of chain transfer to non-conjugated fatty alcohol chains plays an important role in the emulsion co-polymerization with fatty alcohol-modified acrylic monomer. Although the approach of Joshi and Chatterjee of using modified unsaturated fatty acids as macromonomers in an emulsion polymerization seemed very promising, little research along this line seems to have been performed since the original work in 1978.

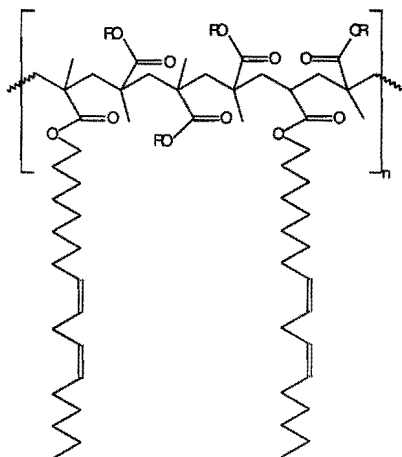


Figure 1.6. Fatty acid modified acrylic polymer.

Mechanical Blend of Alkyd Resin and Acrylic Polymer

An alkyd-acrylic hybrid system composed of a blend of the oil, or alkyd resin, and the acrylic polymer can be formed in a solvent-borne or in a waterborne system. In the solvent-borne system described by Zissell and Southwell [52] and by Athley *et al.* [53], acrylic polymer particles were dispersed in a vegetable oil or an alkyd resin solution. In these systems the dispersed acrylic polymer particles improved the resistance to aging or acted as reservoirs for encapsulated UV absorbers. A waterborne blend of an alkyd emulsion and an acrylic latex was described by Hofland *et al.* [54]. In this system the alkyd emulsion acted as a reactive softener for the acrylic particles. The mechanical blend was formed by emulsion polymerization with secondary nucleation during polymerization resulting in the formation of a generation of all-acrylic particles. The authors reported that a clear film was obtained, because the difference in refractive index between the alkyd resin and the polymer based on the unsaturated monomers, was smaller than 0.025. Since the alkyd resin and the acrylic polymer are incompatible this approach resulted in a coating with a heterogeneous morphology.

1.4 Objectives and Survey of the Thesis

From the research described in the previous section it can be concluded that the different approaches used in the synthesis of oil-, or alkyd-, acrylic hybrid latexes result in hybrid systems with different chemical compositions and various particle morphologies, and gives films with different coating properties. In the introductory section it was described that *the primary aim of this investigation was the development and characterization of oil-acrylic hybrid binders for high performance waterborne coatings*. Continuing the line of research of Nabuurs [9], the approach used for the preparation of oil-, or alkyd-, acrylic hybrid latexes in this thesis has been to perform a free radical polymerization of the acrylic monomer in the presence of an emulsion of oil or alkyd resin. It is proposed that a system with combined positive properties can be obtained from the combination of low molecular weight oil, or alkyd resin, and high molecular weight acrylic polymer. Compatibilization of this hybrid system with oil-acrylic copolymer is expected to increase particle homogeneity and to result in better coating performance. In addition, this approach allows for the use of the versatile range of alkyd resins and modified alkyd resins that have been developed over the years. The use of the emulsion polymerization process, combined with the homogenization technology commonly used for the formation of alkyd emulsions, allows one to take advantage of the positive aspects of emulsion polymerization, *i.e.*, good heat transfer and ease of processing.

When using emulsion polymerization there are two aspects that need to be considered:

- i. **compatibility** between the oil-, or alkyd, resin and the acrylic polymer,
- ii. **secondary nucleation** during emulsion polymerization.

Previous results in our laboratories indicated that a more homogeneous particle morphology resulted in better coating properties. Therefore, research has been focused on the development of oil-acrylic hybrid latexes with a homogeneous intraparticle morphology. Initiation of polymerization by fatty-acid hydroperoxides has been used to increase the amount of copolymer present after the polymerization and thus the compatibility between the two components. Secondary nucleation is avoided by making use of the process of mini-emulsion polymerization.

The second objective of this investigation was to increase the understanding of the processes that take place during film formation of oil/alkyd-acrylic hybrid latexes. The oil/alkyd-acrylic hybrid latexes prepared using the above approach consist of low molecular weight autoxidatively reactive oil, or alkyd resin, high

molecular weight acrylic polymer and copolymer of the resin and the acrylic. It is expected that insight in the relationship between the morphology of the particle on the one hand, and the properties and morphology of the resulting coating on the other hand, provides tools for a better design of hybrid binders.

The research described in this thesis can be divided into two sections. The first part (Chapters 2 and 3) is focused on the preparation and control of particle morphology of oil-acrylic hybrid latexes. The second part (Chapters 4-6) describes the use of oil/alkyd-acrylic hybrid latexes as binders for coatings, as compared to alkyd emulsion binders and an oil/alkyd-acrylic blend. The processes that take place during film formation are characterized and the coating properties analyzed. These two parts are concluded by a general discussion on the preparation of oil/acrylic hybrid latexes and their applicability as a binder system. A more detailed outline of the thesis is given below.

The formation of emulsions of vegetable oils with hydroperoxide functionality is described in **Chapter 2**. The process of emulsification followed by oxidation at high partial oxygen pressure was compared to the oxidation of the oil at elevated temperature followed by emulsification.

Chapter 3 describes the use of fatty-acid hydroperoxides as initiators for the mini-emulsion polymerization of methyl methacrylate. The kinetics of the mini-emulsion polymerization in an ROOH/iron-EDTA/SFS redox system and the characteristics of the particles were examined. Cryogenic electron microscopy was used to compare the morphology of fatty-acid hydroperoxide-initiated and *tert*-butyl hydroperoxide-initiated hybrid latex particles.

The preparation of film-forming alkyd-acrylic hybrid latexes is presented in **Chapter 4**. In this and the following chapters ethyl methacrylate was used as acrylic monomer. The surface properties of films prepared from these hybrid latexes and of individual hybrid particles were studied using Atomic Force Microscopy (AFM). The migration of binder components to the substrate-film and film-air surface was analyzed for films prepared on hydrophobic and hydrophilic surfaces.

Chapter 5 presents a characterization study of the phase separation in the bulk of the film between the oil and acrylic components during film formation and ageing. Fluorescence resonance energy transfer measurements were used to study phase separation for hybrid latexes composed of anthracene-labeled (acceptor) acrylic polymer, and phenanthrene-labeled (donor) oil resin.

A preliminary evaluation of the coating properties of films prepared from a blend of an alkyd emulsion and acrylic latex and from oil-acrylic hybrid latexes is

described in **Chapter 6**. The morphology of films made from the alkyd-acrylic blends was studied by AFM and the effect of variation in composition between alkyd emulsion and acrylic latex is discussed.

1.5 References

1. Z.W. Wicks, F.N. Jones, S.P. Pappas, in *"Organic Coatings. Science and Technology"*, Vol. 2, Wiley, Chichester (1994).
2. Official chair *"Coating Technology"* at Eindhoven University of Technology since 1995.
3. J. Geurts, *"Latexes with Intrinsic Crosslink Activity"*, Ph.D. Dissertation, Eindhoven University of Technology (1997).
4. J.M.G. Verstegen, *"Post-Crosslinking of Functional Polymers Using Photo-Acid Generators"*, Ph.D. Dissertation, Eindhoven University of Technology (1998).
5. T.A. Misev, *"Powder Coatings. Chemistry and Technology"*, Wiley, Chichester (1991).
6. E.M.S. van Hamersveld, F.P. Cuperus, J.T.P. Derksen, J.G.G.S. van Es, A.L. German, Patent Application no. 1009254 (1998).
7. M.A. Winnik, J. Feng, *J. Coat. Tech.*, 68 (852), (1996) 39.
8. R.M. Rynders, C.R. Hegedus, A.G. Gilicinski, *J. Coat. Tech.*, 67 (845), (1995) 59.
9. T. Nabuurs, *"Alkyd-Acrylic Composite Emulsions. Polymerization and Morphology"*, Ph.D. Dissertation, Eindhoven University of Technology (1997).
10. (a) G.J.H. Buisman, *Polym. Paint Col. J.*, 188, (1998) 14. (b) F.M. Witte, C.D. Goemans, R. van der Linde, D.A. Stanssens, *Prog. Org. Coat*, 32, (1997) 241.
11. E.A. Weiss, in *"Oilseed Crops"*, Longman London, (1983) 528.
12. H. Wexler, *Chem. Rev.*, 64 (6), (1964) 591, see for review.
13. Z.W. Wicks, *"Drying Oils"*, in Kirk-Othmer Encyclopedia of Chemical Technology, 4th Ed., Vol. 8, Wiley, New York, (1991) 522.
14. Z.W. Wicks, F.N. Jones, S.P. Pappas, in *"Organic Coatings. Science and Technology"*, Vol. 1, Wiley, Chichester, (1992) 134.
15. R.H. Kienle, C.S. Ferguson, *Ind. Eng. Chem.*, 21, (1929) 349.
16. K.F. Lin, *"Alkyd Resins"*, in Kirk-Othmer Encyclopedia of Chemical Technology, 4th Ed., Vol. 2, Wiley, New York, (1991) 53.
17. F.N. Jones, *"Alkyd Resins"*, in Ullmann's Encyclopedia of Industrial Chemistry, Vol. A1, 5th Ed., VCH, Weinheim, (1985) 409.
18. For review on emulsion polymerization see: (a) Q. Wang, S. Fu, T. Yu, *Prog. Pol. Sci.*, 19, (1994) 703. (b) J.M. Asua (Ed.), *"Polymeric Dispersions: Principles and Applications"*, Nato

- ASI Ser. 335, Kluwer, Dordrecht (1997). (c) P.A. Lovell, M.S. El-Aasser (Eds.), "Emulsion Polymerization and Emulsion Polymers", Wiley, Chichester (1997).
19. Starting with the 'Clean Air Act' in 1970 in the U.S.A.
 20. K.D. Weiss, *Prog. Polym. Sci.*, 22, (1997) 203.
 21. E.M.S. van Hamersveld, F.P. Cuperus, J.T.P. Derksen, *Agro-Food-Ind., Hi-Tech.*, July/August, (1996) 23.
 22. (a) F. Dobler, Y. Holl, in "Film Formation", ACS Symp. Ser. 648, A.C.S. Washington D.C, (1996) 22. (b) M. Visschers, J. Laven, A.L. German, *Prog. Org. Coat.*, 30, (1997) 39.
 23. G. Rødsrud, J.E. Sutcliffe, *Surf. Coat. Int.*, 1, (1994) 7.
 24. C. Kuo, Z. Chen, L. Nirali, S. Dirlikov, *Waterborne, Higher-Solids, and Powder Coat. Symp.*, New Orleans, (1994) 797.
 25. E.J. Kuzma, E. Levine, *J. Coat. Tech.*, 56 (710), (1984) 45.
 26. D.B. Larson, *Polym. Mat., Sci. Eng.*, 55, (1986) 143.
 27. I.G. Farben Industrie, British Patent 362,845, Dec 7, (1931).
 28. J. Schreiber, *Farbe und Lack*, 9 (63), (1957) 443.
 29. J. Brandrup, E.H. Immergut (Eds.), "Polymer Handbook", Wiley Interscience, New York (1973).
 30. W.E. Lawson, L.T. Sandborn, U.S. Patent 1,975,959, Oct 9, (1934).
 31. L.E. Wakeford, D.H. Hewitt, British Patent 573,809, May 4, (1943).
 32. L.E. Wakeford, F. Armitage, British Patent 573,835, Oct 25, (1944).
 33. L.H. Dunlap, U.S. Patent 2,382, 213, Aug. 14, (1945).
 34. H.M. Schroeder, R.L. Terill, *J. Am. Oil. Chem. Soc.*, April, (1949) 153.
 35. D.H. Hewitt, F. Armitage, *J. Oil Col. Chem. Ass.*, 29, 312, June, (1946) 109.
 36. W.J. Muizebelt, J.C. Hubert, R.A.M. Venderbosch, *Prog. Org. Coat.*, 4, (1994) 263.
 37. M.S. Saxena, P.K. Jain, A.K. Vasishtha, *J. Oil Chem. Assoc.*, 65, (1982) 409.
 38. S. Majumdar, D. Kumar, Y.P.S. Nirvan, *J. Coat. Tech.*, 70 (879), (1998) 27.
 39. R. Buter, P.M. Postma, Eur. Patent 0-555-903 A1, (1993).
 40. T. Nabuurs, R.A. Baijaards, A.L. German, *Prog. Org. Coat.*, 27, (1996) 163.
 41. S.T. Wang, F.J. Schork, G.W. Poehlein, J.W. Gooch, *J. Polym. Sci., Polym. Lett.*, 11 (1996) 2069.
 42. D.H. Solomon, *J. Oil Col. Chem. Ass.*, 45, (1962) 88.
 43. J.R. Fletcher, D.P. Kelly, D.H. Solomon, *J. Oil Col. Chem. Ass.*, 46, (1963) 127.
 44. J.J. Hopwood, C. Pallaghy, D.H. Solomon, *J. Oil Col. Chem. Ass.*, 47, (1964) 289.
 45. R. Dhein, L. Fleiter, R. Küchenmeister, *Verfkroniek*, 53 (4), (1980) 145.
 46. W. Weger, *Polym. Paint Colour J.*, June, (1995) 12.
 47. M. Gobec, W. Weger, *Kunst. Nachr.*, 31, (1995) 10.
 48. E. Levine, E.J. Kuzma, *J. Coat. Tech.*, 51 (557), (1979) 35.
 49. M. Gorzinski, German Patent DE 196 47 416 A1, (1996).

50. S.K. Joshi, P.C. Chatterjee, *Pigment and Resin Tech.*, October, (1978) 9.
51. S.K. Joshi, P.C. Chatterjee, *J. Am. Oil Chem. Soc.*, 55, (1978) 607.
52. M.J. Zissell, M.J. Southwell, UK Pat. GB 2 170 810 A, (1986).
53. R.D. Athley, N.W. Heywood, H. Harlan, *Eur. Coat. J.*, 1-2, (1998) 46.
54. A. Hofland, R. van der Linde, R.A. Bayards, Eur. Pat. 0 551 942 A2, (1993).

CHAPTER 2: PREPARATION OF EMULSIONS OF OXIDIZED VEGETABLE OILS

Summary

An introduction to the process of autoxidation is presented in this chapter. The mechanism of fatty-acid hydroperoxide formation and the products resulting from the fatty-acid hydroperoxide decomposition are reviewed. Two methods for the preparation of emulsions of oxidized vegetable oils are described using sunflower oil as a model triglyceride. The first method involved the formation of emulsions of sunflower oil followed by oxidation at high partial oxygen pressure. The effect of temperature, of oxygen pressure and of the presence of metal ions on the formation of fatty-acid hydroperoxides in emulsion was studied. The second method involved the bulk oxidation of sunflower oil, followed by high-pressure emulsification. The effect of temperature on the bulk oxidation of sunflower oil was investigated and the stability of the formed hydroperoxides during emulsification and ageing was monitored. It was shown that both methods could be used for the preparation of emulsions of oxidized vegetable oils with low degree of cross-linking. Each method had its specific advantages for further use in the preparation of oil-acrylic hybrid latexes. Because of the maximum hydroperoxide value (HPV) that could be obtained and its flexibility, bulk oxidation followed by emulsification was the method of choice.

2.1 Introduction

In order to improve their suitability as a paint binder, vegetable oils are often pre-treated to a certain extent. Vegetable oils can be chemically modified by means of hydrogenation, blowing (oxidation), heat bodying (polymerization), or double processing, *i.e.*, moderate heat bodying followed by air blowing [1]. Both non-conjugated and conjugated drying oils can be thermally polymerized by heating under an inert atmosphere to form bodied oils. Bodied oils have higher viscosity than non-bodied oils and are often used in oil-based paints to improve application and performance characteristics [2,3]. The viscosity of drying oils can also be increased by passing air through the oil at relatively moderate temperatures [3]. The autoxidation process causes polymerization at the double bonds with cross-linking of the fatty acids.

In the 1980s Gooch *et al.* [4-6] showed that the properties of emulsions of vegetable oils and alkyd resins could be improved by autoxidative cross-linking at high partial oxygen pressure. They showed that partially cross-linked emulsions of vegetable oil and alkyd emulsions, with an optimum 'swelling ratio' of 3.7, resulted in binders with improved tensile strength and drying time compared to non-treated emulsions. The factors that controlled the autoxidative cross-linking included temperature, oxygen concentration, presence of transition metal ions, concentration of unsaturated and conjugated groups and the type of surfactant used to stabilize the emulsions.

The studies of Gooch *et al.* [4-6] have shown that the process of autoxidative drying can be applied in emulsions to improve the properties of vegetable oil and alkyd resin emulsions as binders. The research described in this chapter was aimed at the preparation of emulsions of unsaturated vegetable oils that were modified with a certain amount of fatty-acid hydroperoxide groups. Fatty-acid hydroperoxides are the products of the first stage of autoxidative drying, as is described in the review on autoxidative drying in the next section (Section 2.2). The use of these oxidized vegetable oil emulsions as part of the initiating system for the mini-emulsion polymerization of acrylic monomers for the preparation of oil-acrylic hybrid emulsions is described in Chapter 3 of this thesis.

Earlier research in our laboratories [7] showed that alkyd resins, treated with air to introduce hydroperoxide groups can be used as part of a redox initiation system for the seeded emulsion polymerization of acrylic monomers. This approach showed very promising results for the development of alkyd-acrylic hybrid binder systems. In the preliminary study the introduction of hydroperoxide groups was performed by purging air through an alkyd emulsion at elevated

temperatures. Competitive decomposition of the formed hydroperoxides and the resultant cross-linking of the alkyd emulsions were not described.

In the present study the controlled formation of fatty-acid hydroperoxides is monitored. In order to enable the fatty-acid hydroperoxides to be used as part of the initiator system, hydroperoxide values (HPV, expressed as $\mu\text{mole active oxygen}/2 \text{ kg of oil}$) varying from 400 to 800 were aimed at. A hydroperoxide value of 400 corresponds to an initiator concentration of about 0.1 mole/L in a 50/50% mixture by weight of sunflower oil to methyl methacrylate. Concurrently, a hydroperoxide value of 400 corresponds to oxidation of about 6% of the sites available for oxidation of sunflower oil.

It is important that the number of reactive sites, *i.e.*, non-conjugated dienes and fatty-acid hydroperoxides, consumed during autoxidation and during initiation is small, since the propensity of the oil to cross-link after application needs to be maintained. Therefore, during oxidation the decomposition of the formed hydroperoxides and resultant cross-linking should to be minimized. Measurement of the solubility of the emulsion in acetone as a method to monitor the formation of polymer products during the autoxidation reaction was introduced by Gooch *et al.* [4-6]. With increasing cross-linking, the transmittance of an emulsion-acetone mixture decreased. A sharp drop of the light transmittance occurred towards the end point of the autoxidative cross-linking. This method was used in the current study to monitor the formation of cross-linked product.

Sunflower oil was used in this study as a model compound for long-oil alkyd resins. The chemical composition of sunflower oil is easily determined and the molecular weight distribution is narrow. This enabled a more detailed characterization of the autoxidation products and allowed a better study of the factors affecting the formation of fatty-acid hydroperoxides. In addition, it was expected that a more detailed characterization of the oil-acrylic products resulting from initiation of polymerization using fatty-acid hydroperoxides was possible.

Two different methods of forming oxidized vegetable-oil emulsions have been investigated:

- i. emulsification of vegetable oil followed by oxidation at high pressure in emulsion, and
- ii. oxidation of vegetable oil followed by emulsification of the oxidized oil.

The vegetable oil emulsions were formed by direct emulsification of the vegetable oil in water using high-pressure homogenization. Stabilization of the emulsions was performed by the addition of anionic surfactant. For many reasons (stability, relative surface area, flow etc.) it was desirable that small

particles were obtained. Walstra [8] showed that high-pressure homogenization is the most effective technique for the formation of small particles. Research on emulsification of alkyd resins by Östberg *et al.* [9] showed that the use of anionic surfactants resulted in the most stable emulsions. In addition to the better stabilization properties of anionic surfactants, it was found by Gooch [6] and Beurde [10] that the use of nonionic surfactants gave a decreased rate of oxidation. Therefore, sodium dodecyl sulfate (SDS) was chosen as anionic surfactant in our research.

The effects of temperature, oxygen pressure and addition of transition metal ions on the formation and decomposition of hydroperoxide groups were studied for emulsions of sunflower oil. Bulk oxidation of sunflower oil was investigated at various temperatures. After oxidation the stability of the formed hydroperoxides upon emulsification and ageing was tested.

2.2 Autoxidative Drying

The autoxidation of natural products is of importance in both the food and the non-food industry. For coating applications, autoxidation is generally considered as a desirable process that results in the formation of a cross-linked network. Catalysts are added to these systems in order to increase and manipulate its effectiveness. The process is being widely used in alkyd resin-based paints, especially for the do-it-yourself (DIY) market.

The process of autoxidation has been the subject of various studies in the past [11-31,33-39]. It is now generally accepted that the autoxidation of organic compounds, RH, involves a radical-catalyzed chain reaction and results in the formation of hydroperoxides, ROOH, as primary products (Eqns. 2.1–2.5).



The formation of the initiating free radical species $\text{X} \cdot$ (Eqn. 2.1) can be inhibited by the presence of natural antioxidant compounds [26], or can be accelerated by

the addition of radical-generating compounds, like *tert*-butyl hydroperoxide [27,28], or high concentrations of tocopherol [29,30].

In 1995 Porter *et al.* [31] presented a detailed overview of autoxidation reactions of monoene lipids, non-conjugated diene lipids and polyene lipids. The binders used for autoxidatively drying coatings normally contain a high content of non-conjugated diene-type of fatty-acid chains [32].

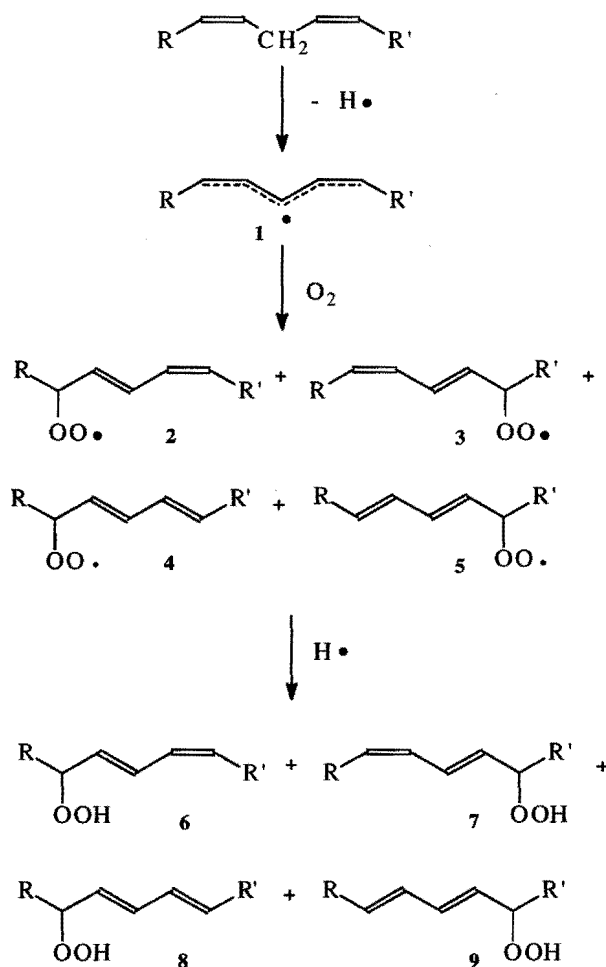
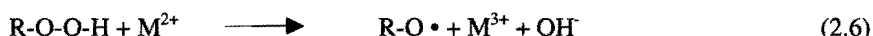


Figure 2.1. Schematic representation of the autoxidation process of non-conjugated diene lipids.

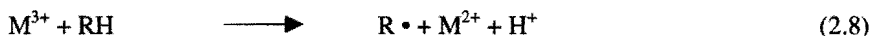
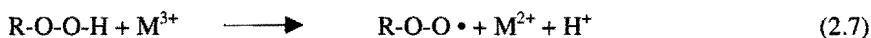
The autoxidative drying of these systems can be described as occurring in two stages. In the first stage (the actual autoxidation) oxygen is incorporated and hydroperoxides are formed as schematically represented in Figure 2.1. The second stage involves the decomposition of hydroperoxides and generation of polymeric and low molecular weight products [33-35].

The initial step of the autoxidation is considered to be the abstraction of a hydrogen atom allylic to two double bonds resulting in pentadienyl radical **1** (Eqns. 2.2 and 2.4). Oxygen addition to **1** generates either one of the two *cis* or *trans* peroxy radicals **2** or **3**. Subsequent hydrogen atom abstraction from a donor such as another non-conjugated fatty-acid chain leads to the *cis,trans* hydroperoxides **6** and **7**, which are the kinetic products of the autoxidation. The concurrent formation of the thermodynamic products, *i.e.*, *trans,trans* hydroperoxides **8** and **9**, involves rearrangement of the intermediate peroxy radicals, **2** and **3**, by β -fragmentation as has been established by Chan *et al.* [11]. Bisallylic hydroperoxides, resulting from oxygen addition to the central carbon of pentadienyl radicals, are normally not observed in autoxidation [36].

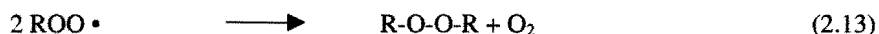
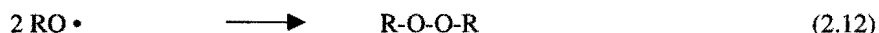
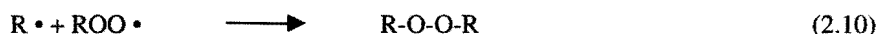
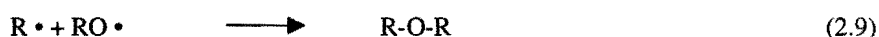
The second stage of autoxidative drying involves the decomposition of hydroperoxides and the formation of low molecular weight and polymeric products. Hydroperoxides can decompose thermally to give radicals $\text{RO}\cdot$ and $\text{HO}\cdot$. At ambient temperature this decomposition reaction is slow. However, divalent ions of a number of transition metals, like Co, Fe and Mn, are effective catalysts [25,37-39]. Initially, these ions act as one-electron donors to give $\text{RO}\cdot$ radicals as represented by Eqn. 2.6.



This is followed by a second step, in which radicals are produced and M^{2+} is regenerated so that a catalytic cycle is established (Eqns. 2.7 and 2.8).



Radicals formed by the decomposition of hydroperoxides can couple to another radical, abstract a hydrogen from a non-conjugated diene, or add to the double bond of a conjugated diene. Reactions such as (2.9)-(2.13) will result in the formation of a network.



A complex mixture of low molecular weight molecules, *i.e.*, hydrocarbons, alcohols, aldehydes, ketones and acids, may result from scission reactions following the decomposition of fatty-acid hydroperoxides [33]. The formation of these products (often referred to as volatile by-products) is considered to be a disadvantage in the use of autoxidatively drying binders, since they contribute to the volatile organic compound content (VOC) of a paint system.

2.3 Experimental

2.3.1 Materials

Commercial grade sunflower oil (SFO) was obtained from Rhenus B.V. (Dodewaard, The Netherlands). The fatty acid composition of the sunflower oil as determined by gas chromatography (GC) of the methyl esters was 5.9% C16, 64.9% C18:2 (non-conjugated), 24.5% C18:1, 4.0% C18, 0.7% C20. Prior to use the SFO was purified by column chromatography using Florisil (60–100 mesh, Merck) to get rid of any peroxides [40]. Sodium hydrogencarbonate (NaHCO₃, Merck), potassium iodide (KI, Merck), sodium chloride (NaCl, Merck), silver nitrate (AgNO₃, Merck), sodium dodecyl sulfate (SDS, very pure Fluka Biochemica) and hydroquinone (HQ, Aldrich) were used as received. Glacial acetic acid (Aldrich), isopropyl alcohol (IPA, Aldrich), acetone (Aldrich) and tetrahydrofuran (THF, Aldrich) were used without further purification. Co-octanoate was obtained from Vliegenthart B.V. An aqueous solution of sodium thiosulfate (0.01 M) was prepared from a titration package (1.0 M, Merck). Aqueous starch dispersion was prepared by dissolving 100 mg of starch in 100 mL of water at 90 °C. Starch dispersion was used after cooling to ambient temperature. Water was doubly distilled and deionized (Millipore Super Q).

2.3.2 Oxidation Procedures

Emulsification and High Pressure Oxidation

The oxidation was carried out according to the conditions O1–O7 given in Table 2.1. All recipes contained 280 g of water, 120 g of sunflower oil (SFO) and 2 g of surfactant (SDS).

A pre-emulsion was created by sonification (Branson Sonifier 250, 70% duty cycle) for 2 minutes while cooling in a water bath. The pre-emulsion was subsequently passed through a high-pressure homogenizer (Gaulin Laboratory Homogenizer, APV capacity 60 L/h) for 5 minutes. The homogenizer was operated at a pressure of 400 bar.

After emulsification the particle size was analyzed and 125 mL of the SFO emulsion was transferred to a high-pressure teflon[®]-coated autoclave (Berghoff Maasen, HR 100). A cross-sectional representation of the autoclave is given in Figure 2.2. After charging the autoclave with the emulsion at atmospheric conditions the magnetic stirrer was engaged at a rotor speed of 850 rev./min. The reactor was flushed twice with oxygen and the oxygen pressure was set to the predetermined vessel pressure.

After setting the oxygen pressure the vessel was heated to the predetermined vessel temperature. During the high-pressure oxidation liquid samples were taken to monitor the progress of the autoxidation using the extraction device. A small amount of hydroquinone was added to the samples to prevent further radical reactions. The start of the reaction, $t = 0$, was defined as the moment when the predetermined temperature of the vessel was reached.

Table 2.1. Formulations and Conditions used for High-Pressure Oxidation

| Code | T (°C) | P (bar) | Cat. |
|------|-----------|------------|-----------------|
| O-1 | 55 | 5 | - |
| O-2 | 55 | 6.5 | - |
| O-3 | 55 | 10 | - |
| O-4 | 80 | 5 | Fe |
| O-5 | 55 | 5 | Co ^a |
| O-6 | 55 | 5 | Co ^b |
| O-7 | 55 | 5 | - |

a) 0.05 % wt./wt. of oil

b) 0.1 % wt./wt. of oil

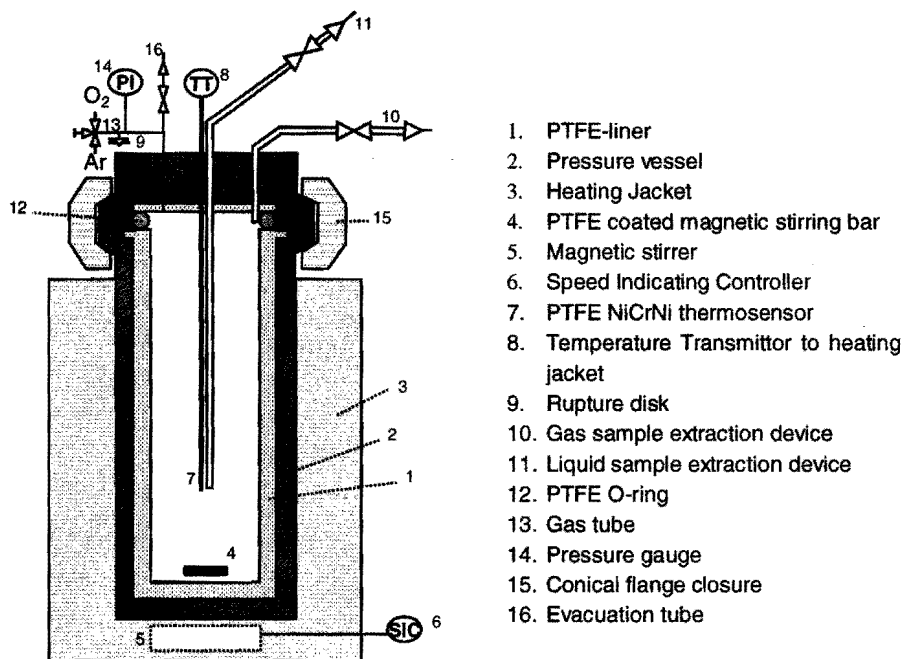


Figure 2.2. PTFE-coated batch reaction autoclave used for the emulsion oxidation experiments. The extraction devices facilitate sampling under the reaction conditions.

SFO Oxidation at Atmospheric Pressure

The oxidation of SFO by oxygen at ambient temperature was carried out in a round-bottomed flask, covered with aluminum foil and equipped with a mechanical stirrer and a gas inlet: 350 mL of SFO was added to the flask and 150 cm³/min. of oxygen gas was blown through the oil at different temperatures. The concentration of hydroperoxide groups (HydroPeroxide Value, or HPV) and the viscosity of the oil were monitored.

2.3.3 Analysis

Hydroperoxide Value

The hydroperoxide value (HPV, expressed as μmole of active oxygen/2 kg of oil) of the samples was determined according to the procedures described in ISO standard 3960.

A sample of the oil, or the emulsion, was dissolved in isopropyl alcohol (10 mL) and an excess of a saturated potassium iodide solution (1 mL) and glacial acetic acid (15 mL) were added successively. The solution was stirred for five minutes, then water (75 mL) and a starch dispersion (5 g/L, 2 mL) were added. The solution was titrated with sodium thiosulfate solution (0.01 N), until the yellow/brown color fully disappeared. The result was compared with a blank without hydroperoxides. The HPV was calculated using the following equation:

$$\text{HPV} = \frac{(V - V_0) \cdot T}{m} \cdot 1000 \quad (2.14)$$

with: HPV = hydroperoxide value given in μmole active oxygen/2 kg of oil

V = volume of titer used

V_0 = volume of titer used in blank determination

T = titer of $\text{Na}_2\text{S}_2\text{O}_3$ solution

m = weighed oil mass

For the calculation of the hydroperoxide value of the oil in emulsion first the solids content of the emulsion was determined gravimetrically.

Transmission/Turbidity

The autoxidation was also monitored by measuring the solubility of the oxidized emulsion in acetone as described by Gooch *et al.* [6]. 70 μL of the emulsion was dissolved in 1.0 mL of reagent grade acetone (maximum solubility of oil in acetone-water mixture). The transmission was measured at 509 nm using a Shimadzu UV 160-A spectrophotometer.

Absorption

At the starting point of the autoxidation reaction ($t = 0$), the oil emulsion does not contain carbon-carbon conjugated double bonds. However, during the autoxidation process the number of conjugated double bonds increases (see Figure 2.1). The amount of conjugated double bonds was determined by measurement of ultraviolet (UV) absorption at 234 nm [30]. To determine the absorption, 1 μL of emulsion was dissolved in 1 mL of tetrahydrofuran, a good solvent for vegetable oil emulsions. The absorption was measured using a

Shimadzu UV 160-A spectrophotometer. The concentration of conjugated double bonds was averaged from three separate measurements.

pH

The pH of the samples taken from the autoclave was measured using an AcQmat pH3000.

Viscosity

The viscosity of the oil at different HPVs was determined using a 'Cannon-Fenske Capillary' (Schott Geräte) with 'Viscositätsmessgerät AVS' (Schott Geräte), 'Durchsicht Thermostat CT 1250/6' (Schott Geräte) and 'Durchflusskühler CK100' (Schott Geräte). To determine the viscosity of the oxidized SFO emulsion the emulsion was coagulated by dropwise addition of a silver nitrate solution. THF was added to the coagulated emulsion and the oil was separated from the water phase. After concentration of the oil by rotary evaporation the viscosity was determined. All viscosity measurements were carried out at 25 °C.

Particle Size Analysis

Particle size analysis was performed by dynamic light scattering (DLS) and by Transmission Electron Microscopy (TEM). Prior to measurement by DLS the sample was diluted 100-500 times with water to obtain the desired translucence. DLS was measured at 90° angle using a Malvern 4700 System equipped with a Malvern RR98, a Malvern PSC7 Stepper motor controller & photomultiplier and Malvern Series 7032 Multi-8 Correlator. The Z-average particle size and the polydispersity of the emulsions were determined using the cumulant method [41, 42]. For analysis by TEM the sample was diluted with water (1000 x) and the sample was stained for 30 minutes in osmium tetroxide vapor. TEM analysis was performed using a Philips EM400, STEM system PW6585.

Size Exclusion Chromatography (SEC)

Size exclusion chromatography was carried out using three linearly placed columns: 300 mm x 7.5 mm Plgel (Polymer Laboratories), 10³ and 10² Å

(Chrompack) and a mobile phase of tetrahydrofuran (stabilized with BHT, degassed with a Viscotek D6 700) at 1 mL/min (Waters 510 Pump). The system was calibrated using polystyrene standards (Polymer Laboratories). The injection volume was 50 μ L (Waters 712 Injector) and detection was accomplished by refractive index using a Waters 410 differential refractometer.

2.4 Results and Discussion

2.4.1 Oxidation of Oil Emulsions

2.4.1.1 Emulsification of Vegetable Oils

Emulsification of the sunflower oil in the water phase was carried out by ultrasonification followed by high-pressure homogenization using SDS as surfactant. It was observed that ultrasonification alone did not result in stable emulsions. Within several hours after ultrasonification phase separation was observed. Most probably, the viscosity of the sunflower oil was too high for ultrasonification to result in an emulsion with a sufficiently small particle size (see Figure 2.3). However, ultrasonification followed by high-pressure homogenization resulted in emulsions with an average particle size of ~150 nm after 5 minutes. After 5 minutes of homogenization no further reduction of the particle size and particle size distribution was observed. During homogenization the temperature of the emulsion increased to approx. 40 °C (5 minutes homogenization). Longer homogenization times resulted in higher temperatures. The increase in temperature during homogenization is the result of energy dissipation as described by Walstra [8]. The development of the particle size and particle size distribution during homogenization is presented in Figure 2.3. The average particle size, as determined by Transmission Electron Microscopy, was in correspondence with the particle size as determined by DLS.

The stability of the SFO emulsion was tested by following the average particle size and the particle size distribution in time at 60 °C. Generally this test is performed at 50 °C. However, since at a later stage the emulsions were exposed to higher temperatures (up to 75 °C) for short periods of time, the test was carried out at 60 °C. Over a period of four weeks no change in particle size and particle size distribution (measured by DLS) was observed. Also, sedimentation

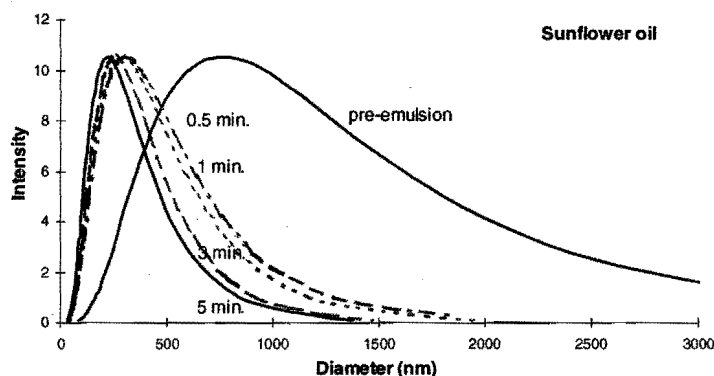


Figure 2.3. Development of particle size distribution during emulsification. Pre-emulsion was prepared by ultrasonification. Final emulsions were made via homogenization after ultrasonification.

and coagulation were not observed. These observations are in contrast with those of Dekker [43], who observed sedimentation and coagulation of alkyd emulsions within 7 days at 50 °C. Dekker argued that this was the result of the limited lifetime of SDS at higher temperatures (due to hydrolysis of the SDS). The different stability observed in our research indicates that hydrolysis of SDS, if any, must occur to a limited extent only. A possible explanation for this could be the difference in chemical structure between an alkyd resin and a triglyceride; alkyd resins contain hydroxyl and carboxylic acid groups that might catalyze hydrolysis. In addition, the particle size in our system was smaller, which increases the emulsion stability. Finally, it was concluded that stable emulsions of sunflower oil can be obtained by using the process of emulsification described above with the use of SDS as surfactant.

2.4.1.2 High Pressure Oxidation of Vegetable Oil Emulsions

Analogous to the research described by Gooch *et al.* [4-6] the effect of temperature, oxygen pressure and metal catalysis on the oxidation of emulsions of sunflower oil was studied. The extent of oxidation was studied by monitoring the hydroperoxide value, the solubility of the emulsion in acetone, the pH of the emulsion and the formation of conjugated double bonds.

Effect of Temperature

In the research performed by Gooch *et al.* [4-6] it was observed that the rate of autoxidative cross-linking was related to the temperature. At temperatures below 50 °C the time to reach 10% transmittance in acetone (the parameter used by Gooch to measure the cross-linking) was reported to increase strongly with decreasing temperature.

The results of the oxidation of sunflower-oil emulsions at 55 and 80 °C at an oxygen pressure of 5 bar are shown in Figure 2.1a-d. Figure 2.1a shows the effect of the temperature on the formation of hydroperoxides. The rate of hydroperoxide formation at 80 °C was higher than that at 55 °C. Both HPV curves of oxidation at 55 and 80 °C showed an increase of HPV in time followed by a decrease. The HPV increases as a result of autoxidation (first stage of autoxidative drying, Section 2.2). When the HPV starts to decrease the rate of decomposition of hydroperoxides (second stage) is higher than the rate of formation. The sharpness and the location of the maximum in the HPV curves in Figure 2.1a indicates that the rate of hydroperoxide formation and decomposition was higher at 80 °C. In addition, at 80 °C the induction period (period of low HPV prior to increase) was shorter. The occurrence of an induction time in the formation of hydroperoxides has been observed previously during the bulk oxidation of vegetable oils. This is generally attributed to the presence of natural antioxidants in the sunflower oil [26,30,40]. More severe cleaning of the sunflower oil prior to emulsification and oxidation, e.g. by additional filtration over florisil and silica gel columns, did not result in shorter induction times. The maximum hydroperoxide value that was reached at the two different temperatures was approximately similar, *i.e.*, about 500 $\mu\text{mole O} / 2 \text{ kg of oil}$. In Figure 2.1b a sharp drop in transmission was observed after approx. 14 hours for oxidation at 80 °C and after approx. 58 hours for oxidation at 55 °C, respectively. The drop in transmission indicates the formation of cross-linked product that is insoluble in acetone. When comparing the drop in transmission in Figure 2.1b with the HPV level at that moment in time in Figure 2.1a it is clear that this coincides with the decrease in HPV. These results indicate that during autoxidation in emulsion the two stages of autoxidative drying (Section 2.2) both occur committantly. Initially, hydroperoxides are formed up to a certain level and no cross-linking takes place. Subsequently, the hydroperoxides start to decompose and cross-linked product is formed.

The relation between the formation of hydroperoxides and their decomposition was also analyzed by measuring the viscosity of the oil at various times

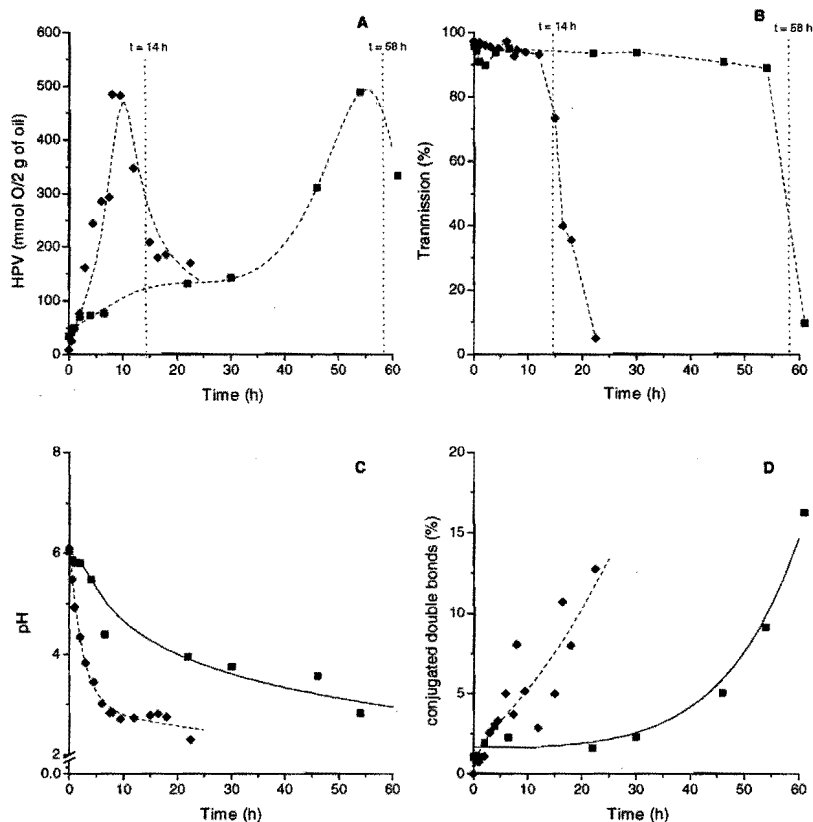


Figure 2.1. Effect of temperature on the oxidation of a sunflower oil emulsion (30 % w/w of oil) in time at 5 bar oxygen pressure, (A) HPV, (B) transmission, (C) pH and (D) conjugated bonds: 55 °C (—■—), 80 °C (---◆---).

during the oxidation. Because of experimental difficulties this analysis was performed during a separate oxidation at 50 °C. The HPV of the oxidation of a sunflower oil emulsion at 5 bar at 50 °C is shown in Figure 2.2a. The transmittance of the emulsion and the viscosity of the oil are presented in Figure 2.2b. After 66 h, a sharp drop in transmittance was observed. Also, at this moment an increase in the viscosity of the oil was observed while the HPV started to decrease at the same time. These results confirm the hypothesis that during oxidation in emulsion initially only hydroperoxides are formed. After a

certain HPV is reached the hydroperoxides start to decompose and cross-linked product is formed.

Figure 2.1c shows that during oxidation the pH decreased to a value of about 2.5. At 85 °C the decrease was stronger than at 55 °C. The decrease in pH could be the result of the formation of hydroperoxides or hydrolysis of the triglycerides [44]. More likely, the decrease in pH was caused by hydrolysis of the SDS. However, coagulation or sedimentation of the emulsion during oxidation at 85 °C was not observed. This indicates that the emulsions were still sufficiently stabilized.

Figure 2.1d shows the percentage of conjugated carbon-carbon double bonds during oxidation. At 55 °C the percentage of conjugated double bonds remained low until about 30 h and then started to increase. At 80 °C an increase was observed right from the start. As described in Section 2.2, the formation of fatty-acid hydroperoxides is accompanied by the formation of carbon-carbon conjugated double bonds (in the case of linoleic acid or linolenic acid). This explains the induction period observed at 55 °C and the strong increase at 85 °C. However, it was observed that after the HPV started to decrease, the percentage of conjugated double bonds kept increasing. This indicates that during hydroperoxide decomposition a different mechanism was responsible for the

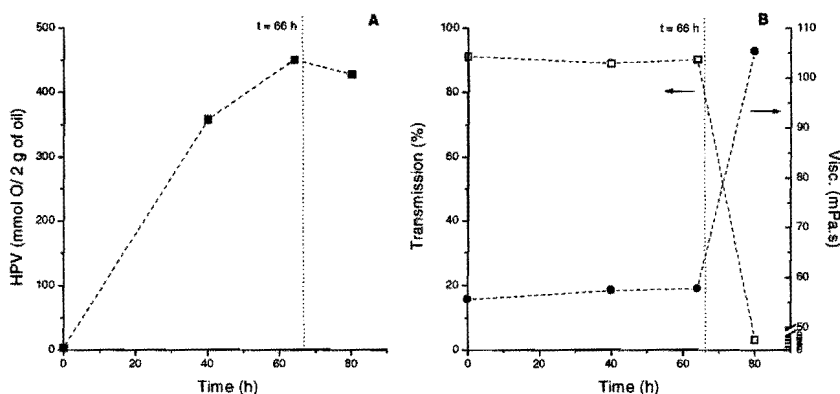


Figure 2.2. High-pressure oxidation of emulsion of sunflower oil at 50 °C at 5 bar oxygen pressure. Development of hydroperoxide value in time (A) and development of transmittance and viscosity of oil in time (B).

formation of conjugated double bonds. A possible explanation for the observed continuing increase in the percentage of conjugated double bonds could be that isomerization of nonconjugated linoleic fatty acid chains occurred, as represented schematically in Figure 2.3.

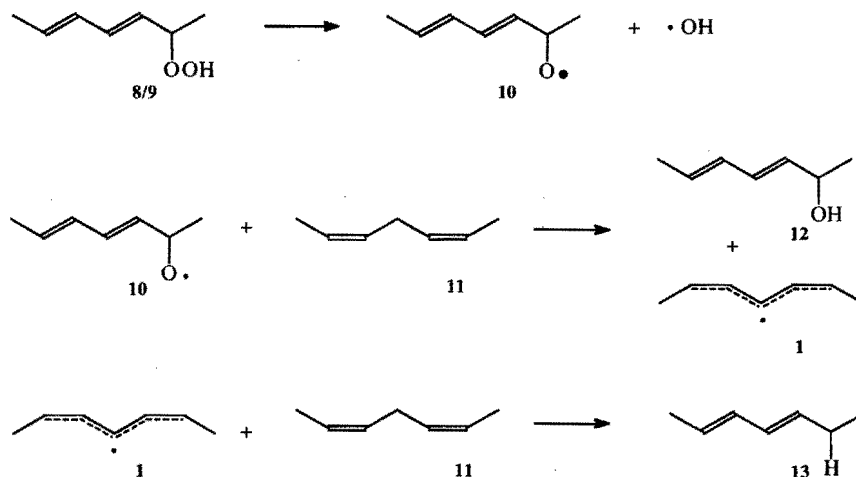


Figure 2.3. Schematic representation of proposed formation of conjugated double bonds by isomerization during decomposition of fatty-acid hydroperoxides.

Decomposition of hydroperoxides 8 or 9 results in the formation of alkoxyradical 10. Proton abstraction from 11 will result in the formation of alcohol 12 and penta-dienyl radical 1, which can form 13 by proton abstraction from 11. Alcohol 12 contains the original conjugated structure of the hydroperoxide. The conjugated structure of compound 13 is additionally formed by this mechanism.

Effect of Oxygen Pressure.

The effect of oxygen pressure on the oxidation of a sunflower-oil emulsion was studied at 5, 6.5 and 10 bar. A temperature of 55 °C was used during oxidation because at this temperature the reaction time, defined as the time needed for the formation of a sufficient concentration of hydroperoxides (HPV 400–800), was acceptable, and the chance of hydroperoxide decomposition was considered to be limited. The results of the oxidation of sunflower-oil emulsions at 5, 6.5 and 10 bar oxygen pressure are presented in Figure 2.1a-d.

Figure 2.1a showed that higher partial oxygen pressure resulted in higher maximum hydroperoxide levels. A direct correlation between the oxygen pressure and the rate of hydroperoxide formation was not observed. By contrast, Gooch *et al.* [4] did observe a decrease in time until the onset of cross-linking by a factor of 2, when increasing the oxygen pressure from 5 to 6.5 bar. However, their oxidation reactions were performed in a stainless steel reactor, where metal ions liberated from the reactor wall could have catalyzed the decomposition of hydroperoxides (see below). The shape of the HPV-curves presented in Figure 2.1a is similar to the curves observed at different temperatures (Figure 2.1a),

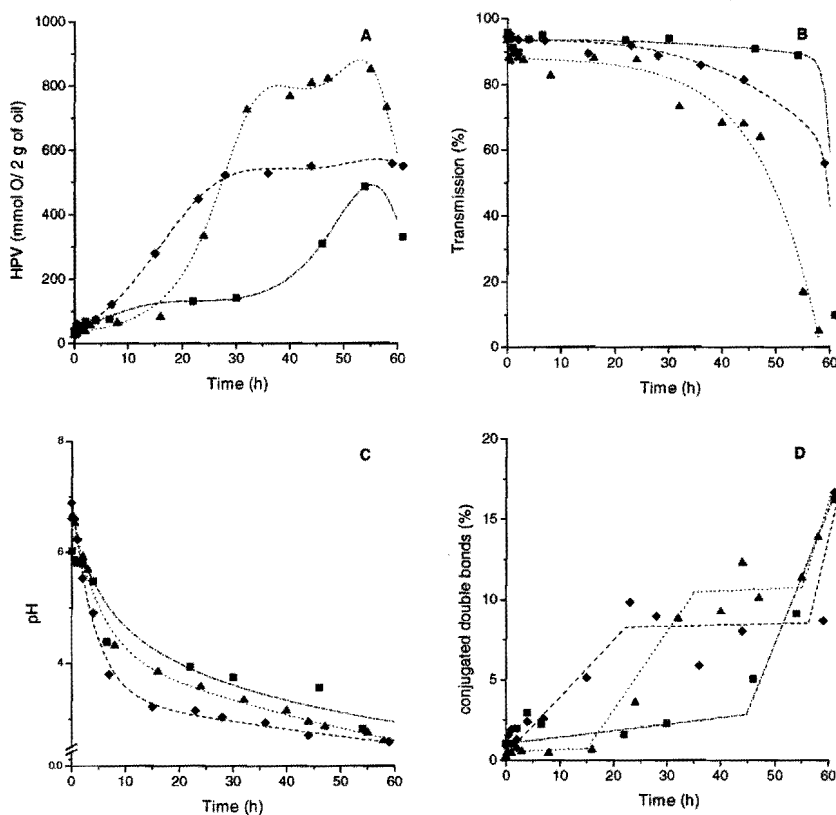


Figure 2.1. Effect of oxygen pressure on the oxidation of sunflower-oil emulsions in time at 55 °C, (A) HPV, (B) transmission in acetone, (C) pH and (D) conjugated bonds: 5 bar (---■---), 6.5 bar (--◆--), 10 bar (---▲---).

showing first an increase in HPV followed by a decrease. However, it seems that at higher oxygen pressures (6.5 and 10 bar) a plateau HPV level is reached instead of a short maximum as observed at 5 bar. A plateau of the percentage of conjugated double bonds was also found for the oxidations performed at 6.5 bar and 10 bar (Figure 2.1d). The presence of this plateau value might indicate that oxidation (no hydroperoxide formation and also no decomposition) stopped when a certain level of HPV was reached. After a stationary period of time (about 25 h. for both 6.5 and 10 bar) the HPV started to decrease. Concurrently, the percentage of conjugated double bonds was increased, indicating that due to hydroperoxide decomposition, isomerization resulting in conjugated bonds started to take place.

The results of the transmission measurements presented in Figure 2.1b, showed that the sharpness of the decrease was less pronounced for the oxidations at 6.5 and 10 bar. The drop in transmission started after approximately 30 h for both oxidations. After this time the transmission decreased slowly until about 50 h, then the transmission dropped more sharply. At the same moment (approx. 50 h) the HPV started to decrease (both for 6.5 and 10 bar). The decrease in transmission after the HPV has started to drop is indicative of the formation of high molecular weight product.

The pH of the emulsions, presented in Figure 2.1c, decreased to a value of about 2.5 during the oxidations. The decrease was stronger at higher oxygen pressure. In conclusion; it appears from Figure 2.1a that the maximum concentration of hydroperoxides that can be formed is dependent on the applied oxygen pressure. Once this value is reached, no further increase in hydroperoxide concentration occurs.

Effect of Metal Catalysis

As described in the previous section (Chapter 2.1), ions from transition metals, like Co, Fe and Mn, can act as catalyst for the decomposition of hydroperoxides. This was also observed by Gooch *et al.* who found that addition of 0.02 % of cobalt naphthenate or 0.02 % of zirconium naphthenate (w/w of alkyd) reduced the reaction time required to cross-link the emulsions to a swelling ratio of 3.7 (swelling ratio defined as the volume ratio of swollen to unswollen polymer [6]) by about two hours. Higher concentrations of transition metal resulted in uncontrollable cross-linking. The object of our study was the formation of emulsions of vegetable oil with a pre-determined concentration of fatty-acid hydroperoxide groups, while keeping the effect of cross-linking limited. Since the

metal ions can act as a catalyst for the decomposition of hydroperoxides, it was expected that the addition of transition metal ions would not be beneficial. Nonetheless, the effect was studied because of the strong effect observed by Gooch *et al.* [4-6].

The results on the oxidation of sunflower oil emulsions at 5 bar at 55 °C with Fe and different concentrations of Co present are shown in Figure 2.1a-d. In Figure 2.1a it was observed that no hydroperoxides are formed at a low concentration of Co ions (0.05 % w/w of oil) and Fe ions. A high concentration of Co ions (0.1 % w/w of oil) resulted in the build up of hydroperoxides after a long period (60 h).

Figure 2.1b showed that the addition of Fe ions resulted in decreased time of reaction to form cross-linked product. Addition of Co ions on the other hand seemed to increase the reaction time. Also, it was observed that the addition of Co ions resulted in an induction period before the decrease in pH started (Figure 2.1c).

From these observations it was concluded that a very complex situation is created with the addition of transition metal catalyst. The presence of Fe ions gives similar results as observed by Gooch *et al.* [4-6], *i.e.*, a decrease in time to form cross-linked products. However, it appeared that the Co ions acted as an inhibitor for the oxidation of sunflower oil in emulsion. A possible explanation for these observations could be found in the distribution of the catalyst between the aqueous phase and the oil phase.

Ösberg *et al.* [45] showed that at pH = 7 most of the Co-catalyst (Co-octanoate) is in the oil phase, while at pH = 3 it's predominantly in the water phase. The distribution of the catalyst between the oil- and aqueous phases was also affected by the surfactant used. During oxidation the pH in our system changed from pH = 7 to pH = 2.5. Therefore, it seems likely that in the beginning of the oxidation the Co is located predominantly in the oil phase of the sunflower oil emulsion, while during the reaction a redistribution of the Co ions towards the aqueous phase occurred. By contrast the Fe ions would have been present in the aqueous phase from the beginning.

From these experiments it was concluded that for our research the presence of metal ions during the oxidation of emulsions at high partial oxygen pressure should be avoided.

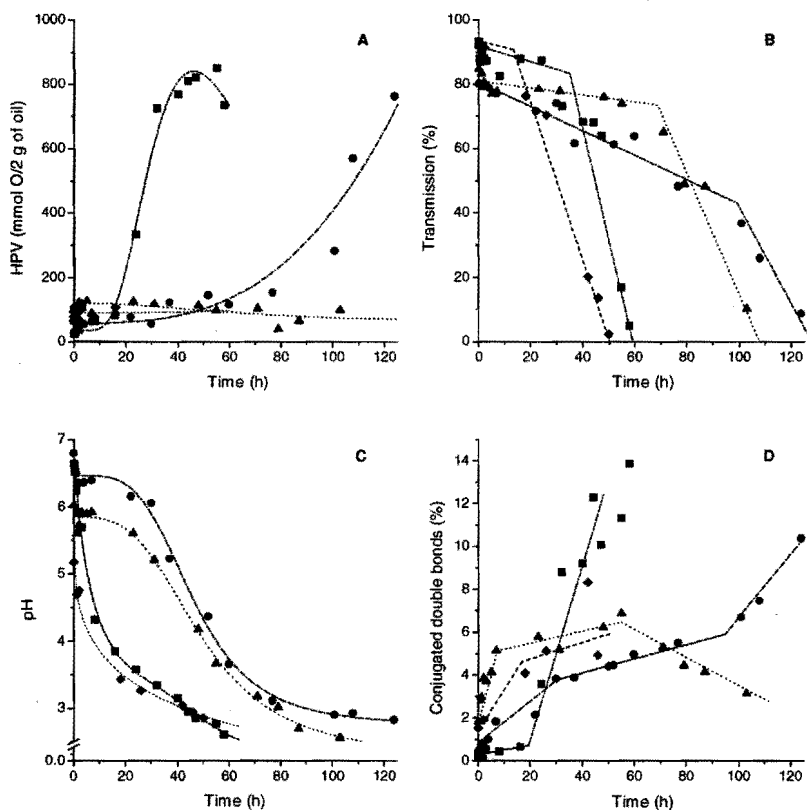


Figure 2.1. Effect of the presence of transition metal ions on the oxidation of sunflower oil emulsions (30 % w/w of oil) in time at 55 °C and 5 bar oxygen pressure, (A) HPV, (B) transmission, (C) pH and (D) conjugated bonds: no catalyst (---■---), Fe (---◆---), Co 0.05 % w/w of oil (---▲---), Co 0.1 % w/w of oil (---●---).

2.4.2 Bulk Oxidation of Sunflower Oil

Emulsions of hydroperoxide-modified vegetable oils can also be prepared by bulk oxidation of the vegetable oil followed by emulsification. In this section results on the effect of temperature on the oxidation of sunflower oil are discussed. For reasons described in the previous section the effect of metal catalysis in bulk oxidation was not studied. The oxidation reactions were

performed in a round-bottomed flask covered with aluminum foil in order to exclude photosensitized oxidation.

Figure 2.2a and Figure 2.2b shows the development of the hydroperoxide value and the viscosity of sunflower oil oxidized at various temperatures. Figure 2.2a shows that at low temperatures (25 °C) the rate of hydroperoxide formation was very slow. After 160 h a HPV of 40 $\mu\text{mol O}_2/\text{kg}$ of sunflower oil was obtained. At higher temperatures the rate of hydroperoxide formation increased. When the oxidation was performed above approx. 75 °C the rate of hydroperoxide formation was very high. However, the early maximum value of HPV in Figure 2.2a and the strong increase in viscosity in Figure 2.2b showed that the fatty-acid hydroperoxides were sensitive towards decomposition at that temperature. From these observations it was concluded that the aimed HPV with low viscosity could best be prepared by bulk oxidation at 50-75 °C. Using these temperatures HPVs up to 1300 $\mu\text{mol O}_2/\text{kg}$ of oil could be obtained.

An indication for the formation of cross-linked product during oxidation was obtained by measuring the viscosity of the oxidized sunflower oil. A more accurate analysis of oxidized sunflower oil (HPV = 580) by GPC showed that a limited amount of dimeric, trimeric, or oligomeric, product was formed when sunflower oil was oxidized at 50 °C (see Figure 2.3, dimer formation

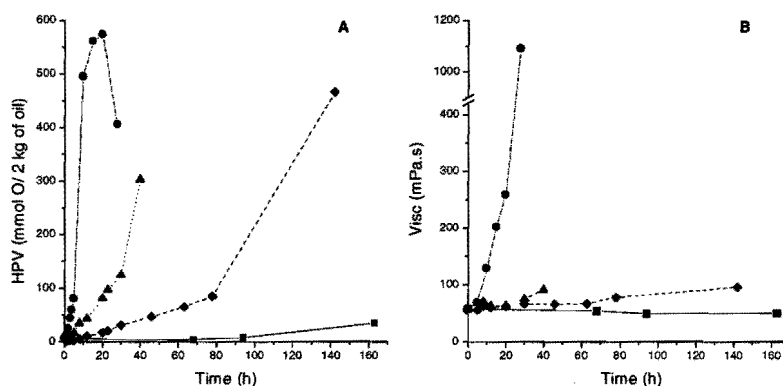


Figure 2.2. Oxidation of sunflower oil in time at different temperatures, (A) hydroperoxide value and (B) viscosity: bulk oxidation at 25 °C (—■—), 55 °C (—◆—), 75 °C (—▲—) and 100 °C (—●—).

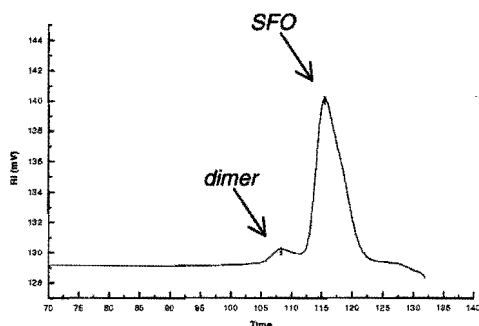


Figure 2.3. GPC-graph of oxidized sunflower oil, HPV = 580. SFO, retention time = 116 min; dimer retention time = 108 min.

below 3 %). This result is confirmed by the observations of Neff *et al.* [16] for the oxidation of glyceryl trislinoleate. Neff *et al.* found no evidence of dimer or oligomer formation in samples of highly oxidized trilinolein (HPV 2950 $\mu\text{mole O}_2/\text{kg}$ of oil). It was argued by the authors that dimerization was not observed because further intramolecular oxidation of mono-hydroperoxides to *bis*- and *tris*-hydroperoxides was more favorable than intermolecular condensation to form dimers. Analysis of the possible formation of *bis*- and *tris*-hydroperoxides during bulk oxidation was beyond the aim of the present study.

The stability of the formed hydroperoxides upon storage and during emulsification was investigated. Hydroperoxide value and viscosity of oxidized sunflower oil showed no change upon storage at 5 °C during a period of 4 weeks. Storage at 20 °C showed a small decrease in HPV (from HPV = 413 to HPV = 406) and an increase in viscosity (from $\eta = 301 \text{ mPa}\cdot\text{s}^{-1}$ to $\eta = 370 \text{ mPa}\cdot\text{s}^{-1}$). This indicated that oxidized sunflower-oil emulsions could best to be stored at 5 °C (or below).

The stability of hydroperoxides during emulsification was also investigated. Emulsions from sunflower oils with different hydroperoxide values were formed using ultrasonification followed by high-pressure homogenization. During emulsification a large part of the energy supplied to the system is dissipated as heat [8]. It might be expected that this could result in the decomposition of a small amount of hydroperoxides, in turn resulting in a decrease in HPV. However, it was observed that emulsification of oxidized sunflower oils (HPV's varying between 200 and 1300 $\mu\text{mole O}_2/\text{kg}$ of oil) did not result in a detectable decrease in HPV. The emulsions formed by ultrasonification followed by high-

pressure homogenization showed similar particle size and particle size distributions as non-oxidized sunflower-oil emulsions (see Section 2.4.1.1).

2.5 Conclusions

The research presented in this chapter shows that two methods can be used for the preparation of emulsions of vegetable oils modified with fatty-acid hydroperoxides. The first method involves emulsification of sunflower oil followed by oxidation in emulsion at high partial oxygen pressure. Stable emulsions with average particle size of about 150 nm can be formed using ultrasonification followed by high-pressure homogenization. The formation and decomposition of hydroperoxides during oxidation of sunflower oil emulsions at high partial oxygen pressure is related to the oxygen pressure applied and the temperature. The presence of metal ions should be avoided. Optimal conditions for the formation of emulsions with HPVs varying between 400 and 800 $\mu\text{mole O}_2/\text{kg}$ of oil, while maintaining a low degree of cross-linking, are 50-60 °C as reaction temperature and an oxygen pressure of about 10 bar.

The second method that was applied involved bulk oxidation of sunflower oil followed by emulsification. An oxidation temperature of 50 °C was found to result in the formation of high HPV levels, up to 1300 $\mu\text{mole O}_2/\text{kg}$ of oil, while maintaining a low degree of cross-linking. Emulsification by ultrasonification followed by homogenization and/or ageing at 5 °C does not result in a decrease in the HPV.

When comparing the two methods, it is concluded that the first method results in a faster formation of hydroperoxides. However, the second method results in higher HPVs and allows for the addition of other components, *i.e.*, alkyd resin and monomer, prior to emulsification. When using the first method, polymerizations need to be carried out using the oxidized emulsion as a seed. For each polymerization with different oil or alkyd composition a new seed will need to be made. When using the second method emulsions with different compositions of oil, alkyd and acrylic can be prepared from a single batch of oxidized oil. Because of the latter reason the second method will be used in the following chapters of this thesis.

2.6 References

1. W. Lühs, W. Friedt, "Designer Oil Crops", VCH Publishers, Weinheim, (1994) 73.
2. Z.W. Wicks, F.N. Jones, S.P. Pappas, "Organic Coatings: Science and Technology", Wiley, New York, Vol. 1, (1992) 133.
3. M.W. Formo (Ed.), "Bailey's Industrial Oil and Fat Products", Wiley, New York, Vol. 1, (1979) 177, 687; Vol. 2, (1982) 343.
4. J.W. Gooch, G.C. Wildman, B.G. Bufkin, *J. Coat. Tech.*, 56 (711), (1984) 33.
5. J.W. Gooch, G. Bufkin, G.C. Wildman, *U.S. Patent 4,419,139*, (1982)
6. J.W. Gooch, Ph.D. Dissertation, University of Southern Mississippi, (1980).
7. T. Nabuurs, "Alkyd-Acrylic Composite Emulsions. Polymerization and Morphology", Ph.D. Dissertation, Eindhoven University of Technology (1997).
8. P. Walstra, *Chem. Eng. Sci.*, 48 (2), (1993) 333.
9. G. Östberg, B. Bergenståhl, M. Huiden, *J. Coat. Tech.* 66 (832), (1994) 37.
10. J.P.E. Beurde, "Initiatorinbouw in Alkyd ten behoeve van Graft-hybriden", Graduation Report, Eindhoven University of Technology (1994).
11. H.W. Chan, G. Levett, J.A. Matthew, *Chem. Phys. Lip.*, 24, (1979) 245.
12. E.N. Frankel, W.E. Neff, E. Selke, D. Weisleder, *Lipids*, 17 (1), (1982) 11.
13. W.J. Muizebelt, J.C. Hubert, R.A.M. Venderbosch, *Prog. Org. Coat.*, 24, (1994) 263.
14. W.J. Muizebelt, J.J. Donkerbroek, M.W.F. Nielen, J.B. Hussem, M.E.F. Biemond, R.P. Klaasen, K.H. Zabel, *J. Coat. Tech.*, 70 (876), (1998) 83.
15. W.J. Muizebelt, M.W.F. Nielen, *J. Mass Spec.*, 31, (1996) 545.
16. W.E. Neff, E.N. Frankel, K. Miyashita, *Lipids*, 25 (1), (1990) 33.
17. S. Huang, E.N. Frankel, J.B. German, *J. Agric. Food Chem.*, 43, (1995) 2345.
18. S. Huang, A. Hopia, K. Schwarz, E.N. Frankel, J.B. German, *J. Agric. Food Chem.*, 44, (1996) 444.
19. R. Yamauchi, N. Miyake, K. Kato, Y. Ueno, *Lipids*, 28 (3), (1993) 201.
20. C.C. Whittern, E.E. Miller, D.E. Prat, *J. Am. Oil Chem. Soc.*, 61 (6), (1984) 1075.
21. A. Kamal-Eldin, L-Å. Appelqvist, *Lipids*, 31 (7), (1996) 671.
22. K.E. Peers, D.T. Coxon, *Chem. Phys. Lip.*, 32, (1983) 49.
23. R.S. Farag, S.A. Osman, S.A.S. Hallabo, A.A. Nasr, *J. Am. Oil Chem. Soc.*, 55, (1978) 703.
24. C.F. Hendriks, P.M. Heertjes, H.C.A. van Beek, *Ind. Eng. Prod. Res. Dev.*, 18 (3), (1979) 216.
25. W.A. Waters, *J. Am. Oil Chem. Soc.*, 48, (1971) 427.
26. J.P. Cosgrove, D.F. Church, W.A. Pryor, *Lipids*, 22 (5), (1987) 299.
27. J.L. Courtneidge, *J. Chem. Soc., Chem. Commun.*, (1992) 1270.
28. J.L. Courtneidge, M. Bush, *J. Chem. Soc., Perkin Trans. I*, 1, (1992) 1531.

29. K. Mukai, K. Sawada, Y. Kohno, J. Terao, *Lipids*, 28 (8), (1993) 747.
30. J. Cillard, P. Cillard, M. Cormier *J. Am. Oil Chem. Soc.*, 57 (8), (1980) 255.
31. N.A. Porter, S.E. Caldwell, K.A. Mills, *Lipids*, 30 (4), (1995) 277.
32. E.M.S. van Hamersveld, Chapter 1 of this thesis, Table 1.1.
33. R.A. Hancock, N.J. Leeves. *Prog. Org. Coat.*, 17, (1989) 321.
34. K. Miyashita, K. Kanda, T. Takagi, *J. Am. Oil Chem. Soc.*, 68 (10), (1991) 748.
35. R. Cueto, G.L. Squadrito, W.A. Pryor, in "*Methods in Enzymology*", Vol. 233, Acad. Press, New York, (1994) 174.
36. F. Halsbeck, W. Grosch, J. Firl, *Biochim. Biophys. Acta*, 705, (1983) 185.
37. C.E.H. Bawn, *J. Oil Col. Chem. Soc.*, 26 (398), (1953) 443.
38. G. Minotti, S.D. Aust, *Lipids*, 27 (3), (1992) 219.
39. R. Yamauchi, N. Yamamoto, K. Kato, *Lipids*, 30 (5), (1995) 395.
40. D.K. Park, J. Terao, S. Matsushita, *Agric. Biol. Chem.*, 49 (9), (1981) 2071.
41. R. Pecora, "*Dynamic Light Scattering*", Plenum Press, New York, (1985) 50.
42. R. Finsy, N. de Jeager, R. Sneyers, E. Geladé, *Part. Part. Syst. Character.*, 9, (1992) 125.
43. G.H. Dekker, "*The Preparation and Application of Alkyd Emulsions*", in *Waterborne Coatings and Additives*, 6, (1996) 22.
44. J.J. Engel, in "*Proc. of the 10th Water-Borne and Higher Solids Coatings Symp.*", New Orleans, LA February, (1983) 32.
45. G. Östberg, B. Bergenståhl, K. Sörensen, *J. Coat. Tech.*, 64 (814), (1992) 33.

CHAPTER 3: FATTY-ACID HYDROPEROXIDE-INITIATED MINI-EMULSION POLYMERIZATION OF MMAⁱ

Summary

The use of oxidized triglycerides as initiators for the mini-emulsion polymerization of acrylic monomer is described. Unsaturated triglycerides, as in, e.g., sunflower, were treated with molecular oxygen to generate fatty-acid hydroperoxide groups. Oil-acrylic hybrid latexes were formed using fatty-acid hydroperoxides as initiators for the mini-emulsion polymerization of acrylics in an ROOH/Fe²⁺-EDTA/SFS redox system. The mini-emulsion system was established with *n*-hexadecane as hydrophobe. The kinetics of the mini-emulsion polymerization and the characteristics of the particles were examined. Cryogenic transmission electron microscopy (cryo-TEM) analysis of the hybrid latexes obtained by initiation with the fatty-acid hydroperoxides did not show intraparticle heterogeneity. Initiation by *tert*-butyl hydroperoxide resulted in the formation of heterogeneous particles. This indicates that the use of fatty-acid hydroperoxides resulted in the formation of oil-acrylic copolymer, which acted as a compatibilizer. It is concluded that the use of fatty-acid hydroperoxide-initiated mini-emulsion polymerization provides a promising system of combined alkyd-acrylic properties.

ⁱ This chapter has been published:

E.M.S. van Hamersveld, J.J.G.S. van Es and F.P. Cuperus, *Colloids and Surf. A*, 151 (1-3), (1999) 285.

3.1 Introduction

The development of a waterborne coating system which combines the positive properties of oils or alkyd resins (e.g., autoxidative curing, high gloss and penetration in wood) with the fast drying and color retention of acrylic latexes has been the object of several studies during recent years [1-6]. Generally, it is believed that the positive properties of both systems can best be combined in a homogeneous mixture of the oil, or alkyd, resin and the acrylic polymer. However, such a homogeneous mix is opposed by the incompatibility of the acrylic polymer and the alkyd resin.

In the past several approaches have been used to solve this problem. A detailed description of the different approaches used was presented in Chapter 1 of this thesis. The approaches of Buter [1] and of Weger *et al.* [2,3] were based on the organic synthesis of an alkyd-acrylic copolymer by graft polymerization of acrylic onto conjugated fatty-acids, and by copolymerization of acrylics with fatty-acid-functionalized acrylics, respectively, followed in both cases by synthesis of the alkyd. After synthesis these co-polymers were emulsified. In both cases this resulted in particles with a core-shell structure.

The process of emulsion polymerization was used by Nabuurs [4]. He first formed an alkyd emulsion by homogenization. The alkyd emulsions were used as a 'seed' for the batch- and semi-batch emulsion polymerization of acrylics initiated by a water-soluble initiator. This process of 'alkyd emulsion-seeded' polymerization resulted in the formation of a secondary generation of all-acrylic particles. It was argued that depending on the surfactant, either micellar or homogeneous nucleation occurred. When using build-in surfactant, formation of a secondary generation of all-acrylic particles was not observed. However, phase separation between the oil and the pMMA did still occur. Possibly, the extent of grafting resulting from the polymerization of the acrylic in the presence of the alkyd was not sufficient to compatibilize the two. By initiation from the alkyd it was expected that a higher degree of grafting and more homogeneous particle morphology would be obtained.

The previous studies show that the chance of obtaining homogeneous oil-acrylic hybrid latexes by emulsion polymerization increases when two criteria are met. First, the compatibility of the oil, or alkyd, resin and the acrylic polymer has to be increased. Second, the nucleation process has to be controlled.

It is well established [7-11] that in mini-emulsion polymerization the main loci of nucleation are the sub-micron monomer droplets. A mini-emulsion is formed by using a mixed surfactant system (ionic surfactant and non-ionic hydrophobe or

co-surfactant) and high shear. Higuchi and Misra [12] have shown that diffusion of the monomer (Ostwald ripening) is retarded by the addition of the hydrophobe (or co-surfactant), a compound with low water solubility. Cetyl alcohol and hexadecane have often been used as hydrophobes and, more recently, Miller *et al.* [13-15] introduced the additional use of a small amount of polymer beside to the hydrophobe. Homogeneous nucleation can further be reduced by using an oil-soluble initiator [9] and redox initiation [16]. Recently, Wang *et al.* [6] have reported the mini-emulsion polymerization of acrylics in the presence of an alkyd resin. The stability of the mini-emulsion using pMMA as hydrophobe compared to a macro-emulsion was described. Initiation of the mini-emulsion by sodium persulfate resulted in the formation of alkyd-acrylic hybrid latex. However, the morphology of the resulting alkyd-acrylic hybrid latex was not discussed.

In this chapter the results of mini-emulsion polymerization of MMA in the presence of partly oxidized sunflower oil are described. The hydroperoxide groups of the sunflower oil were used as oil-soluble initiator in a fatty-acid hydroperoxide/ Fe^{2+} /ethylenediaminetetraacetic acid/sodium formaldehyde sulfoxylate (SFO-HP/ Fe^{2+} -EDTA/SFS) redox initiation system. The use of fatty-acid hydroperoxide as oil-soluble initiator is intended to result in the formation of sunflower oil-poly(methyl methacrylate) block copolymers, which could then act as compatibilizer in the oil-acrylic hybrid particles. The kinetics of the SFO-HP/ Fe^{2+} -EDTA/SFS-initiated mini-emulsion polymerization of MMA in the presence of sunflower oil has been investigated. The effect of using fatty-acid hydroperoxides as initiating groups on the particle morphology is compared with the morphology of particles resulting from a *tert*-butyl hydroperoxide-initiated mini-emulsion polymerization.

3.2 Experimental

3.2.1 Materials

Sunflower oil (SFO, Rhenus B.V., The Netherlands) was purified by filtration over a florisil (Merck) column. Sodium dodecyl sulfate (SDS: Fluka BioChemica, very pure), ethylene diaminetetraacetic acid disodium salt (EDTA: Merck), sodium formaldehyde sulfoxylate (SFS: Merck), sodium hydrogencarbonate (Boom B.V.), ferrous sulfate (Merck), hexadecane (HD: Merck), *tert*-butyl hydroperoxide (*t*-BHP, 70%, Merck) and hydroquinone (Aldrich) were used as supplied.

The monomer methyl methacrylate (MMA: Merck), inhibited with 100 - 200 ppm of hydroquinone, was purified by filtration over an inhibitor removal column (Aldrich). Reagent grade water was obtained using a Waters Millipore purifying system.

3.2.2 Sunflower Oil Oxidation

The oxidation of sunflower oil was performed as described in the previous chapter [17].

3.2.3 Mini-Emulsion Preparation and Polymerization

The general recipe for the mini-emulsion polymerizations is shown in Table 3.1. The oil (oxidized SFO-HP with a known HPV or non-oxidized SFO) was mixed with the monomer and the hydrophobe. An emulsion was created by dispersing the oil-monomer solution into an SDS-water solution. The emulsion was sonicated (Branson Sonifier 250, 70% duty cycle) for 2 minutes while cooling in a water bath and subsequently passed through a high-pressure homogenizer (NS 1001-Panda, Niro-Soavi) for five recycle passes. The homogenizer was operated with the primary stage emulsification valve at 50 bar and a second stage homogenization valve at 500 bar.

The mini-emulsion was transferred into a 250-mL four-necked glass reactor that was equipped with a condenser plus nitrogen outlet, a nitrogen inlet tube, a thermometer and a mechanical stirrer. A concentrated solution of SFS was added and the system was purged with nitrogen and heated to 30 °C. A teflon[®]-coated paddle stirrer operating at 200 rev./min provided agitation.

The polymerization was started by the subsequent addition of SFS and complexed Fe^{2+} from concentrated solutions in water ($[\text{SFS}] = 2.5 \text{ M}$, $[\text{Fe}^{2+}] = 25 \text{ mM}$). At intervals, samples were taken for measuring the conversion and for analyzing the particle size of the mini-emulsion. The conversion was measured gravimetrically. The samples were injected into a pre-weighed aluminum dish containing an aqueous 1% (w/w) hydroquinone solution. Before measuring the dry solids content the samples were dried for 24 h at room temperature and for 12 h at 40 °C in vacuum (25 mbar).

Table 3.1. Typical Recipe for Mini-Emulsion Polymerization

| | Amount | Concentration (mM ^a) |
|---|--------------|-------------------------------------|
| H ₂ O (milli Q) | 200 g | |
| Methyl methacrylate (MMA) | 25 g | |
| Sunflower oil (SFO/ SFO-HP) ^b | 25 g | |
| NaHCO ₃ | 0.336 g | 20 |
| Sodium docecy sulfate (SDS) | 0.404 g | 7 |
| Hexadecane (HD) | 0.96 g | 21 |
| FeSO ₄ x 6H ₂ O | 0.014 g | 0.25 |
| EDTA x 2Na | 0.039 g | 0.53 |
| Sodium formaldehyde sulfoxylate | 0.177 g | 7.5 |
| Tert-butyl hydroperoxyde (t-BHP) ^b | 82.1 μ L | 3 |

a) Concentrations based on water

b) In case of initiation by fatty-acid hydroperoxide, oxidized sunflower oil (SFO-HP) was used instead of tert-butyl hydroperoxide

3.2.4 Analysis

Droplet and Particle Size

Particle size analysis was performed by dynamic light scattering using a Malvern Autosizer IIc (Malvern Instruments). The Z-average particle size and the polydispersity of the droplets and particles were determined using the cumulant-method [18,19]. Prior to measurement the sample was diluted 100-500 times with water to obtain the desired translucence. If the conversion was less than 80% a small amount of an aqueous 1% (w/w) hydroquinone solution was added to the latex and residual monomer was removed under vacuum by rotary evaporation. All particle size measurements were obtained at 25 °C.

The morphology of the pre-emulsion and the hybrid particles was examined with cryogenic Transmission Electron Microscopy (TEM) according to procedures described by Frederik *et al.* [20,21].

Molecular Weight

Oligomers and polymers obtained during oxidation and mini-emulsion polymerization were dissolved in THF at a concentration of 0.1 g/mL. The molecular weight was determined using gel permeation chromatography [GPC; Waters; columns: 300 x 7.5 μ gel (Polymer Laboratories), 10^3 and 10^2 Å (Chrompack); calibrated using polystyrene standards (Polymer Laboratories)].

3.3 Results and Discussion

3.3.1 Sunflower Oil Oxidation

The reaction of organic compounds with O_2 is known as autoxidation. The primary product of the autoxidation reaction of unsaturated fatty-acids is a fatty-acid hydroperoxide [22]. During autoxidation the formation of hydroperoxides is followed by decomposition of the hydroperoxide and a complex sequence of radical reactions [23]. A detailed description of the reactions taking place during autoxidation is presented in Chapter 2 of this thesis.

In the present study autoxidation was used to form a limited amount of fatty-acid hydroperoxide groups without cross-link formation in the oil phase. The hydroperoxides thus obtained were used as initiators during the mini-emulsion polymerization. However, the ability of the oil to form a cross-linked structure by autoxidation after application had to be maintained. In practice this meant that only a few percent of the available double bonds could be used for formation of hydroperoxides and that dissociation of the hydroperoxides to form a network had to be avoided. From previous studies on hydroperoxide formation in oil and oil emulsions, it was concluded that hydroperoxide formation can best be performed with molecular oxygen at 50 °C [24]. At this temperature the rate of hydroperoxide formation is slow, but dissociation is avoided.

Oils with HPVs ranging from 200 to 1500 μ mole O/2 kg of oil were synthesized. Different HPVs refer to different concentrations of initiator groups. Hence, oils with different HPVs were used to study the effect of initiator concentration on the rate of polymerization.

3.3.2 Mini-Emulsion Polymerization

3.3.2.1 Monomer Droplet Formation

In the mini-emulsion polymerization of MMA in the presence of sunflower oil mixing was provided by sonification followed by homogenization. The monomer, the hydrophobe (*n*-hexadecane) and the resin were mixed with the surfactant-water solution according to the recipe described in Table 3.1. The mixture was sonificated for 2 minutes and passed through a high-pressure homogenizer, operating at a pressure of 500 bar, for five recycle passes. During homogenization a turbulent flow is generated, which results in the break up of the oil-monomer droplets [26]. The average droplet size of the mini-emulsions after homogenization was approximately 130 nm, as determined by DLS. A typical number-average size distribution of a monomer-oil emulsion after homogenization is shown in Figure 3.1.

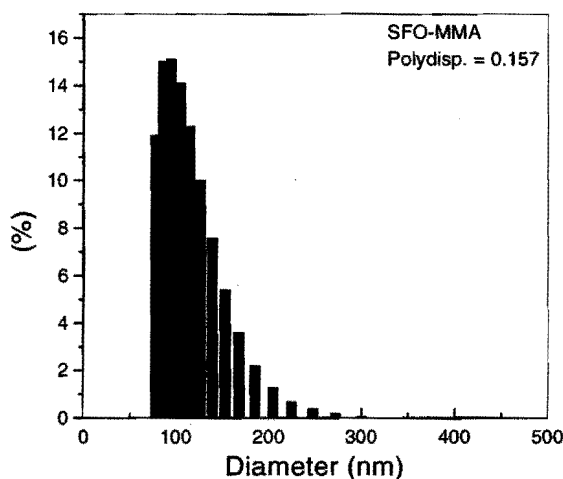


Figure 3.1. Number-average size distribution of SFO-MMA mini-emulsion after homogenization.

A qualitative analysis of the homogeneity and the average particle size of the mini-emulsion droplets prior to polymerization was obtained by cryogenic transmission electron microscopy (cryo-TEM). With the use of cryo-TEM it is possible to analyze particle morphology of monomer-droplets and emulsions without extensive pre-treatment. A thin aqueous film of the emulsion was fixated

by vitrification in liquid ethane and imaged at -170°C . This technique is especially useful when working with monomer-droplets and with emulsions, which contain low molecular weight components such as vegetable oils. For analysis with conventional TEM techniques these emulsions would require extensive chemical fixation by staining and drying. This could result in changes in microstructure. In Figure 3.2 a cryo-TEM image of an oil-acrylic monomer emulsion is presented. The image shows that the mini-emulsion droplets were homogeneous and confirmed the size of the droplets, as measured with DLS. A quantitative analysis of the average droplet size was not made using cryo-TEM images because of the possible occurrence of size segregation in the sample [27].

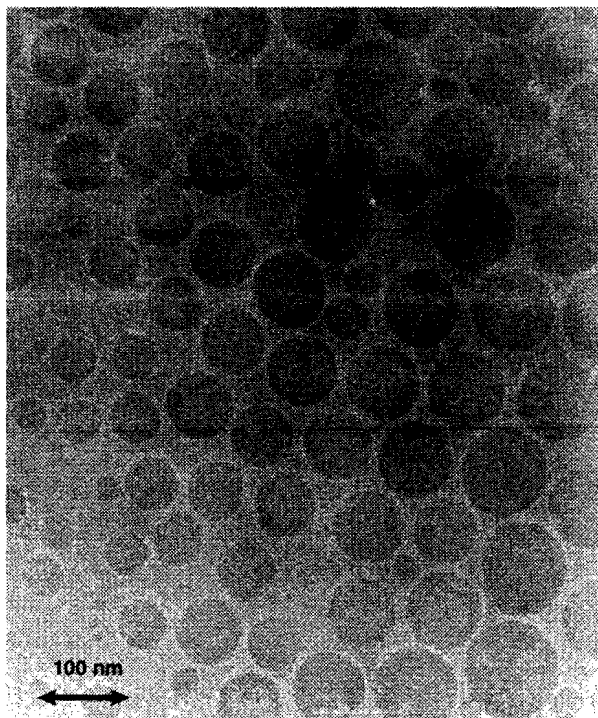


Figure 3.2. Cryo-TEM image of monomer droplets of SFO-HP / MMA mini-emulsion after homogenization (20 % w/w). Standard recipe with HPV = 730 μmole active O/2 kg of oil, ratio SFO-HP : MMA = 50 : 50 w/w.

Using the method reported by Ugelstad *et al.* [7] the relationship between the monomer droplet sizes and the distribution of emulsifier molecules was calculated for our system. Table 3.2 shows that for oil-monomer droplet sizes below 0.7 μm all emulsifier molecules are needed to cover the droplet surface. For the size of monomer-oil droplets obtained after homogenization a surface coverage of 20% was calculated. From these calculations it follows that surfactant has the tendency to be located at the surface of the particles, rather than being molecularly dissolved. Nucleation will therefore mainly take place in the monomer-oil droplets (droplet nucleation).

Table 3.2. Calculated Surface Coverage of Emulsifiers^a

| Average diameter of oil-acrylic droplets (μm) | Number of droplets per cm^3 of $\text{H}_2\text{O} \times 10^{-12}$ | Number of emulsifier molecules per cm^3 of H_2O | | |
|--|--|--|---------------------------------|----------------------|
| | | Droplets $\times 10^{-18}$ | Aqueous phase $\times 10^{-18}$ | Surface Coverage (%) |
| 2 | 0.06 | 1.50 | 2.72 | 100 |
| 1 | 0.48 | 3.00 | 1.22 | 100 |
| 0.7 | 1.39 | 4.28 | - | 98.4 |
| 0.5 | 3.82 | 6 | - | 70.0 |
| 0.2 | 59.97 | 15 | - | 28.1 |
| 0.15 | 141.50 | 20 | - | 21.1 |
| 0.1 | 477.50 | 30 | - | 14.1 |

a) Assumptions: (1) One SDS molecule will occupy an area of 50 \AA^2 of the surface of the droplet, (2) all droplet surface is fully covered with SDS, (3) the amount of monomer dissolved in the aqueous phase is negligible

3.3.2.2 Particle Morphology

The cryo-TEM image shows the monomer-oil droplets before polymerization, and suggests a homogeneous structure. In order to determine the effect of initiation by the triglyceride molecules, the particle morphology of particles resulting from SFO-HP-initiation and from *t*-BHP-initiation were studied. Figure 3.3 shows the images of the cryo-TEM analysis of the particles resulting from *t*-BHP-initiated (Figure 3.3a) and from SFO-HP-initiated (Figure 3.3b) mini-emulsion polymerizations.

Since no specific staining or coloring was used in the cryo-TEM analysis of the particles the contrast between the different phases of the particles is small

(determined by specific interactions between the electron beam and the specimen). However, in Figure 3.3a it can clearly be seen that the *t*-BHP-initiated particles are not homogeneous. The image shows spherical particles that are composed of a dark colored area and a light colored area. Depending on the spatial orientation of the particle the light colored area is located at the side of the particles or in the center. For particles oriented with the light colored area at the side it was observed that the light colored phase was not protruding from the particle but that particles were truly spherical. Therefore, it was concluded that the morphology of these particles could best be described as core-shell. The core, however, was not necessarily located in the center.

In contrast to the results obtained for the *t*-BHP-initiated system, the SFO-HP-initiated system shows no visibly separated domains (Figure 3.3b). These results indicate that initiation by fatty-acid hydroperoxide groups resulted in the formation of particles with a more homogeneous morphology. Initiation by fatty-acid hydroperoxides results in the formation of triglyceride-modified acrylic molecules. During polymerization only a few percent of the triglyceride molecules contain a hydroperoxide group available for initiation [28] and, of these, only a small fraction would be used for initiation. However, the cryo-TEM analysis suggests that the small amount of oil-acrylic co-polymers thus obtained is enough to ensure compatibilization within the oil-acrylic hybrid particles.

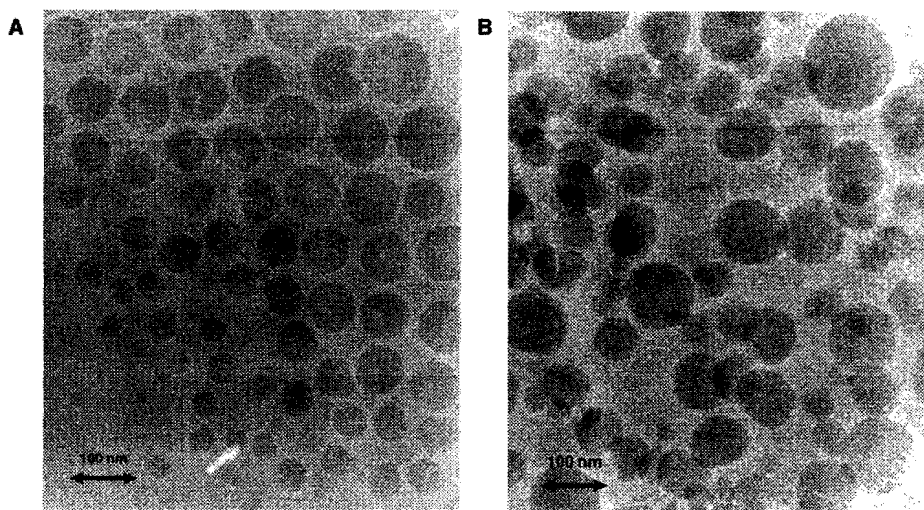


Figure 3.3. (a) Cryo-TEM image of hybrid latex of SFO and pMMA initiated by *t*-BHP. (b) Cryo-TEM image of hybrid latex initiated by fatty-acid hydroperoxides (SFO-HP).

3.3.2.3 Mini-emulsion Polymerization of MMA Initiated by Fatty-Acid Hydroperoxide Groups

The redox initiation system hydroperoxide/sodium formaldehyde-sulfoxylate (SFS)/ EDTA-chelated Fe^{2+} was chosen in this study. It enabled the use of fatty-acid hydroperoxides as initiating groups, resulting in the *in situ* formation of compatibilizing molecules. In the past this redox system has been used in several studies with various hydroperoxides [29-31]. Andersen and Proctor [29] were the first to study the kinetics of this system. Recently, Wang *et al.* [31] published a detailed kinetic study on the mini-emulsion polymerization of styrene initiated by the cumene hydroperoxide/ Fe^{2+} -EDTA/SFS redox system. They described the initiation process as taking place at the interface between the oil and aqueous phases and found that aqueous phase nucleation was reduced by using an oil-soluble hydroperoxide initiator.

In this study the effect of the polymerization temperature, the concentration of SFS, the HPV and the Fe^{2+} concentration on the rate of polymerization were studied for the SFO-HP-initiated mini-emulsion polymerization of MMA. The results of the particle size and size distribution analysis and the measurements of the molecular weight of the pMMA formed at various conditions are shown in Table 3.3. The conversion vs. time curves of MMA for the polymerizations are presented in Figure 3.4a-d. For all of the conversion vs. time curves it was observed that no gel effect occurred and that 100% conversion was not reached. Also, in the mini-emulsion copolymerization of acrylics in the presence of alkyd resin, reported by Wang *et al.* [6], the gel effect was not observed. Therefore, it was assumed that in the presence of oil or alkyd the heat of reaction could be removed effectively in the latex particles. A possible explanation for the limited conversion was given by Wang *et al.* [31]. They observed the same limited conversions in the redox-initiated mini-emulsion polymerization of styrene and described this as being caused by the formation of a glassy polystyrene layer in the outer layer of the particles. In accordance to this, the limited conversion observed in our system could be caused by the formation of glassy poly(methyl methacrylate) in the outer layer of the particle hindering the diffusion of the monomer and the fatty-acid hydroperoxide to the surface. However, in the system of Wang and Schork *et al.* [6], which used MMA/BA with a glass transition temperature of less than room temperature, the limited conversion was also observed. Schork also observed this effect with polyester- and urethane-acrylic hybrids [32]. These results suggest that the observed limited

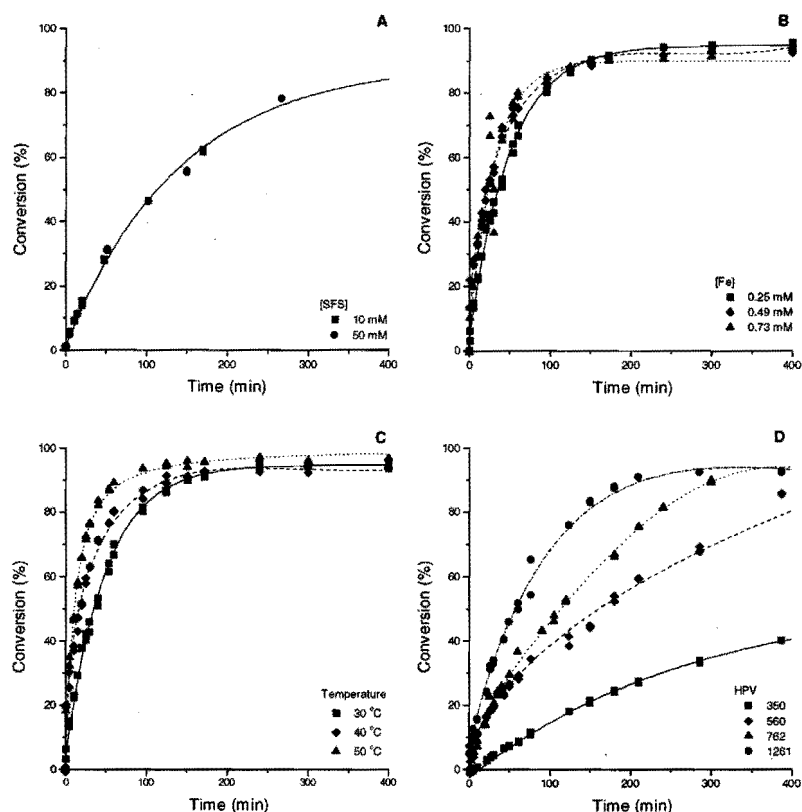


Figure 3.4. Conversion vs. time curves for (A) various concentrations of SFS; (B) various concentrations of Fe^{2+} ; (C) various temperatures; and (D) various hydroperoxide concentrations. Standard conditions: $T = 30^{\circ}C$; $[SFS] = 7.5 \text{ mM}$; $[Fe] = 0.25 \text{ mM}$; HPV = $1300 \mu\text{mole O} / 2 \text{ kg of oil}$.

conversions can also be caused by chain transfer. In the present case, chain transfer to the 1,4-double bonds present in the fatty-acid chains, resulting in a non-reactive allylic radical, may be the cause. With decreasing of monomer concentration at higher conversion the chance of chain transfer to fatty-acid chains increases.

The mechanism of interfacial initiation of the mini-emulsion polymerization of styrene initiated by CHP was described by Wang *et al.* [31] as consisting of three stages, *i.e.*, diffusion, initiation and regeneration. Diffusion of the different components through either the water or the oil phase to the interface was considered as the first stage. This was followed by generation of free radicals and initial polymerization at the interface in the second stage and regeneration of

the Fe^{2+} by the SFS in the aqueous phase in the third stage. The schematic representation of the initiation process at the interface as proposed by Wang *et al.* [31] is redrawn for our system in Figure 3.5.

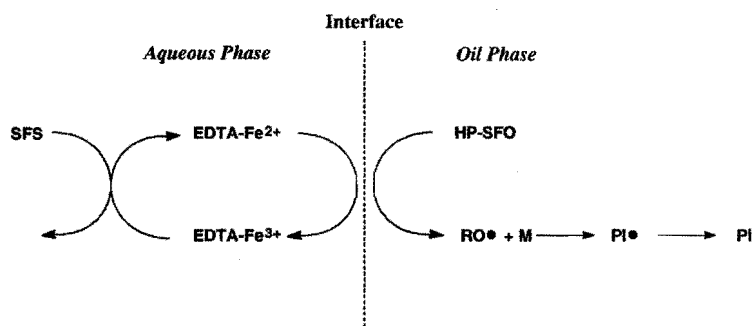


Figure 3.5. Schematic representation of the initiation process at the water-oil interface.

Table 3.3. Data of the Average Particle Size and Particle Size Distribution, Number-Average (M_n) and Weight-Average (M_w) Molecular Weights of the pMMA Fraction of SFO-HP-Initiated Mini-Emulsion Polymerizations of MMA under Various Conditions.

| Variations ^a | | | | Z-Average | Polydis- | M_n | M_w |
|-------------------------|---------------------|------------------------------|--------------------|-----------|----------|----------------------|----------------------|
| $\Delta[\text{SFS}]^b$ | $\Delta[\text{Fe}]$ | $\Delta T(^{\circ}\text{C})$ | ΔHPV | (nm) | Persity | ($\times 10^{-3}$) | ($\times 10^{-3}$) |
| 10 | | | | 122.7 | 0.107 | 46.8 | 146.0 |
| 50 | | | | 153.4 | 0.087 | 43.7 | 138.6 |
| 7.5 | 0.73 | | | 165.6 | 0.153 | 41.9 | 129.4 |
| 7.5 | 0.49 | | | 164.4 | 0.139 | 43.9 | 135.8 |
| 7.5 | 0.25 | 30 | 1300 | 140.3 | 0.135 | 41.3 | 123.7 |
| | | 40 | | 159.1 | 0.151 | 39.5 | 132.1 |
| | | 50 | | 124.9 | 0.120 | 38.6 | 126.9 |
| | | | 350 | 131.2 | 0.171 | 60.6 | 190.1 |
| | | | 560 | - | - | 52.3 | 158.3 |
| | | | 762 | - | - | 53.5 | 141.4 |
| | | | 1261 | - | - | 43.4 | 111.9 |

a) Standard conditions: $T = 30^{\circ}\text{C}$; $[\text{Fe}] = 0.25 \text{ mM}$; $[\text{SFS}] = 7.5 \text{ mM}$; $\text{HPV} = 1300 \mu\text{mole O}/2 \text{ kg of oil}$

b) $\text{HPV} = 1225 \mu\text{mole O}/2 \text{ kg of oil}$

Figure 3.4a suggests that a variation in the concentration of SFS did not affect the rate of polymerization. This is in contrast to the observations of Wang *et al.* [31]. Figure 3.4b shows that the concentration of Fe^{2+} did not have a large effect on the rate of polymerization either. Since neither the SFS concentration nor the Fe^{2+} concentration influenced the polymerization rate, it was concluded that the diffusion of the components through the water phase in the first stage and the regeneration of Fe^{2+} in the third stage of the initiation mechanism were not of influence in the SFO-HP-initiated mini-emulsion polymerization of MMA, in contrast to the observations of Wang *et al.* [31].

Figure 3.4c and Figure 3.4d show that the polymerization rate increased with temperature and with HPV (concentration of ROOH). The initial polymerization rate was found to depend on the 1.65 power of the concentration of ROOH from the slope of the curve of the logarithm of the polymerization rate vs. the HPV, as shown in Figure 3.6.

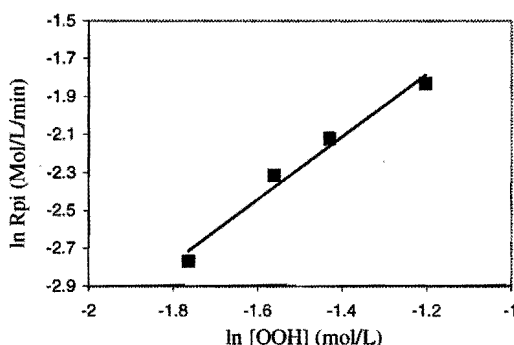


Figure 3.6. Logarithmic plot of R_{pi} vs. $[\text{OOH}]$.

In addition, Table 3.3 showed that the molecular weight of the PMMA decreased with increasing concentration of ROOH. From the above observations it was concluded that, according to the initiation mechanism described by Wang, the rate polymerization would be determined by the diffusion of the SFO-HP through the oil phase, or by the generation of free radicals at the oil-water interface. A triglyceride molecule is a relatively large molecule ($M_w \sim 900$). Therefore it seems likely that in the mini-emulsion polymerization of MMA initiated by fatty-acid hydroperoxides in an $\text{ROOH}/\text{Fe}^{2+}$ -EDTA/SFS redox system, diffusion of the fatty-acid hydroperoxide to the oil-water interface is the limiting step in the initiation mechanism.

After dialysis of the polymerized hybrid latexes it was found that 4–7% of the initial hydroperoxide groups were still present. This means that during polymerization most of the hydroperoxide groups were used for initiation. This may also indicate that in the course of the polymerization the diffusion of initiator groups to the water-oil interface was limited. The presence of residual hydroperoxides is expected to be beneficial: as they are intermediate groups in the autoxidative cross-linking it is very well possible that the non-used hydroperoxide groups will decrease the overall cross-linking time of the hybrids after application.

3.4 Conclusions

From the study presented in this chapter it was concluded that oil-acrylic hybrid latexes could be formed using fatty-acid hydroperoxides as initiating groups for the mini-emulsion polymerization of MMA. During polymerization nucleation predominantly, if not exclusively takes place in the monomer-oil droplets. The use of fatty-acid hydroperoxides as oil-soluble initiators in the ROOH/Fe²⁺-EDTA/SFS redox initiation system results in the formation of triglyceride-modified poly-acrylic molecules. These molecules act as compatibilizers between the oil phase and the pMMA phase resulting in more homogeneous particles. The diffusion of the fatty-acid hydroperoxide molecules from the oil phase to the oil-water interface probably determines the rate of polymerization. Only a small number of the available sites for cross-linking of the oils are used for initiation of the mini-emulsion polymerization and, therefore, the autoxidative cross-linking capabilities of the oils are not significantly affected.

3.5 References

1. R. Buter, EP 0-555-903 A1, (1993).
2. W. Weger, *Polymer Paint Colour Journal*, June, (1995) 12.
3. M. Gobec, W. Weger, *Kunstharz Nachrichten*, 31, (1995) 10.
4. T. Nabuurs, "Alkyd-Acrylic Composite Emulsions. Polymerization and Morphology", Ph.D. Dissertation, Eindhoven University of Technology, (1997).
5. T. Nabuurs, R.A. Bayards, A.L. German, *Prog. Org. Coat.*, 27, (1996) 163.
6. S.T. Wang, F.J. Schork, G.W. Poehlein, J.W. Gooch, *J. Appl. Polym. Sci.*, 60, (1996) 2069.
7. J. Ugelstad, M.S. El-Aasser, J.W. Vanderhoff, *J. Polym. Sci., Polym. Lett.*, 11, (1973) 503.

8. F.K. Hansen, J. Ugelstad, *J. Polym. Sci., Polym. Chem.*, 17, (1973) 3069.
9. Y.T. Choi, M.S. El-Aasser, E.D. Sudol, J.W. Vanderhoff, *J. Polym. Sci., Polym. Chem.*, 23, (1985) 2973.
10. K. Fontenot, F.J. Schork, *J. Appl. Polym. Sci.*, 49, (1993) 66.
11. J. Reimers, F.J. Schork, *J. Appl. Polym. Sci.*, 59, (1996) 1833.
12. W.I. Higuchi, J. Misra, *J. Pharm. Sci.*, 51 (5), (1962) 459.
13. C.M. Miller, E.D. Sudol, C.A. Silebi, M.S. El-Aasser, *Macromolecules*, 28, (1995) 2754.
14. C.M. Miller, E.D. Sudol, C.A. Silebi, M.S. El-Aasser, *Macromolecules*, 28, (1995) 2765.
15. C.M. Miller, E.D. Sudol, C.A. Silebi, M.S. El-Aasser, *Macromolecules*, 28, (1995) 2772.
16. C.C. Wang, N.S. Yu, C.Y. Chen, J.F. Kuo, *J. Appl. Polym. Sci.*, 60, (1996) 493.
17. E.M.S. van Hamersveld, Chapter 2 of this thesis, Section 2.2.2.
18. R. Pecora, in "Dynamic Light Scattering", Plenum Press, New York, (1985) 50.
19. R. Finsy, N. de Jaeger, R. Sneyers, E. Geladé, *Part. Part. Syst. Charact.*, 9, (1992) 125.
20. P.M. Frederik, M.C.A. Stuart, P.H.H. Bomans, W.M. Busink, K.N.J. Burger, A.J. Verkleij, *J. Microscopy*, 161 (2), (1991) 253.
21. P.M. Frederik, M.C.A. Stuart, P.H.H. Bomans, D.D. Lasic, in "Handbook of Non-medical Applications of Liposomes", Vol I, D.L. Lasic, Y. Barenholz (Eds.), CRC Press, New York, Ch VII. (1996).
22. R.D. Mair, R.T. Hall, in "Organic Peroxides". Vol. II, D. Swern (Ed.), Wiley Interscience, New York, Ch VI (1971).
23. N.A. Porter, S.E. Caldwell, K.A. Mills, *Lipids*, 30, (1995) 277 (for a review).
24. (a) A. Overeem, "Hybrid Acrylic-Oil Emulsions. Build-in of Initiator groups in Vegetable Oils.", Master Thesis, (1995), Agricultural Research Institute, Wageningen. (b) E.M.S. van Hamersveld, Chapter 2 of this thesis.
25. (a) J.L. Courtneidge, M. Bush, *J. Chem. Soc., Perkin Trans. I*, 1, (1992) 1531. (b) J.L. Courtneidge, M. Bush, S. Loh, *J. Chem. Soc., Perkin Trans. I*, 1, (1992) 1539.
26. P. Walstra, *Chem. Eng. Sci.*, 48 (2), (1993) 333.
27. Y. Talmon, *Ber. Bunsenges. Phys. Chem.*, 100, (1996) 364.
28. Note that for an HPV of $700 \cdot 10^{-3}$ / 2 kg of oil only 6.1% of the unsaturated groups of the oil contain a hydroperoxide group.
29. H.M. Andersen, S.L. Proctor, *J. Polym. Sci. A*, 3, (1965) 2343.
30. E.S. Daniels, V.L. Dimonie, M.S. El-Aasser, J.W. Vanderhoff, *J. Appl. Polym. Sci.*, 41, (1990) 2463.
31. C.C. Wang, N.S. Yu, C.Y. Chen, J.F. Kuo, *Polymer*, 37 (12), (1996) 2509.
32. F.J. Schork, personal communication (1998).

CHAPTER 4: MORPHOLOGY DEVELOPMENT OF FILMS PREPARED FROM ALKYD-ACRYLIC HYBRID LATEXES: SURFACE PROPERTIESⁱ

Abstract

This chapter describes the research performed on the synthesis of film forming alkyd-acrylic hybrid emulsions and on the analysis of the surface properties of dry films from these hybrids. Mini-emulsion polymerization was used for the preparation of alkyd-acrylic hybrid latexes with compositions varying from 25 w% to 75 w% of alkyd resin. The hybrids were prepared using EMA as monomer with either internal initiation by fatty-acid hydroperoxides or external initiation by tert-butyl hydroperoxide in an ROOH/Fe²⁺-EDTA/SFS redox system. For particles prepared with either initiation system a homogeneous particle morphology was observed using cryo-TEM.

Atomic force microscopy (AFM) was used to study the topography and surface morphology of films prepared from the hybrid latexes and of individually adsorbed particles. It was shown that phase separation between the alkyd resin and the acrylic polymer occurred during adsorption and drying of individual particles. ESCA analysis and contact angle measurements of surfaces (top and bottom) of films prepared on hydrophilic and hydrophobic glass suggested phase separation between the alkyd resin and the acrylic polymer and migration of surfactants to the surfaces.

ⁱ Part of this chapter has been accepted for publication:

E.M.S. van Hamersveld, J.J.G.S. van Es, A.L. German, F.P. Cuperus, P. Weissenborn, and A.-C. Helligren, *Prog. Org. Coat.*, (1999).

4.1 Introduction

The ongoing research on the development of high performance binders for low VOC waterborne coatings has most recently focused on binders consisting of two, or more, chemically different components. Examples of such waterborne binders are blends of latexes of low Tg and high Tg polymers [1-3], polyurethane-acrylic hybrids [4-7], and alkyd-acrylic hybrids [8-14]. The combination of two, or more, components creates the opportunity to combine specific properties of each of the components and/or to reduce the need for additives. Often, one of the components ensures good film formation and reduces, or eliminates, the need for organic coalescing agents. Other properties, for instance hardness, are incorporated in the second component.

The successful use of binders consisting of two, or more, components depends on the synergistic effects of the components that can be realized. For waterborne binder systems these synergistic effects will be determined predominantly by the morphology of the blend or the hybrid prior to application and by the changes that take place during film formation. For example, blends of acrylic latexes of high Tg and low Tg gave films that showed hard spheres embedded in a soft matrix [3]. The morphology of the coating will also be determined by the degree of deformation of individual particles during film formation [15]. Therefore, it is important to study how the particle morphology of hybrid particles can be translated to film morphology and film properties after film formation.

Research on the preparation of oil-acrylic hybrid latexes in our laboratory [16] has shown that for the system comprising poly(methyl methacrylate) (PMMA) and sunflower oil the morphology of the hybrid particles can be controlled by proper choice of the type of hydroperoxide used. Use of *tert*-butyl hydroperoxide (*t*-BHP, external initiator) in an iron-EDTA/SFS redox system resulted in particles that showed phase separation, whereas initiation by sunflower oil hydroperoxide (SFO-HP, internal initiator) resulted in a homogeneous particle morphology.

This chapter describes the preparation of film forming alkyd-acrylic hybrid latexes using mini-emulsion polymerization of EMA in alkyd-monomer droplets and the film formation of the hybrids thus obtained. Initiation of the polymerization was accomplished by using fatty-acid hydroperoxides or *tert*-butyl hydroperoxide. The morphology of the hybrid particles was studied using cryo-TEM. The film formation was studied by analysis of the surface properties of films applied from the hybrid latexes. Analysis of the bulk properties of films from the hybrid latexes will be described elsewhere [17]. The surface properties were analyzed by atomic force microscopy (AFM), ESCA and contact angle measurements.

First, an introduction to the film formation process of polymer latexes is given, followed by that of waterborne alkyd resins, as a number of distinct differences exist.

4.2 Film Formation

The formation of a coherent film from waterborne latexes or alkyd resin emulsions is an important aspect in the formation of a coating. During film formation the water evaporates and particles in the latex start packing. For both polymer latexes and resin emulsions the film formation process can be described as occurring in three stages.

4.2.1 Film Formation of Polymer Latexes

Film formation from polymer latexes is a complex multistage process. Because of the industrial importance of polymer latexes this process has been the subject of various studies in the past 40 years. Various models have been proposed to describe the process. However, discussions still remain as to the exact mechanisms that determine the transformation of a colloidal polymer dispersion into a polymer layer with good cohesive properties. It is now generally accepted that the process of film formation of polymer latexes can be described as occurring in three stages. An idealized representation of the different stages involved in the film formation process is presented in Figure 4.1.

Stage 1. In the initial stage water evaporates and the concentration of the particles increases. With the evaporation of the water, the inter-particle distance decreases, until the particles come into contact with each other. This results in a dense packing of particles with water filling the interstices.

Stage 2. The second stage involves the evaporation of the interstitial water along with the deformation and compaction of the particles. This stage, also called coalescence, results in a honeycomb-like structure of deformed particles. The exact mechanism of the relation between the particle deformation and the water loss is still subject of discussion.

Stage 3. The final stage involves interdiffusion of macromolecules across particle-particle boundaries, leading to a homogeneous continuous film. During this stage the honeycomb structure disappears and the mechanical strength of the film increases.

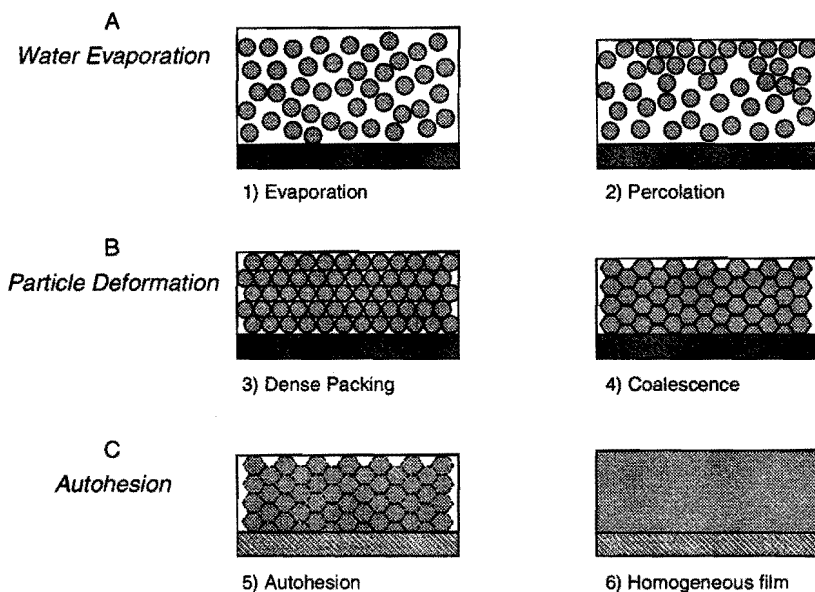


Figure 4.1. Idealized representation of the film formation process of polymer latexes.

Many theoretical and experimental investigations have been devoted to these three different stages.

Most of the theoretical work performed on film formation has been aimed at describing the deformation of densely packed particles during the evaporation of interstitial water in the coalescence stage. Dobler and Holl have presented a detailed review of the literature dealing with the deformation step in 1996 [15]. A brief description of the main theories, namely the dry sintering theory by Dillon *et al.* [18], the capillary theory by Brown [19], the wet sintering theory by Vanderhoff *et al.* [20,21], and Sheetz's surface layer theory [22] is presented below.

Dillon and co-workers [18] proposed the dry sintering theory in 1951. The theory was based on drying of the latex prior to the deformation of the particles. According to the theory the particles are deformed by viscous flow driven by the particle-air interfacial tension.

Brown [19] criticized this theory, because deformation was also observed for slightly cross-linked particles. In the capillary theory of Brown the deformation of particles and the evaporation of water occur simultaneously. Deformation of the particles was suggested to occur when the promoting forces for deformation are stronger than the resisting forces. The capillary pressure, determined by the

interfacial pressure of the air-water interface and the radius of the particles, was considered as the main promoting force.

In the wet sintering theory of Vanderhoff *et al.* [20,21] the evaporation of water and the deformation of particles also occurred simultaneously. The main driving force for deformation in this theory was suggested to be the particle-water interfacial tensions. The Laplace equation was used to show that polymeric material is pushed from the center of the particle to the contact area, thus increasing the size of this area and deforming the particles.

The theory of Sheetz [22] involves the formation of a surface layer of deformed particles formed by capillary forces. This surface layer covers the drying latex. In order to leave the latex water has to diffuse through this layer. This leads to an osmotic pressure that causes the deformation of particles beneath the layer.

As mentioned in the beginning of this section the deformation of particles during film formation is still a point of discussion in literature. The main theories described above were proposed in the 1960s. The work published after this time has not resulted in new main theories. However, this work has resulted in verification and/or improvement of the different main theories. A review of these verifications and improvements is presented by Dobbler and Holl [15].

Experimental research performed on film formation of polymer latexes has been aimed at all three stages of film formation. Traditionally film formation was studied by measuring the evaporation rate of water [23-28] and the build-up of mechanical strength [26] and barrier properties [25,28] of the film. This was combined with analysis of the film structure by electron microscopy (SEM, TEM) [28,29]. In recent years several new experimental techniques have been developed for the analysis of the wet stage packing and deformation of particles in Stage 2 and for analysis of the interdiffusion of polymer chains and development of mechanical properties in Stage 3. These techniques include dielectric analysis [26,30,31], environmental scanning electron microscopy (ESEM) [23,32-35], cryogenic electron microscopy [36,48], neutron scattering (SANS) [29,37-39], ellipsometry [23,32,33], dynamic mechanical analysis (DMTA) [29,40-43], minimal film formation temperature measurements (MFFT) [44-46], UV-visible transmission measurements [47,28], direct fluorescence energy transfer measurements (DET) [48-54] and atomic force microscopy (AFM) [4,6,28,55-60]. The use of these techniques has resulted in a more detailed understanding of the parameters influencing the film formation process. For instance, Keddie *et al.* [23,32,33] introduced the existence of an intermediate stage, defined as II', depending on the MFFT of the polymer particles and the conditions (humidity and temperature) of film formation. Detailed reviews on the

recently developed experimental techniques and resulting advances in the studies on film formation of polymer latexes were presented in 1997 by Richard [61] and Winnik [62].

4.2.2 Film Formation of Alkyd Emulsions

The process of film formation of alkyd emulsions, or emulsions of other low molecular weight resins, has received less attention in literature. The only model described until now, was proposed by Beetsma and Hofland [63-65]. This model is based on the reversion of the process of emulsification by phase inversion [66]. The film formation of alkyd emulsions can be described as occurring in three stages. An idealized representation of the various stages of film formation of alkyd emulsions is shown in Figure 4.2.

Stage 1. In the initial stage water evaporates and the concentration of particles increases. This stage is similar to Stage 1 of film formation of polymer latexes.

Stage 2. At a certain concentration of water the alkyd droplets will come into contact with each other and partial interfacial diffusion of alkyd chains will take place: the oil-in-water (O/W) emulsion inverts to a water-in-oil (W/O) emulsion. This transition involves a one-phase system, a bicontinuous micro-emulsion of the aqueous phase and the oil phase. The occurrence of this phase inversion depends on the droplet viscosity (pseudo T_g). For instance, short oil alkyds may not invert (resin is solid at room temperature).

Stage 3. The final stage involves the evaporation of the water from the aqueous domains in the water-in-oil emulsion. Transport of water to the surface takes place by means of diffusion. The build-up of mechanical strength of the alkyd film takes place by autoxidative drying after Stage 3.

Visual evaluation of the drying of alkyd emulsions on a glass or quartz plate was presented as experimental argumentation for the model described [64,65]. After some time four different stages were visible on the plate. The central zone of the drying film consists of an O/W emulsion and has a white color. This zone is surrounded by a gray W/O phase. Between the two phases a transparent zone is observed: the bicontinuous phase. In this bicontinuous phase the composition of the film is such that the water and oil are miscible in a metastable sense. The inhomogeneities in this phase are smaller than the wavelength of visible light, which results in a transparent phase. In the outer zone of the film also a clear film was observed. Weight loss measurements and optical microscopy were also used to study the film formation of alkyd emulsions by Caprati *et al.* [67].

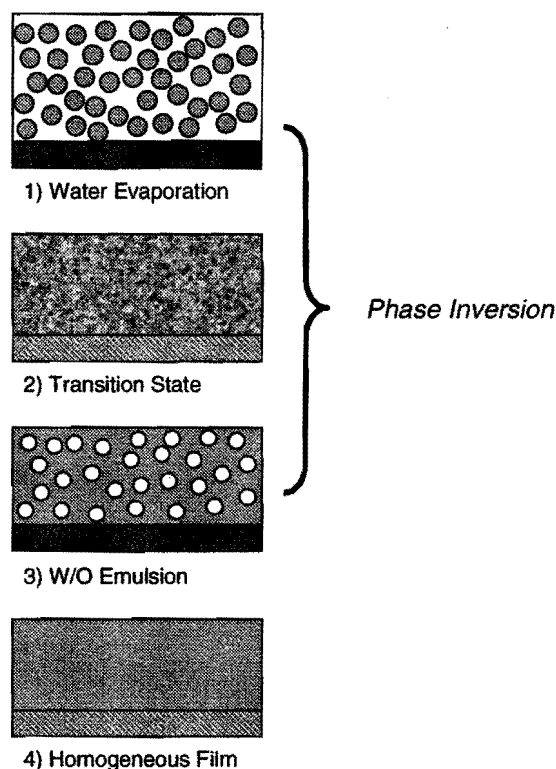


Figure 4.2. Idealized representation of the film formation process of alkyd emulsions.

However, these results were not used to describe a model for the process.

The major difference between the film formation of polymer latexes and that of alkyd emulsions is the disappearance of the interfaces between the alkyd droplets upon concentration by water evaporation in Stage 2 of the film formation process. Because of the low viscosity of the alkyd, chains of different droplets can merge within a few seconds. Also, during Stage 3 of film formation of alkyd emulsions it is suggested that transport of water is realized by means of diffusion. For polymer latexes, on the other hand, this transport takes place by capillary flow.

4.3 Experimental

4.3.1 Materials

Rhenus B.V. (Dodewaard, The Netherlands) kindly provided the sunflower oil (SFO). Before use the sunflower oil was purified by filtration over a florisil column (Merck, Belgium). Oxidized sunflower oil (SFO-HP, HPV = 1225 $\mu\text{mole O}/2 \text{ kg}$ of oil [68]) was prepared according to the procedure reported in Chapter 2 of this thesis. The alkyd resin was kindly supplied by DSM Resins (AH98, Zwolle, The Netherlands). The alkyd resin was based on mixed fatty acids and pentaerythritol with an oil length of 83%, an acid value of 9.3 mg of KOH/g and a hydroxyl number of 29.2 mg of KOH/g. Sodium hydrogencarbonate (NaHCO_3 , 99.5%, Merck, Germany), sodium dodecyl sulfate (SDS, 99+%, Merck, Germany), ethylene-diaminetetraacetic acid disodium salt (EDTA, 99+%, Aldrich, Belgium), sodium formaldehyde-sulfoxylate (SFS, 97%, Merck, Germany), ferrous sulfate hexahydrate ($\text{FeSO}_4 \cdot 6\text{H}_2\text{O}$, Aldrich, Belgium), hexadecane (HD, 99%, Aldrich, Belgium), aqueous *tert*-butyl hydroperoxide (*t*-BHP, 70% aqueous solution, Merck, Germany), (3,3)-dimethylbutyl dimethylchlorosilane (DDCS, Aldrich), hydrochloric acid (HCl, 37%), ammonia (NH_3 , 25%), hydrogen peroxide (H_2O_2 , 30%), non-ionic surfactant (B-048, Akzo-Nobel, Sweden), Co-siccative (WEB-Co, 8% Co, Servo Delden, The Netherlands) and poly(ethyleneimine) (PEI, Mw 70.000, 30% aqueous solution, Polysciences Inc., U.S.A.) were used as supplied. The monomer ethyl methacrylate (EMA, 99%, Aldrich, Belgium), inhibited with 100 – 200 ppm of hydroquinone, was purified by filtration over an inhibitor-removal column (Aldrich, Belgium). Water was purified using a Waters Millipore purifying system (MilliQ).

4.3.2 Oil/Alkyd-Acrylic Hybrid Preparation

The oil/alkyd-acrylic hybrid latexes were prepared in a batch mini-emulsion polymerization under a nitrogen blanket at 30 °C. The hybrids were composed of different proportions of sunflower oil (SFO), or oxidized sunflower oil (SFO-HP), and alkyd resin, to monomer (EMA). The general recipe for the mini-emulsion polymerization is shown in Table 4.1. The polymerization of the pure acrylic (Ac1) was performed at 50 w% solids content using 10 mM *t*-BHP. The SDS and the NaHCO_3 were dissolved in the water. The emulsion was premixed by ultrasonification (3 min, ampl. 10 μm) and homogenized by high-pressure homogenization at 1000 bar (5 bar inlet pressure) at 25–35 °C using a Microfluidizer TM-120 from Microfluidics, Boston, USA. The mini-emulsion was

transferred to a glass reactor that was equipped with a teflon[®]-coated mechanical stirrer operating at 200 rev./min. The polymerization was started by the subsequent addition of SFS (15 mM) and complexed Fe^{2+} (0.25 mM) from concentrated aqueous solutions. In case of initiation by fatty-acid hydroperoxide, SFO-HP was used instead of SFO and *t*-BHP was not used. The final conversion was determined gravimetrically after 10 hours. A sample of the emulsion was injected into a pre-weighed aluminum dish containing an aqueous 1% (w/w) hydroquinone solution to stop the reaction. Before measuring the dry solids content the samples were dried for 24 h at room temperature and for 12 h at 40 °C in vacuum (25 mbar).

Table 4.1. Typical Composition of Mini-Emulsion Recipe used for Preparation of Oil/Alkyd-Acrylic Hybrid Latexes.

| | Amount added (g) | Concentration (mM) ^a |
|-------------------------------------|---------------------|------------------------------------|
| Water | 100.0 | |
| NaHCO ₃ | 0.163 | 20.0 |
| SDS | 0.68 | 23.6 |
| HD | 2.04 | 90.3 |
| Monomer | 41.4 | |
| Sunflower oil (SFO) ^b | 13.6 | |
| Alkyd resin | 27.3 | |
| <hr/> | | |
| <i>Initiator composition</i> | (mL) | |
| SFS ^c | 0.60 | 15.0 |
| <i>t</i> -BHP ^b | 0.103 | 7.5 |
| Fe^{2+} -EDTA ^d | 1.00 | 0.25 |

a) Concentrations based on water

b) When initiation was performed with fatty-acid hydroperoxides, SFO-HP (HPV = $1225 \cdot 10^6$ mole O/2 kg of oil) was used and no *t*-BHP was added

c) From freshly prepared stock solution of SFS (2.5 M)

d) From freshly prepared stock solution of $\text{FeSO}_4 \cdot 6 \text{H}_2\text{O}$ and Na-EDTA (25 mM Fe^{2+} , with Fe-EDTA molar ratio of 1 : 2.1)

4.3.3 Analysis

Particle Size

The particle size analysis was performed by dynamic light scattering with a Autosizer IIc from Malvern Instruments, United Kingdom. The Z-average particle

size and the polydispersity of the particles were determined using the cumulant method [69]. Prior to measurement the sample was diluted 100-500 times with water to obtain the desired translucence. All particle size measurements were carried out at 25 °C and in duplicate.

Zeta-potential

The electrophoretic mobility value of the latex particles was determined using a Zetasizer 4 from Malvern Instruments, United Kingdom. Prior to measurement the samples were diluted 100-500 times. The zeta-potential measurements were carried out at 25 °C and in duplicate.

Scanning Electron Microscopy (SEM)

Scanning electron microscopy (Cambridge Stereoscan 200) was used to visualize the individually adsorbed latex particles (sample preparation is described in Section 4.3.4.1). The surfaces of the SEM samples were coated with a thin gold-palladium layer.

Viscosity

The viscosity of the latexes was determined using a Brookfield Synchro-Lectric viscometer (model LVT) operating with spindle LV3 at 30 rev./min.

Particle Morphology

The morphology of the hybrid particles was examined with cryogenic Transmission Electron Microscopy (cryo-TEM) according to procedures described by Frederik *et al.* [70,71]. The samples for cryo-TEM were prepared from hybrid latexes with ~40% solids content. Dipping a bare specimen grid into and withdrawing it from the latex yielded a thin aqueous film. After dipping the film was vitrified in liquid ethane. The vitrification process is extremely fast (10^{-2} ms, Bachmann and Mayer [72]). The time between dipping and vitrification was approximately 1 sec.

Molecular Weight

The molecular weight of the polymers was determined using gel permeation chromatography (GPC). GPC was carried out on a Waters modular GPC instrument (pump model 510, injector WISP 712). Tetrahydrofuran (AR stabilized

from Biosolve), at a flow rate of 1 mL/ min, was used as eluent. Detection was carried out by refractive index (Waters 410 differential refractive index detector) and UV detection (Waters 486 UV detector at 254 nm) at 40 °C. The system was calibrated using polystyrene standards (Polymer Laboratories). The data was analyzed using Millennium HPLC software including GPC option. 4 Columns in series were used: mixed B (300*7.5 mm each) from Polymer Millipore.

4.3.4 Surface Properties

4.3.4.1 Atomic Force Microscopy (AFM)

AFM experiments were carried out using a Nanoscope III Multimode microscope (Digital Instruments, Santa Barbara, U.S.A.). AFM images were obtained under ambient conditions while operating the instrument in tapping mode. Commercial etched silicon nitride cantilevers of 125 μm (spring constant 20-100 N/m, resonance freq. 298–369 kHz) were used (Nanoprobe™ TESP, Digital Instruments, Santa Barbara, U.S.A.). Height and phase images were obtained simultaneously. Images were obtained at a scan rate of 1 Hz, with 512 lines. Scanned images were of different size ranging from 500 x 500 nm^2 to 10 x 10 μm^2 squared.

Films to be imaged were prepared by placing a drop of latex onto freshly cleaved mica. The drop was spread out on the mica using the top of a pipette. The films were allowed to air dry at ambient temperature for 24 h prior to imaging.

To obtain images of individual particles, the particles were adsorbed onto a flat surface using the adsorption method described by Johnson [73]. However, the silane-modified glass cover slips used by Johnson were replaced by PEI-modified mica plates. Modification of freshly cleaved muscovite mica was carried out by immersion in an $\text{NaHCO}_3/\text{Na}_2\text{CO}_3$ buffered solution (pH 9.9) of branched PEI (200 ppm). This created a surface with an electropositive charge at neutral pH [74,75]. After 3 hours of immersion/adsorption the surface-treated mica was rinsed thoroughly with water and immediately used for particle adsorption.

Particles were adsorbed for 30 minutes onto the PEI-modified mica from a 0.1 mM NaHCO_3 suspension with a particle volume fraction (ϕ) of 10^{-4} . The mica sheets were withdrawn from the suspension and gently rinsed by immersion in water to remove non-adsorbed particles. Excess water was removed by blotting with filter paper and the sample was dried at ambient condition (2 h) prior to imaging.

4.3.4.2 Static Contact Angle Measurements

Static contact angle measurements were used to characterize the film-air surface and the film-substrate surface of films prepared from different hybrid latexes. Films were prepared by application of the latexes onto clean glass plates and onto flat bottomed culture dishes with a hydrophilic surface and also onto glass plates and dishes treated with an alkyl silane to give a hydrophobic surface. The classification of "hydrophilic surface" and "hydrophobic surface" was arbitrarily taken as wetting by water (contact angle, $\phi < 10^\circ$), and adhesional wetting of water ($\phi > 80^\circ$), respectively [76].

Hydrophilic glass surfaces were obtained by thoroughly cleaning the glass objects. Cleaning was carried out by boiling the glass objects for 5 min in a solution of HCl and H₂O₂ (5 parts of H₂O, 1 part of 37% aqueous HCl and 1 part of 30% aqueous H₂O₂), followed by rinsing with ethanol and water, subsequent boiling in a solution of NH₃ and H₂O₂ (5 parts H₂O, 1 part of 25% aqueous NH₃ and 1 part of 30% H₂O₂) and rinsing with ethanol and water. The cleaned glass surfaces were stored in ethanol. Hydrophobic glass surface was obtained by overnight gas treatment of the cleaned glass surfaces with (3,3)-dimethylbutyl-dimethylchlorosilane.

Prior to application of the latexes 3% non-ionic surfactant (B-048) (w/w of total solids) and 0.05% Co (w/w of oil/alkyd phase) were added to the latex, successively, and the latex was allowed to equilibrate for 48 h and 24 h, respectively. Films were prepared in the culture dishes by placing a small amount of latex onto the glass and spreading the film. Latex was added until the surface of the dish was covered. Because of differences in spreading-wetting on hydrophilic surfaces and adhesional wetting on hydrophobic surfaces this resulted in thin films (50-200 μm) on the hydrophilic and thick films (0.5-2 mm) on the hydrophobic surfaces, respectively. After drying for more than 5 days the films were carefully removed from the glass surface using a razor blade. The contact angle of a milliQ water droplet on the bottom surface and top surface of the film were measured using a Ramé Hart A-100 goniometer (sessile drop method). A schematic representation of the apparatus is given in Figure 4.3.

The angles on left and right sides of the 2D-droplet projection were measured. The contact angles for droplets were measured at two different locations on the film.

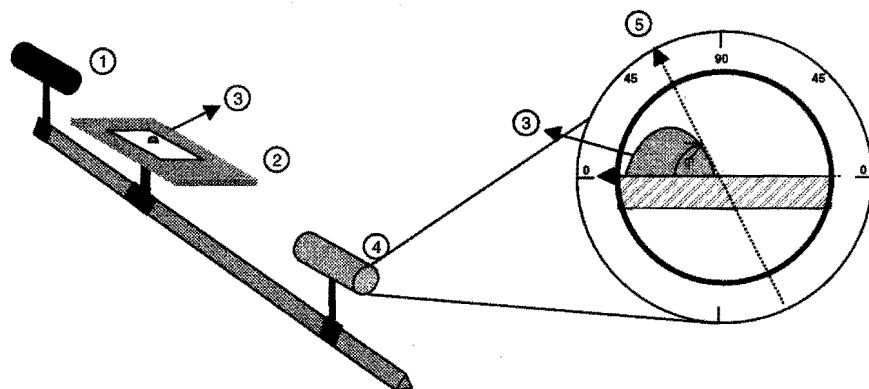


Figure 4.3. Schematic representation of contact angle measurement setup. (1) = light source, (2) = equalized plate, (3) = droplet (2-D projection), (4) = optical lens, (5) = measured contact angle (ϕ).

4.3.4.3 Electron Spectroscopy for Chemical Analysis (ESCA)

The chemical compositions of free films (film-substrate interface and film-air interface) dried on hydrophilic and hydrophobic glass surfaces were analyzed by ESCA (also known as X-ray photoelectron spectroscopy, XPS). ESCA was carried out using a Kratos (AXIS-HS) ESCA spectrometer with a monochromatic Al K α X-ray source (operating at 15 kV; 20 mA), and a hemispherical analyzer. The integrated peak intensities for C 1s, O 1s, Na 1s and S 2p signals were computed using a desktop computer and associated ESCA software. To help resolve the energies of individual carbon bands separate high-resolution carbon spectra were measured using a lower energy pass of 20 eV. Due to instrumental parameters, uncertainties in atomic cross-sections and electron inelastic mean free paths, the accuracy of the ESCA method for quantitative purposes is normally not better than 10% [77]. When using ESCA the chemical composition of a spot with a spot size of about 1 mm² with about 10 nm depth is analyzed. The preparation of the films on the hydrophilic and on the hydrophobic substrate is described in Section 4.3.4.2. Free films were obtained by breaking the culture dishes and carefully removing the film from the glass surface using a razor blade. The films were dried for more than 7 days at ambient conditions followed by 4 days in vacuum (25 mbar, 25 °C) prior to analysis.

4.4 Results and Discussion

4.4.1 Oil/Alkyd-Acrylic Hybrid Latexes

Latex Properties

High-solids oil/alkyd-acrylic hybrid latexes with different compositions of vegetable oil, alkyd resin and acrylic polymer were prepared by mini-emulsion polymerization. The mini-emulsion polymerization was initiated using an ROOH/Fe²⁺-EDTA/SFS redox initiation system. The results of the analysis of the different hybrid latexes are presented in Table 4.2. In Table 4.2 the columns entitled H3 represent hybrids initiated by fatty-acid hydroperoxide groups (SFO-HP), whereas columns entitled H4 refer to hybrids initiated by *tert*-butyl hydroperoxide (*t*-BHP), respectively. The values 25–75 represent the percent ratio of oil/alkyd (1:3 mixture) of oil, alkyd and EMA monomer in the initial mixture.

The results presented in Table 4.2 showed that for the mini-emulsion polymerization of the hybrid latexes final conversions of monomer to polymer of less than 100% were obtained. The final conversion generally varied between 75 and 95%. This contrasts the result obtained for the mini-emulsion polymerization of pure EMA, which showed 100% conversion. The limited final conversions of monomer to polymer were also noted in Chapter 3 of this thesis and by others and were ascribed to the formation of a glassy polymer layer at the surface of the particles [12]. In the case of alkyd-acrylic hybrids it may also have been caused by dominant transfer of propagating radicals to pentadienyl groups of unsaturated fatty-acid chains at relatively high conversions (in a 50/50 mixture of oil/alkyd and EMA the ratio of monomer to pentadienyl groups is approx. 1 to 1 at 80% conversion).

Measurements of the particle size of the hybrids (D_{av}) at the end of the polymerization showed that the particle size apparently increased when the fraction of oil was increased (Table 4.2). At fractions lower than 40 (corresponding to less than 40% of oil/alkyd by weight) the average particle size remained constant.

Table 4.2. Composition and Properties of Oil/Alkyd-Acrylic Hybrids Investigated

| | Ac1 | Ak1 | H1-50 | H2-50 | H3-25 | H3-40 | H3-50 | H3-50 | H3-60 | H3-75 | H4-25 | H4-40 | H4-50 | H4-50 | H4-60 | H4-75 |
|--------------------------|-------|------------------|-------|-------|-------|-------|-------|-------|-------|-------|-------|-------|-------|-------|-------|-------|
| SFO (w%) | - | 33.7 | 32.3 | 50 | - | - | - | 3.6 | 6.7 | - | 8.3 | 12.2 | 16.7 | 17.1 | 20.0 | 25 |
| SFO-HP (w%) | - | - | 16.7 | - | 8.3 | 12.8 | 16.7 | 13.6 | 13.6 | 25 | - | - | - | - | - | - |
| Alkyd (w%) | - | 66.3 | - | - | 16.7 | 26.8 | 32.3 | 33.4 | 39.7 | 50 | 16.7 | 26.8 | 32.3 | 33.7 | 40.9 | 50 |
| EMA (w%) | 100 | - | - | - | 75 | 60.4 | 50 | 49.4 | 40.0 | 25 | 75 | 70.0 | 50 | 50.3 | 39.1 | 25 |
| MMA (w%) | - | - | 50 | 50 | - | - | - | - | - | - | - | - | - | - | - | - |
| Properties | | | | | | | | | | | | | | | | |
| Solids (w%) | 50.0 | 50.0 | 18.6 | 16.9 | 42.3 | 39.8 | 43.8 | 41.8 | 41.2 | 42.3 | 41.4 | 41.2 | 40 | 40.6 | 40.6 | 39 |
| Final conv. (%) | 100 | - | 87 | 70 | 93 | 85.7 | 89 | 87.1 | 83.2 | 73.1 | 87 | 87 | 75 | 83.9 | 79.1 | 40 |
| pH | 8.5 | 7.0 | 8.0 | 8.4 | 7.4 | 7.0 | 7.1 | 6.9 | 6.8 | 6.9 | 7.2 | 7.5 | 8.0 | 7.3 | 7.2 | 7.1 |
| D _{av} (nm) | 180 | 230 ^a | 180 | 200 | 123 | 130.7 | 155 | 151.2 | 160.2 | 203 | 137 | 127.2 | 138 | 143.6 | 157.6 | 192 |
| Z _{potential} | -57 | - | -43.2 | -43.6 | -50.4 | - | -52.7 | - | - | -53.4 | -49.7 | - | -53.5 | - | - | -53.3 |
| Br. Visc (LV3) | 155 | - | - | - | 95 | 67 | 178 | 45 | 34 | 30 | 102 | 160 | 119 | 64 | 72 | 82.5 |
| Mn (x10 ⁻³) | 139.1 | - | 54.6 | 38.7 | 40.7 | 24.1 | 19.8 | 18.9 | 15.5 | 12.3 | 40.9 | 26.0 | 21.6 | 3.5 | 4.2 | 12.1 |
| Mw (x 10 ⁻³) | 876.5 | - | 210.9 | 111.4 | 266.4 | 134.7 | 123.0 | 133.2 | 82.7 | 56.8 | 553.4 | 224.6 | 219.0 | 81.0 | 109.1 | 59.0 |

a) Measured with Malvern Mastersizer

b) Low conversion, reaction not performed in duplo

According to Walstra [78] the most important factors that determine the droplet size are the amount of energy used to create the droplets and the type and efficiency of the emulsifier used. Here, in all cases the latexes were stabilized using similar amounts of sodium dodecyl sulfate (SDS) and a similar homogenization pressure (which corresponds to similar energy input) was used. When using mini-emulsion polymerization nucleation is directed towards the particles. During the polymerization the initially formed monomer droplets are transformed into polymer particles. Therefore, it was expected that the use of similar amounts of SDS and a similar homogenization pressure would result in latexes with the same particle size. An explanation for the observed dependence of the final latex particle size on the chemical composition could be a difference in volume contraction: the polymerization of the monomer will result in contraction and, thus, in reduction of particle size. This effect will be stronger when the fraction of monomer in the particles is higher.

The molecular weight values of the polymers formed at different compositions showed a decrease when the fraction of oil/alkyd was increased, as shown in Figure 4.2. Two effects may have caused this dependence on composition. First, when increasing the ratio of oil/alkyd to monomer the concentration of pentadienyl groups present in unsaturated fatty-acid side chains increases. This promotes the chance for chain transfer of a propagating acrylic polymer radical to a pentadienyl group. Second, when increasing the ratio of oil/alkyd to monomer for the preparation of H3 the amount of SFO-HP was increased. With the increase of SFO-HP the HPV of the total mixture was increased, which resulted in a decrease in the molecular weight. This was also observed for MMA mini-emulsion polymerization (Chapter 3). The preparation of the H4 hybrids was performed using a constant *t*-BHP concentration. When decreasing the fraction of acrylic monomer the ratio of initiator to monomer increased, which could also account in part for the decrease in molecular weight.

From these results it was concluded that mini-emulsion polymerization of EMA with sunflower-oil hydroperoxide (SFO-HP) or with *tert*-butyl hydroperoxide as part of the redox initiation system could be used for the preparation of oil/alkyd-acrylic hybrid latexes with compositions varying from 25% to 75% (w/w) of oil/alkyd. The morphology of the hybrids prepared and the surface properties of films prepared from these hybrids are discussed in the next section.

Characterization of Hybrid Particles by Cryo-TEM

The morphology of the H3 and H4 hybrid particles was analyzed with cryo-TEM. In Chapter 3 it was observed that initiation by fatty-acid hydroperoxides resulted in a more homogeneous particle morphology, compared to initiation by *t*-BHP. The phase separation between the oil/alkyd phase and the acrylic phase was not observed in the Cryo-TEM images of H3-50 (SFO/AH98 and pEMA initiated by SFO-HP) and H4-50 (SFO/AH98 and pEMA initiated by *t*-BHP), as represented in Figure 4.4a and Figure 4.4b. Possibly, the use of the more hydrophobic monomer pEMA prevented phase separation and resulted in homogeneous particles. This effect was also observed by Nabuurs when butyl methacrylate, dispersed in emulsified alkyd droplets in the presence of free surfactant, was polymerized [14].

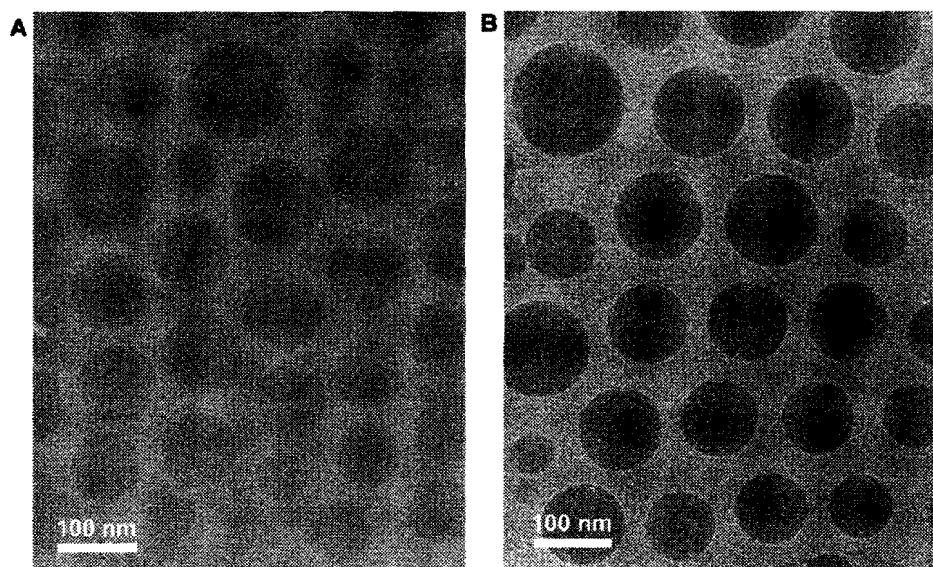


Figure 4.4. (a) Cryo-TEM image of SFO/AH-98 and pEMA initiated by fatty-acid hydroperoxides (H3-50). (b) Cryo-TEM image of SFO-AH-98 and pEMA initiated by *t*-BHP (H4-50).

A cryo-TEM image of a larger area, as presented in Figure 4.5, showed some interesting features. Clusters of deformed particles resembling the honeycomb structures that were described for Stage 2 of the film formation process of polymer latexes, were observed. Areas containing particle morphologies that might result from phase inversion or that indicated that phase inversion had occurred were not observed. During the time between dipping of the sample and vitrification some water might have evaporated from the thin film, thereby increasing the packing density of the particles. However, an increase to a concentration of 50% or higher does not seem likely. Figure 4.5 also shows that a large number of particles are not deformed. This indicates that the observed particle deformation occurred during evaporation of water (Stage 1 of film formation of polymer particles). These results suggest that initially the hybrids show film formation behavior similar to film formation of polymer latexes. An experimental setup with controlled atmosphere (temperature, relative humidity) and controlled time between dipping and vitrification would allow a more detailed study of this phenomenon.

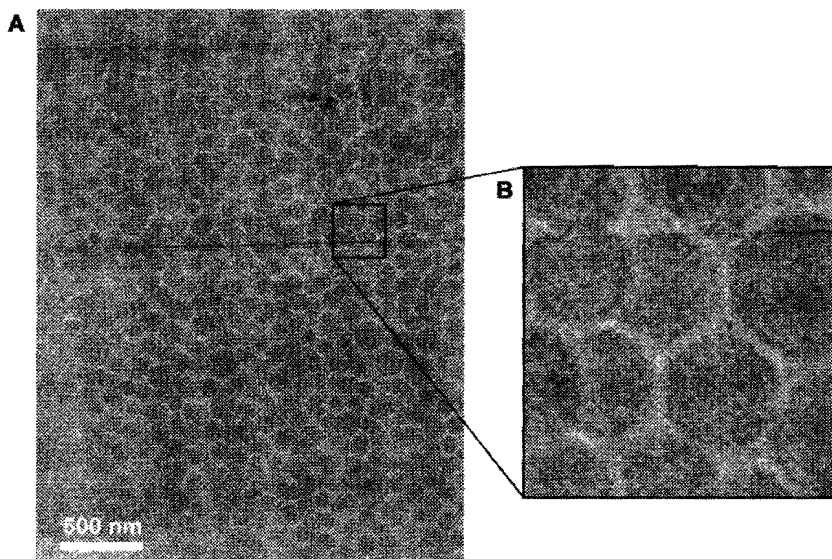


Figure 4.5. Cryo-TEM image of thin film of H4-50 hybrid latex (~40 w%) (A), enlarged area showing deformed particles (B).

4.4.2 Surface Properties

4.4.2.1 Atomic Force Microscopy

Atomic force microscopy (AFM) was used to image the morphology and topography of the surfaces of coatings from alkyd-acrylic hybrid latexes and to monitor the processes taking place during film formation.

Since its invention in 1986 [79] AFM has become a powerful technique to image the topography of a sample surface with high resolution and without the use of special sample preparation. The development of tapping mode AFM [80] allowed the imaging of soft samples such as polymers with less destruction of the surface by the tip. Tapping mode AFM has already been used to study latex dispersion coatings [6,57-60,81-83] and individual particles [57,58,84,85]. A recent development in tapping mode AFM, phase imaging, presents the possibility to obtain an image of the sample surface resulting from shifts in phase angles of tip vibration, because of variation in tip-sample interactions [86]. This phase image thereby provides information about the viscoelastic properties of the surface of the sample and, therefore, is especially useful for the study of heterogeneous surfaces [87].

Hybrid Films

Hybrid latexes H3-50 and H4-50 yielded clear, glossy films with smooth surfaces. AFM analysis of these films gave little information because of high degree of deformation of the particles. It was expected that more information on the effect of hybrid particle morphology on the surface properties could be obtained from analysis of films prepared from hybrid latexes with high T_g polymer, *i.e.*, hybrids of sunflower oil and pMMA (H1 and H2, [88]). Hybrid H1 was prepared by mini-emulsion polymerization using internal initiation by sunflower oil hydroperoxides, while H2 was prepared by initiation using *tert*-butyl hydroperoxide as part of the redox system. This resulted in particles with an apparently homogeneous structure for H1 and particles that showed phase separation for H2, respectively, as judged by cryo-TEM (Figures 3.3a and 3.3b).

Hybrid latexes, composed of high T_g acrylic polymer (pMMA) and sunflower oil, gave white non-transparent films. Typical height and phase images of films from hybrid latexes H2 and H1 are shown in Figure 4.6a and Figure 4.6b.

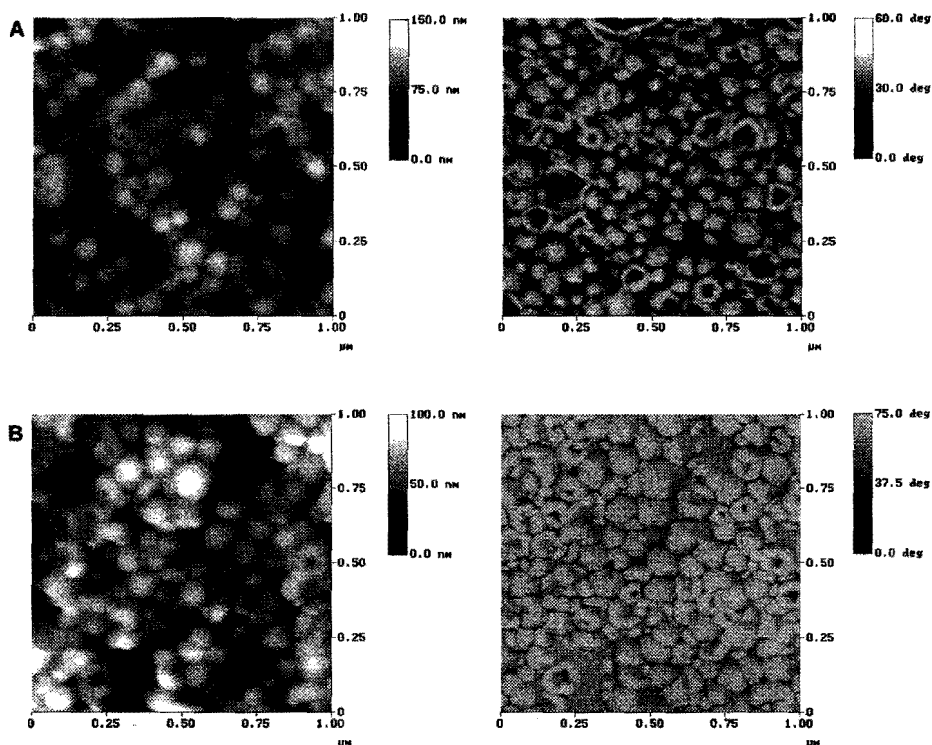


Figure 4.6. Height (left) and phase (right) images of coatings from H2 hybrid (*t*-BHP initiation) (A) and from H1 hybrid (SFO-HP initiation) (B)

The height image of the film from H2 (top-left) showed that the hybrid latex particles had a spherical shape and that a number of particles had an open structure. Large areas of hexagonally close-packed clusters that characterize fcc packing [89], as imaged by Juhue and Lang [81] and by Zhang *et al.* [90], were not observed. Possible explanations for low ordering, *i.e.*, high film thickness ($>50\ \mu\text{m}$), broadness of particle size distribution, and/or effects of surfactants [58], could have played a role in our films. In addition, the observed effect could have been caused by (partial) depletion of oil from the particles during film formation. However, the open structure of the particles has, to the best of our knowledge, not been observed previously. The open structure observed for the particles in the film of hybrid H2 (initiated by *t*-BHP) is in agreement with the morphology of the latex particles, as observed by cryo-TEM (Figure 3.3a).

Surprisingly, the height and phase images of films prepared from H1 (initiated by SFO-HP) with an apparently homogeneous morphology (as judged by cryo-TEM; see Figure 3.3b) also gave images with 'open' particles. A possible explanation

for the observed particle structure of coatings from hybrid H1 could be that the particles had a core-shell structure, or that microdomains of phase separated material were present that were not observed with cryo-TEM (because no staining was used). Alternatively, phase separation between alkyd resin and the acrylic polymer in the apparently homogeneous particles could have taken place during film formation. Deformation occurs when the capillary and interfacial forces that act upon the particles during film formation overcome the mechanical rigidity of the latex particles. Deformation of particles was observed in the phase images of films from H1 and H2.

Individual Particles

Since films prepared from the hybrid binders with the lower T_g acrylic polymer (H3-50 and H4-50) were not suitable for AFM imaging, attention was directed to imaging of individual latex particles. Recently, Johnson and Lenhoff [73,84] showed that images of individual latex particles (styrene) could be obtained from samples that were prepared by electrostatic adsorption onto alkyl-silane-modified glass. Samples prepared from strongly diluted dispersions did not result in individual particles as was shown by Butt *et al.* [57,58,83] and Granier *et al.* [85]. In this research the adsorption method of Johnson [73] was used to adsorb individual particles of the hybrid latexes. However, instead of using polished glass cover slips coated with a thin layer of silane, muscovite mica sheets with a layer of adsorbed poly(ethyleneimine) (PEI) were used as substrate for the adsorption of the negatively charged particles. The branched PEI on the mica generates a positive surface potential in water at pH 7-8 due to protonation of the primary and secondary amine groups [74,75]. Figure 4.7 gives a schematic representation of the PEI-modified mica surface and the proposed adsorption of acrylic particles.

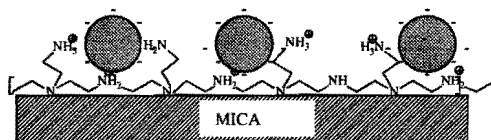


Figure 4.7. Schematic representation of PEI-modified mica surface with adsorbed particles.

Since the PEI-modified mica has a high positive charge ($> +50$ mV) and the polymer particles have a negative charge (~ -50 mV), it was possible to adsorb particles onto PEI-modified mica by electrostatic attraction. The magnitude of the

electrostatic attraction between the PEI-modified mica and polymer particles was sufficient to hold particles in place during imaging by AFM in tapping mode. Figure 4.8 shows a typical topographic surface plot, top view image and cross-section of all-acrylic particles (Ac1) adsorbed onto PEI-modified mica. The particles were adsorbed as small clusters of particles and as individual particles. The top view image showed that capillary and interfacial forces acting at particle-particle contact resulted in particle deformation. Deformation of the individual particles resulting from capillary forces between the drying particle and the modified mica surface could not be visualized by AFM because of experimental restrictions. This deformation could be determined when the height of the particles after drying was compared with the height of the particles prior to drying. Measurements of the height of the adsorbed latex particles in fluid conditions (prior to drying) were not successful because the adsorbed particles were 'pushed away' by the tip. From comparison of the mean height of the particles Ac1 (163 ± 5 nm) with the average particle size measured by dynamic light scattering (180 nm, Table 4.2) and from SEM imaging (Figure 4.9) of the adsorbed particles it was concluded that deformation resulting from capillary forces between the drying particle and the mica surface was small.

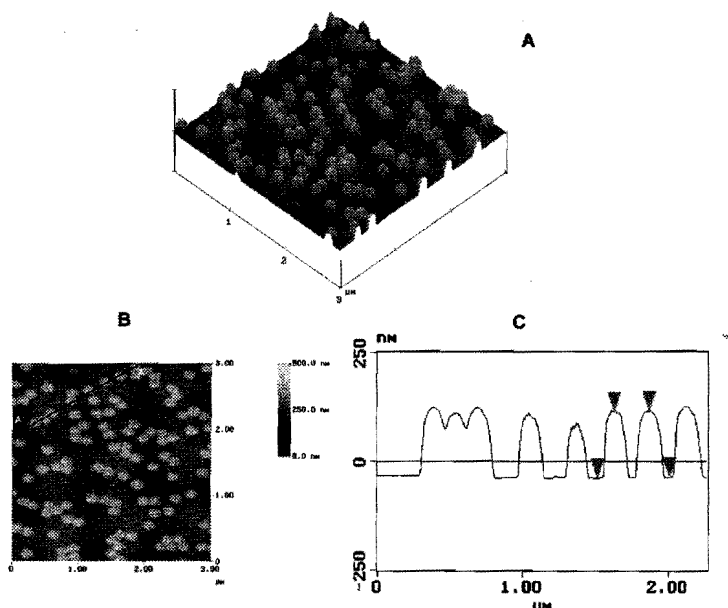


Figure 4.8. (A) AFM topographic surface plot of poly(ethyl methacrylate) latex particles adsorbed and dried onto PEI-modified mica; (B) top-view of adsorbed latex particles, and (C) cross-section along line AA'.

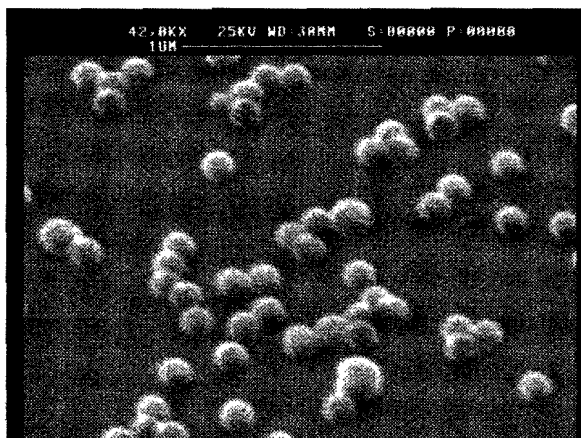


Figure 4.9. SEM image of Ac1 particles adsorbed and dried onto PEI-modified mica. Image tilted 50°.

Since the zeta-potential and particle size of the hybrid latexes H3-50 and H4-50 were not significantly different (in terms of influencing their adsorption behavior) from latex Ac1 (Table 4.2), the optimized conditions for adsorption of Ac1 particles were used for the adsorption of individual particles of hybrids H3-50 and H4-50. Figure 4.10 shows a typical surface plot, top view image and phase image of hybrid particles H4-50 adsorbed and dried onto PEI-modified mica. The cross-sectional profile and the surface plot of the adsorbed H4-50 particles (prepared using *t*-BHP initiation) showed that the particles were significantly deformed. The height of the particles was low compared to the particle size measured by dynamic light scattering. Also, the slope of the side of the particles was less steep than was observed for the cross-section of the all-acrylic particles (Ac1). The deformed structure was also observed with SEM.

The most surprising observation was made with the phase image. The phase image of adsorbed H4-50 particles showed three different regions of tip-surface interaction or viscoelasticity. Large areas of uncovered mica are represented in a light color, where the light color indicates weak tip-surface interactions. Light spheres surrounded by a dark area were also observed. The dark color represents strong tip-surface interactions. These observations suggest that phase separation between the alkyd resin and the acrylic polymer had occurred during the adsorption or during the drying of the individual particles. Apparently, the alkyd resin had 'leaked' out of the particle and spread on the mica

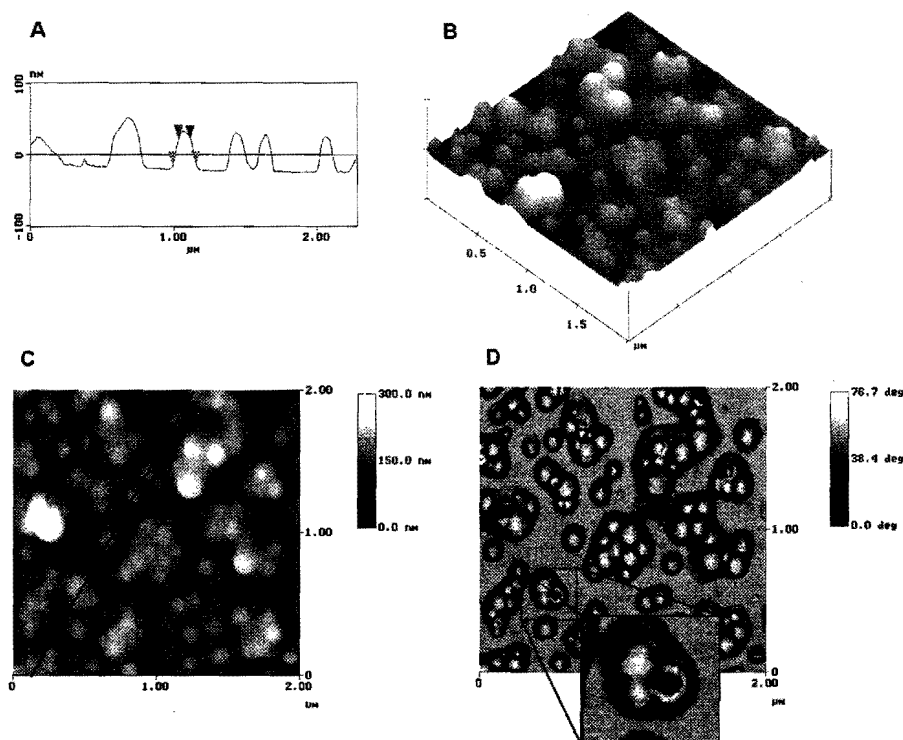


Figure 4.10. AFM analysis of particles of hybrid H4-50 adsorbed and dried onto PEI-modified mica. (A) cross-sectional profile, (B) topographic surface plot, (C) top-view topographic image, and (D) phase image.

surface, resulting in large dark areas with strong tip-surface interaction. One could argue that the observed tip-surface interaction surrounding the particles, is a tip effect resulting from the strong deformation of the particles. However, analysis of strongly deformed Ac1 particles (annealing at 90 °C) did not show this effect.

A further indication that the oil/alkyd had leaked out was the observation that particles with an increased oil/alkyd content were surrounded by a larger area of dark material as shown in Figure 4.11. Imaging of particles with a decreased content of oil/alkyd (H4-25) showed images similar to the ones obtained for all-acrylic particles.

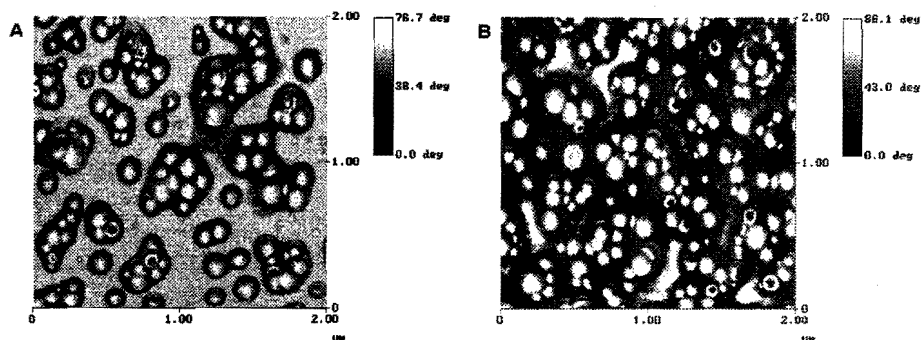


Figure 4.11. AFM phase images of H4 hybrids adsorbed onto PEI-modified mica; (A) image of H4-50 particles, and (B) image of H4-60 particles.

Adsorbed individual particles of hybrid H3-50 (prepared using SFO-HP initiation) showed similar topographic and phase images as observed with hybrid H4-50. Figure 4.12a and Figure 4.12b show the topographic image and the phase image of the adsorbed H3-50 particles, respectively. In the phase image (Figure 4.12b) the same features, *i.e.*, light areas of mica and light 'open' particles surrounded by dark material were observed.

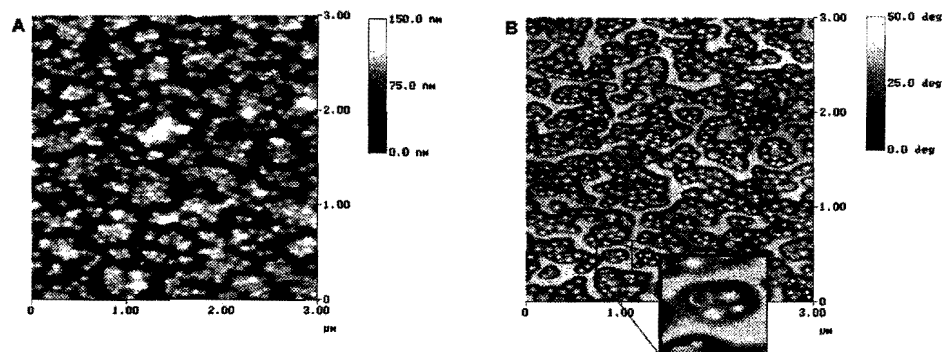


Figure 4.12. AFM top-view topographic image (a) and phase image (b) of hybrid H3-50 adsorbed and dried onto PEI-modified mica.

For both hybrids H4-50 and H3-50 a homogeneous particle morphology was observed in the cryo-TEM analyses. H3-50 was initiated internally by sunflower oil hydroperoxide (SFO-HP) and H4-50 was initiated externally by *tert*-butyl hydroperoxide (*t*-BHP). Both systems showed oil/alkyd depletion and particle deformation after adsorption onto modified mica and drying. Thus, it appears that

the particle morphology, which is achieved by initiating the polymerization internally by SFO-HP or externally by *t*-BHP, is lost during adsorption and drying of the particles.

To explain the rupture of the particles requires an analysis of the forces acting upon the associated and free particles. For individual particles adsorbed onto the PEI-modified mica surfaces the final stages of water evaporation would be expected to induce a relatively strong capillary force. This force may be capable of 'sucking' the particle towards the mica surface (analogous to the capillary forces in normal film formation). Additional forces due to gravity and Van der Waals attraction would be expected to contribute to the flattening and deformation (see Figure 4.13a and Figure 4.13b). Accepting that particle deformation occurs, the and rupture of the particle 'shell' and release of the oil/alkyd would be the result of the internal particle stresses caused by changes in particle shape. For associated particles the capillary forces are compounded with other interfacial forces and the effect is the same as for individual particles, namely particle rupture. This is consistent with general literature describing forces operating during latex film formation [15,24,34,44,45,91].

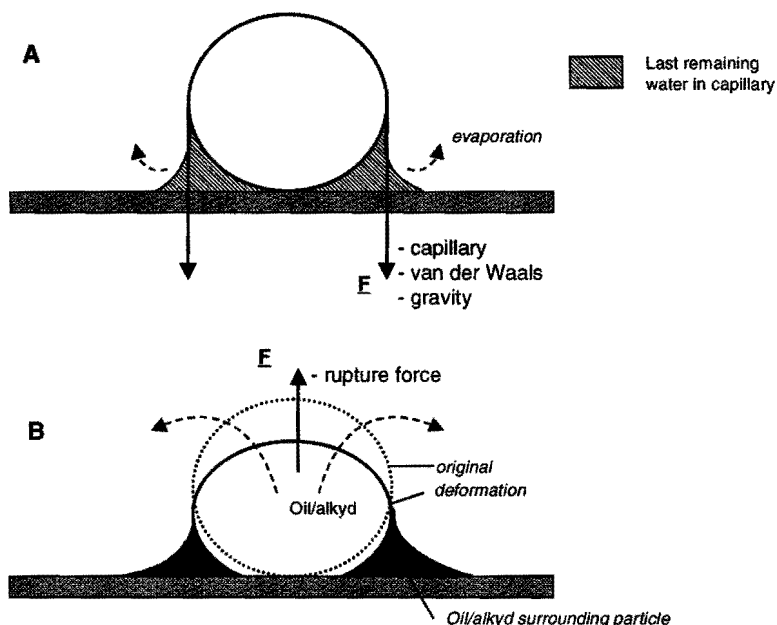


Figure 4.13. Forces acting upon an individual particle adsorbed onto PEI-modified mica.

From these results it was concluded that the forces acting on a layer of singularly adsorbed particles during drying destroy the morphology characteristics that were established during the mini-emulsion polymerization. To what extent this takes place in films of multiple layers of particles will be the objective of further study (see Chapter 5).

4.4.2.2 Surface Properties of Films

ESCA and contact angle measurements were used to analyze the surface of films prepared from the hybrid latexes H3 and H4. The results of these analyses were compared to those obtained from films prepared from the alkyd emulsion (Ak1). The films were prepared on hydrophobic and hydrophilic glass surfaces to enable evaluation of any phase separation and surfactant migration during film formation. The basis for the interpretation of the results is that relatively hydrophilic phases will have a tendency to migrate to the hydrophilic glass surface and relatively hydrophobic phases will migrate to the hydrophobic interfaces (hydrophobic glass surface and air).

Since ESCA operates under a low vacuum it was necessary to de-gas the films prior to analysis. This was carried out by storing the films, prior to their removal from the culture dishes, in a vacuum oven at 25 °C for 5 days. However, once the films were placed under even lower vacuum in the ESCA chamber the samples continued to de-gas. This was believed to be due to the volatile low molecular weight aldehydes formed upon cross-linking of the fatty-acid chains. Surface analysis was started only when a sufficiently low vacuum had been obtained.

A typical ESCA scan and wide angle scans of oxygen and carbon are presented in Figure 4.14. The presence of aldehyde or ketone groups (functional group C=O with chemical shift of 187.90 eV in wide angle scan) was observed for the top surface of both H3 and H4 films and in the alkyd film. This group was not observed in the bottom surface of the H3 film, as shown in Figure 4.14. The bottom surface of the H4 films showed a small amount of carbon at 287.9 eV. The presence of keto groups at the surfaces indicates the presence of byproducts formed upon cross-linking of fatty acids.

Figure 4.14a shows a sulfur peak at approximately 165 eV. This originated from the SDS used in the mini-emulsion polymerization. The presence of the sulfur peak allowed calculation of the SDS concentration at the surface. The results are shown in Table 4.3, together with the results from contact angle measurements and other observations on the spreading, removing and thickness of the films.

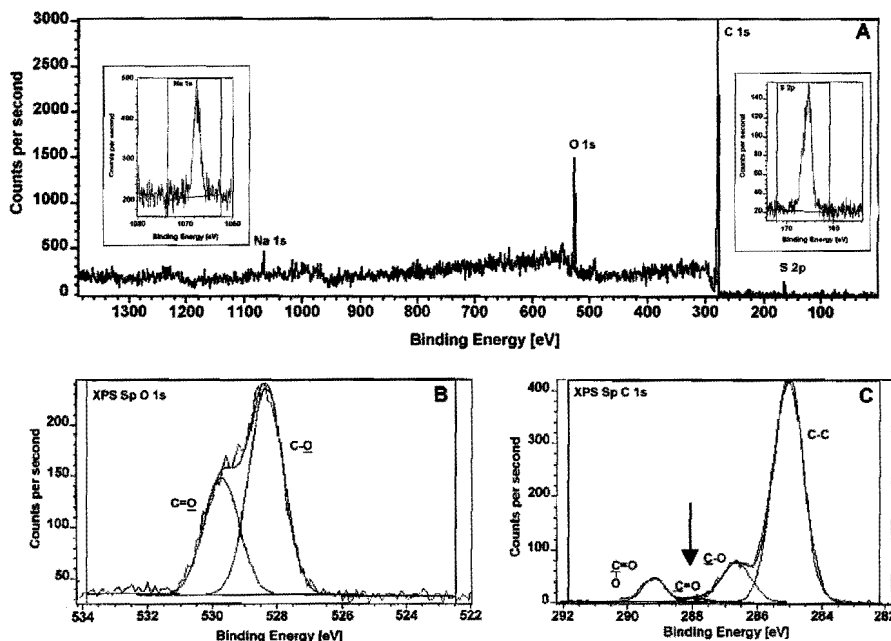


Figure 4.14. (a) Typical ESCA survey scan of bottom side of H4-50 film on hydrophobic glass, (b) the wide-angle scan of oxygen and (c) that of carbon.

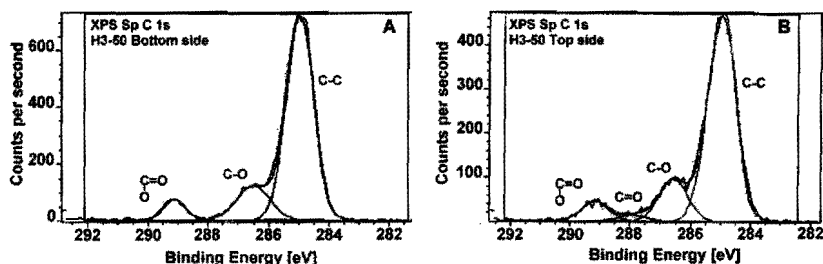


Figure 4.15. Wide angle ESCA scan of carbon: (a) bottom side of film from H3-50, (b) top side of film from H3-50.

Given the difficulties in removing the films from the hydrophilic glass surfaces and variations in film roughness and thickness, the results presented in Table 4.3 need to be considered as a whole and from a broad perspective. The contact angles should not be taken as absolute values, but emphasis should be placed on the difference between the top and bottom contact angles in each system.

Further, the composition of the films is complex (Table 4.1) and contains two surfactants, SDS and Berol 048. The bulk film concentrations of the SDS and Berol 048 were approximately 0.8 w% and 2.5 w%, respectively. The ESCA results can only be related to the migration of SDS.

The contact angle results for the pure alkyd emulsions were as expected. On hydrophilic glass the surfactants in the water phase help with the spreading of the emulsion over the glass surface. During drying the surfactants remained at the bottom of the film, which gave near 0° contact angle. The alkyd rich phase was left at the top of the film, which gave a higher contact angle. Calculations of the SDS concentration at the bottom and top surfaces from ESCA confirm the migration of the SDS towards the hydrophilic glass interface.

For the hydrophobic glass, the surfactants could not assist with the spreading of the emulsion and a thick film resulted. The contact angle results suggest that the film is homogeneous and that alkyd and/or surfactants are equally present at the bottom and top of the film. More surfactant appeared to have migrated to the top surface than in the hydrophilic case. I view of the measured contact angles (59° versus 85°).

The contact angle results for the H3 hybrids (SFO-HP initiation) indicate that the top and bottom surfaces were similar and, therefore, that preferential migration or phase separation of any species (including alkyd and acrylic) toward the hydrophilic and hydrophobic interfaces had not occurred. ESCA indicated that the SDS had migrated preferentially towards the bottom of the films. Comparing the contact angle results for the H3-50 and the H3-60 hybrids shows that the H3-60 had slightly higher angles consistent with higher alkyd concentration in the film and suggesting that alkyd is present at the interfaces.

In contrast to the H3 hybrids, the results obtained for the H4 hybrids (*t*-BHP initiation) indicate a significant phase separation within the film. The ESCA results show that SDS had migrated towards the hydrophobic interfaces more than towards the hydrophilic interfaces. More importantly, the differences in SDS concentration at the top and bottom compared to the H3 hybrids indicate that surfactant migration occurred to a greater extent in the H4 hybrids. The contact angle results for the hydrophobic glass suggests that a more hydrophobic species (possibly alkyd) had separated towards the hydrophobic glass interface. Hence, the H4 hybrid appears to be more prone to phase separation.

More detailed comparison between the contact angle results for H3 and H4 is difficult. It should be noted that removal of the H4 films from the glass was easier than removal of the H3 films. The H3 films adhered strongly to the glass and could not be cleanly removed. Hence the contact angle and ESCA results for H3

Table 4.3. Results from Contact Angle Measurements and ESCA Analysis of Films from Emulsion and Hybrid samples on Hydrophilic and Hydrophobic Glass Surfaces.

| Sample | Glass | Surface | SDS conc. (%) ^a | Contact angle (°) | Comments about film | | |
|--------|-------------|---------|-------------------------------|----------------------|------------------------|-----------------------|-----------------------------|
| | | | | | spreading ^b | removing ^b | film thickness ^c |
| Ak1 | Hydrophilic | Top | 0 | 85 | 1 | 5 | 1 |
| | | Bottom | 16.4 | Close to zero | | | |
| | Hydrophobic | Top | | 59 | 5 | 1 | 4 |
| | | Bottom | | 69 | | | |
| H3-50 | Hydrophilic | Top | 20.0 | 45 | 2 | 5 ^e | 2 |
| | | Bottom | 31.9 | 54 | | | |
| | Hydrophobic | Top | 0 | 36 | 4 | 4 ^e | 4 |
| | | Bottom | 29.7 | 47 | | | |
| H3-60 | Hydrophilic | Top | | 56 | | | |
| | | Bottom | | — ^f | | | |
| | Hydrophobic | Top | | 45 | | | |
| | | Bottom | | 56 | | | |
| H4-50 | Hydrophilic | Top | 64.8 | 38 | 2 | 3 | 3 |
| | | Bottom | 22.3 | 41 | | | |
| | Hydrophobic | Top | 30.1 | 24 | 3 | 3 | 4 |
| | | Bottom | 97.3 ^d | 50 | | | |
| H4-60 | Hydrophilic | Top | | 35 | | | |
| | | Bottom | | 49 | | | |
| | Hydrophobic | Top | | 27 | | | |
| | | Bottom | | 40 | | | |

^a Calculated from surface S in ESCA spectrum. Bulk concentration SDS 0.8%wt. ^b Spreading/removing; 1 = good, 5 = very difficult. ^c Film thickness 1 = ~ 50 μm -5 = ~ 1 mm. ^d Large difference in concentration of SDS observed between various measurements. ^e Top surface very uneven. ^f Not measurable.

are in part for the bulk close to the bottom surface of the film. Film removal also induced roughness that may be significantly different between H3 and H4 films and will affect droplet spreading. The H4 films showed stronger migration of SDS to the bottom surface than H3 films. The poor adhesion of the H4 films may be caused by greater surfactant migration or alkyd/oil phase separation. The surfactants and alkyd may then be left behind on the glass slide or the surfactants may dissolve in the water when measuring contact angle.

The results presented in Chapter 3 showed that for MMA mini-emulsion polymerization the hybrid particles obtained by internal initiation (fatty-acid hydroperoxides) are more homogeneous than when using *t*-BHP in the redox initiation system, probably because of the formation of compatibilizing species. Therefore, it is expected that for the EMA mini-emulsion polymerization described in this chapter, the series H3 (internal initiation by fatty acid hydroperoxides) would afford the more homogeneous films. The contact angle and ESCA results do not clearly show that phase separation between the alkyd and the acrylic phase occurred during film formation of the H3 and H4 hybrid latexes, because of the influence of surfactant migration and degassing of the films. However, since surfactant migration appears to be more significant in the H4 hybrid, this could be due to more dominant alkyd/acrylic phase separation. This would indicate that the films from H4 hybrids are less homogeneous than those from H3 hybrids. Further investigation is necessary using methods such as DMTA or fluorescence microscopy, which give information about the bulk of the film.

4.5 Conclusions

The research described in this chapter shows that stable high-solids (40-45 w%) alkyd-acrylic hybrid latexes composed of long oil-alkyd and pEMA can be prepared. The chemical composition of the hybrid latexes can be varied from 25% up to 75% of alkyd. The use of mini-emulsion polymerization initiated by hydroperoxides (externally by *t*-BHP, internally by SFO-HP) results in hybrid latexes with apparently homogeneous particle morphology as shown with cryo-TEM.

Cryo-TEM analysis also shows that during evaporation of water the hybrid particles deform to yield a honeycomb structure in a manner similar as generally described for Stages 1 and 2 of the film formation process of polymer latexes.

A new method for the adsorption of individual latex particles onto PEI-modified mica surface allows AFM images of individual hybrid particles to be obtained. The images show that the homogeneous particle morphology of the hybrid latexes is lost during adsorption and drying. Both externally initiated and internally initiated alkyd-acrylic hybrid particles apparently show phase separation between the alkyd resin and the acrylic polymer.

Analysis of the surface properties of films from the hybrid latexes applied on hydrophobic or hydrophilic glass surfaces do not confirm the phase separation, observed by AFM for individually adsorbed particles. Contact angle measurements combined with ESCA analysis show migration of surfactant to the film-glass interface and film-air interface. The migration is less for internally initiated hybrids, which may have been due to a lesser tendency to show phase separation between the alkyd resin and the acrylic polymer due to the presence of compatibilizer. In general it is concluded that the prepared hybrid particles deform strongly during film formation, giving macroscopically homogeneous films. Research aimed at analysis of the bulk properties of the hybrid latexes during film formation is needed to further confirm these conclusions.

4.6 References

1. M.A. Winnik, J. Feng, *J. Coat. Tech.*, 68 (852), (1996) 39.
2. J. Feng, M.A. Winnik, R.R. Shivers, B. Club, *Macromolecules*, 28, (1995) 7671.
3. A.J. Fream, S. Magnet, *Farg Lack Scand.*, 1, (1998) 4.
4. R.M. Rynders, C.R. Hegedus, A.G. Gilicinski, *J. Coat. Tech.*, 67 (845), (1995) 59.
5. A.G. Gilicinski, C.R. Hegedus, *Polym. Mat. Sci. Eng.*, 73, (1995) 142.
6. A.G. Gilicinski, C.R. Hegedus, in "Film Formation in Waterborne Coatings", M.A. Winnik, T. Provder, M. Urban (Eds.), ACS Symp. Ser. 648, (1996) 286.
7. R. Tennebroek, J. Geurts, A. Overbeek, A. Harmsen, *Eur. Coat. J.*, 11, (1997) 1016.
8. W. Weger, *Polym. Paint Col. J.*, (1995) 12.
9. R. Buter, P.M. Postma, European Patent 0-555-903 A1, (1993).
10. M. Gobec, W. Weger, *Kunstharz Nachrichten*, 31, (1995) 10.
11. T. Nabuurs, R.A. Bayards, A.L. German, *Prog. Org. Coat.*, 27, (1996) 163.
12. S.T. Wang, F.J. Schork, G.W. Poelzin, J.W. Gooch, *J. Appl. Polym. Sci.*, 60, (1996) 2069.
13. A. Hofland, R. van der Linde, R.A. Bayards, European Patent 0551-942 A2, (1993).
14. T. Nabuurs, "Alkyd-Acrylic Composite Emulsions. Polymerization and Morphology", Ph.D. Dissertation, Eindhoven University of Technology (1997).

15. For reviews on film formation of latexes see: (a) F. Dobbler, Y. Holl, in "Film Formation in Waterborne Coatings", M.A. Winnik, T. Provder, M. Urban (Eds.), ACS Symp. Ser. 648, (1996) 22. (b) F. Dobler, Y. Holl, *TRIP*, 4 (5), (1996) 145.
16. E.M.S. van Hamersveld, Chapter 3 of this thesis.
17. E.M.S. van Hamersveld, Chapter 5 of this thesis.
18. R.E. Dillon, L.A. Matheson, E.B. Bradford, *J. Coll. Sci.*, 6, (1951) 108.
19. G.L. Brown, *J. Polym. Sci.*, 22, (1956) 423.
20. J.W. Vanderhoff, H.L. Tarkowski, M.C. Jenkins, E.B. Bradford, *J. Macromol. Chem.*, 1, (1966) 131.
21. J.W. Vanderhoff, *Br. Polym. Sci.*, 2, (1970) 161.
22. D.P. Sheetz, *J. Appl. Polym. Sci.*, 9, (1965) 3759.
23. J.L. Keddie, P. Meredith, R.A.L. Jones, A.M. Donald, *Macromolecules*, 28, (1995) 2673.
24. C. Gauthier, A. Guyot, J. Perez, O. Sindt, in "Film Formation in Waterborne Coatings", M.A. Winnik, T. Provder, M. Urban (Eds.), ACS Symp. Ser. 648, (1996) 163.
25. F. Dobbler, T. Pith, M. Lambla, Y. Holl, *J. Coll. Int. Sci.*, 152 (1), (1992) 12.
26. S. Cleeve, D. Elliot, T. Strivens, *J. Therm. Anal.*, 38, (1992) 531.
27. E.F. Redknap, *J. Oil Chem. Assoc.* 49, (1966) 1023.
28. J. Mulvihill, A. Toussaint, M.B. de Wilde, *Prog. Org. Coat.*, 30 (1997) 127.
29. J. Richard, in "Film Formation in Waterborne Coatings", M.A. Winnik, T. Provder, M. Urban (Eds.), ACS Symp. Ser. 648, (1996) 118.
30. J.W. Schultz, R.P. Chartoff, *J. Coat. Technol.*, 68 (861), (1996) 97.
31. R.M. Hill, L.A. Dissado, T.A. Strivens, *Adv. Org. Coat. Sci. Technol. Ser.*, 13, (1991) 71.
32. J.L. Keddie, P. Meredith, R.A.L. Jones, A.M. Donald, in "Film Formation in Waterborne Coatings", M.A. Winnik, T. Provder, M. Urban (Eds.), ACS Symp. Ser. 648, (1996) 332.
33. J.L. Keddie, P. Meredith, R.A.L. Jones, A.M. Donald, *Polym. Mat. Sci. Eng.*, 73, (1995), 144.
34. S.T. Eckersley, A. Rudin, in "Film Formation in Waterborne Coatings", M.A. Winnik, T. Provder, M. Urban (Eds.), ACS Symp. Ser. 648, (1996) 2.
35. C. He, A.M. Donald, *Langmuir*, 12, (1996) 6250.
36. J. Dubochet, M. Adrain, J. Lepault, A. McDowall, *Trends Biochem. Sci.*, 10, (1985) 143.
37. K. Hahn, G. Shuller, R. Oberthür, *Coll. Polym. Sci.*, 264, (1986) 1092.
38. L.H. Sperling, A. Klein, J.N. Yoo, K.D. Kim, N. Mohammadi, *Polym. Adv. Tech.*, 1, (1990) 263.
39. Y. Chevalier, *TRIP*, 4 (6), (1996) 197.
40. A. Zosel, *Polym. Adv. Tech.*, 6, (1995) 263.
41. M.P.J. Heuts, R.A. le Fèvre, J.L.M. van Hilst, G.C. Overbeek, *Polym. Mat. Sci. Eng.*, 73, (1995) 140.
42. A. Zosel, G. Ley, *Prog. Coll. Polym. Sci.*, 101, (1996) 86.

43. A. Zosel, G. Ley, *Macromolecules*, 26, (1993), 2222.
44. P.R. Sperry, B.S. Snijder, M.L. O'Dowd, P.M. Lesko, *Langmuir*, 10, (1994) 2619.
45. B.S. Snyder, P.R. Sperry, M.L. O'Dowd, P.M. Lesko, Z. Fu, E. Boczar, A. Kirk, B.C. Dione, A. Koller, *Polym. Prepr.*, 35, (1994) 299.
46. M.J. Devon, J.L. Gardon, G. Roberts, A. Rudin, *J. Appl. Polym. Sci.*, 39, (1990) 2119.
47. A. van Tent, K. te Nijenhuis, *J. Coll. Int. Sci.*, 150, (1992) 97.
48. C. Zhao, Y. Wang, Z. Hruska, M.A. Winnik, *Macromolecules*, 23, (1990) 4082.
49. J. Feng, H. Pham, V. Stoeva, M.A. Winnik, *J. Polym. Sci.: Polym. Phys.*, 36, (1998) 1129.
50. P. Marion, J. Lang, D. Juhu , *22th Fatip c Congr.*, Brussel, (1996) A-71.
51. E. P rez, J. Lang, *Langmuir*, 12, (1996) 3180.
52. J. Feng, M.A. Winnik, A. Siemiar czuk, *J. Polym. Sci.: Polym. Phys.*, 36, (1998) 1115.
53. J. Feng, M.A. Winnik, *Polym. Mater. Sci. Eng.*, 73, (1995) 252.
54. P. Marion, G. Beinert, D. Juhu , J. Lang, *J. Appl. Polym. Sci.*, 64, (1997) 2409.
55. A.C. Gilcinski, C.R. Hegedus, *Prog. Org. Coat.*, 32, (1997) 81.
56. B. Gerharz, R. Kuopka, H. Petri, H.-J. Butt, *Prog. Org. Coat.*, 32 (1997) 75.
57. H.-J. Butt, R. Kuopka, B. Christensen, *Coll. Polym. Sci.*, 272, (1994) 1218.
58. H.-J. Butt, B. Gerhartz, *Langmuir*, 11, (1995) 4735.
59. F. Lin, D.J. Meier, *Langmuir*, 11, (1995) 2726.
60. F. Lin, D.J. Meier, *Langmuir*, 12, (1996) 2774.
61. J. Richard, in *"Polymeric Dispersions: Principles and Applications"*, J.M. Asua (Ed.), NATO ASI Ser. 335, Kluwer, Dordrecht, (1997) 397.
62. M.A. Winnik, in *"Emulsion Polymerization and Emulsion Polymers"*, P.A. Lovell, M.S. El-Aasser (Eds.), Wiley, New York, (1997) 467.
63. J. Beetsma, *Pig. Res. Tech.*, 27 (1), (1998) 12.
64. J. Beetsma, *22th Fatip c Congr.*, Brussels, (1996) 157.
65. A. Hofland, in *"Film Formation of Waterborne Coatings"*, M.A. Winnik, T. Provder, M. Urban (Eds.), ACS Symp. Ser. 648, (1996) 183.
66. G.  stberg, B. Bergenst hl, *J. Coat. Tech.*, 68 (858), (1996) 39.
67. J.J. Caprari, O. Slutzy, P.L. Pessi, *Pitture e Vern. Eur.*, 9, (1993) 17.
68. R.D. Mair, R.T. Hall, in *"Organic Peroxides"*, Vol II, D. Swern (Ed.), Wiley, New York, (1971).
69. R. Pecora, in *"Dynamic Light Scattering"*, Plenum Press, New York, (1985) 50.
70. P.M. Frederik, M.C.A. Stuart, P.H.H. Bomans, W.M. Busink, K.N.J. Burger, A.J. Verkleij, *J. Microscopy*, 161 (2), (1991) 253.
71. P.M. Frederik, M.C.A. Stuart, P.H.H. Bomans, D.L. Lasic, in *"Handbook of Nonmedical Applications of Liposomes"*, D.L. Lasic, Y. Barenholz (Eds.), Vol. 1, CRC Press, New York, (1996), Ch. VII.

72. L. Bachmann, E. Mayer, in "Cryotechniques in Biological Electron Microscopy", R.A. Steinbrecht, K. Zierold (Eds.), Springer-Verlag, Berlin, (1987) 3.
73. C.A. Johnson, "Adsorption Behavior of Proteins and Colloidal Particles Studied using Atomic Force Microscopy", Ph.D. Dissertation, University of Delaware (1997).
74. P.M. Cleasson, O.E.H. Paulson, E. Blomberg, N.L. Burns, *Coll. Surf. A.*, 123-124, (1997) 341.
75. P.M. Cleasson, E. Blomberg, O.E.H. Paulson, M. Malmsten, *Coll. Surf. A.*, 112, (1996) 131.
76. D.J. Shaw., in "Introduction to Colloid and Surface Chemistry", 4th Ed., Butterworth-Heideman Ltd., Oxford, (1992) 151.
77. D. Briggs, "Handbook of X-ray and Ultraviolet Photoelectron Spectroscopy", Heyden, London (1977).
78. P. Walstra, *Chem. Eng. Sci.*, 48 (2), (1993) 333.
79. G. Binnig, C. Quate, G. Gerber, *Phys. Rev. Lett.*, 56, (1986) 930.
80. Q. Zhong, D. Innes, K. Kjoller, V.B. Elings, *Surf. Sci. Lett.*, 290, (1993) L688.
81. D. Juhue, J. Lang, *Langmuir*, 9, (1993) 792.
82. F. Sommer, T.M. Duc, R. Pirri, G. Meunier, C. Quet, *Langmuir*, 11, (1995) 440.
83. B. Gerharz, H.-J. Butt, *Prog. Coll. Polym. Sci.* 100, (1996) 91.
84. C.A. Johnson, A.M. Lenhoff, *J. Coll. Int. Sci.*, 179, (1996) 587.
85. V. Granier, A. Sartre, M. Joanicot, *J. Adhes.*, 42, (1993) 255.
86. D.A. Chernoff, "High Resolution Chemical Mapping Using Tapping Mode AFM with Phase Contrast", Proc. Microscopy and Microanalysis (1995).
87. G. Bar, Y. Thomann, R. Brandsch, H.J. Cantow, M.H. Whangbo, *Langmuir*, 13, (1997) 3807.
88. See Chapter 3 for preparation.
89. K.J. Lissant, *J. Coll. Int. Sci.*, 22, (1966) 462.
90. P.C. Zhang, J. Lui, C.H. Chew, L.M. Gan, S.F.Y. Li, *Talanta*, 45, (1998) 767.
91. M. Visschers, J. Laven, R. van der Linde, *Prog. Org. Coat.*, 31, (1997) 311.

CHAPTER 5: MORPHOLOGY DEVELOPMENT OF FILMS PREPARED FROM ALKYD-ACRYLIC HYBRID LATEXES: TIME-RESOLVED FLUORESCENCE MEASUREMENTS.

Abstract

This chapter describes the use of fluorescence resonance energy transfer (FRET) measurements for determination of the initial degree of mixing of oil-acrylic hybrid latexes and of the processes that take place during film formation and aging of films prepared from these latexes. Hybrid latexes were prepared using phenanthrene-labeled fatty-acid esters as donor and anthracene-labeled acrylic polymers as acceptor. The latexes were prepared by external initiation using tert-butyl hydroperoxide (t-BHP) or by internal initiation using fatty-acid hydroperoxides (SFO-HP) in an ROOH/Fe²⁺-EDTA/SFS redox initiation system. Static fluorescence measurements showed that use of the most common type of alkyd resin, which contains isophthalic acid in the copolyester backbone, in the hybrid composition was not possible because of high background levels. Thus, only oils/fatty-acid esters were used in the present study. Films prepared from hybrid latexes and from solvent-borne systems with a similar chemical composition were analyzed. The fluorescence decay profiles were analyzed by fitting the decay profiles to a sum of exponential terms and by calculation of the area under the fluorescence decay curve. These methods showed that four different types of relaxation could describe the fluorescence profile of films prepared from oil-acrylic hybrid latexes. Also, it was shown that the type of initiation had a strong influence on the initial degree of mixing of the oil and acrylic phases. However, after longer periods of aging the degree of mixing in both systems was similar.

5.1 Introduction

The properties of films prepared from latexes consisting of two, or more, components are for a great part determined by the distribution of these components in the film. The distribution of the components is determined by the particle morphology prior to casting the film and by the interparticle diffusion of the components during film formation. In addition, the miscibility/compatibility and the preparation conditions are also of influence on the distribution of the components. For latexes consisting of one polymer component it is generally accepted that build up of the mechanical and permeation properties of the latex film during film formation is related to interparticle polymer diffusion. However, in the case of latexes consisting of two components the effect of diffusion may be more profound and result in a strong change of film properties. For example, due to difference in hydrophobicity, or surface tension, one of the components may preferentially migrate to the surface during film formation. The preferential migration of one of the components to the surface can be put to advantage, *i.e.*, in the case of self-stratifying coatings [1], but it can also result in heterogeneous films with inferior properties.

In recent years two experimental methods have been developed for the study of diffusion of polymer molecules across particle boundaries. These methods involve small angle neutron scattering (SANS) and fluorescence resonance energy transfer (FRET). SANS was first reported by Hahn *et al.* in 1986 [2] for the study of interdiffusion of a pBMA latex system. This method involves the mixing of a deuterated latex with a non-deuterated latex. The diffusion of the polymer chains during film formation was analyzed by following the radius of gyration of the deuterated latex particles. The method of fluorescence resonance energy transfer measurements was developed for studies of polymer diffusion during latex film formation by Pekcan *et al.* in 1990 [3]. This method is based on the preparation of one batch of latex labeled with a small amount of fluorescent dye (the donor, D) and the preparation of another batch of latex labeled with a second dye (the acceptor, A). Polymer diffusion during film formation was analyzed using fluorescence decay measurements. During the last ten years this technique has become a widely accepted approach to study interparticle diffusion of homopolymer latexes during film formation [4-6]. Also, it has been utilized to probe the morphology of some core-shell latex systems and it has provided information on concentration gradients that may exist when going from the core out to the shell [7-9].

Analysis of the fluorescence decay data is based on the fact that direct energy transfer between the donor and acceptor takes place when the distance of donor to acceptor is small, *i.e.*, 50 Å in the case of phenanthrene-anthracene couple used in this study. The efficiency of this energy transfer is governed by the relation $E = R^6/(R^6 + r^6)$, where R is the characteristic (or Förster) distance between a donor and an acceptor, 23 Å for phenanthrene-anthracene, and r is the actual distance between the donor and acceptor.

So far, two methods have been employed for the analysis of the fluorescence decay data. The first method is derived directly from the Förster equation and involves fitting the fluorescence decay data of the donor to one or more mathematical models that have been well established for simple systems. When no acceptor is present the decay of the donor can be described by a single exponential [4]:

$$I(t) = I(0) \exp(-t/\tau_0) \quad (5.1)$$

where τ_0 is the fluorescence lifetime of the excited species. In a system where the donor (D) molecules are close enough to an acceptor (A) species, the decay can be described with a stretched exponential equation [4]:

$$I(t) = I(0) \exp[-(t/\tau_0) - \beta(t/\tau_0)^{1/2}] \quad (5.2)$$

where β is a time-independent parameter proportional to the local concentration of the acceptor [4]. This expression presumes a globally uniform mixing of D and A. In reality a film will contain both mixed areas where energy transfer will take place and unmixed areas of no transfer. A linear combination of the two equations (5.1) and (5.2), weighted by the pre-exponential factors B_1 and B_2 , is often used to model such a film [4,6-9]:

$$I(t) = B_1 \exp[-(t/\tau_0) - \beta(t/\tau_0)^{1/2}] + B_2 \exp(t/\tau_0) \quad (5.3)$$

The volume fraction of mixing (f_m) can be calculated from the expression:

$$f_m = B_1/(B_1 + B_2) \quad (5.4)$$

If D and A are the only species that can participate in the energy transfer process, and if the decay lifetime of D is negligibly affected by the presence of A at longer distance, then first-order and stretched exponential equations can be satisfactorily used to characterize the system. However, the simplicity of these models can lead to their being applied incorrectly, as Vogelsang and Hauser have pointed out [10].

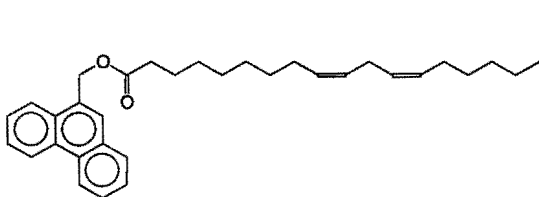
When other components in the system can fluoresce at the excitation wavelength and/or participate in energy transfer, the use of simple models becomes

questionable. In such cases, where curve fitting becomes more complicated, the modified analysis described by Feng *et al.* [6] can be used. This analysis involves the use of the area underneath the fluorescence decay profile ($I(t)$) as an indication for the degree of mixing. The volume fraction of mixing can then be calculated according to:

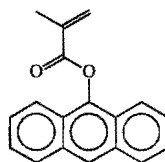
$$f_A' = (A - A_D) / (A(\infty) - A_D) \quad [6-9] \text{ (5.5)}$$

where A , A_D , and $A(\infty)$ are determined after normalization and integration of the decay profiles. A_D is the area under the decay profile of a system containing only the donor, and $A(\infty)$ is the area of the decay profile obtained for a completely mixed system of donor and acceptor. In this chapter both methods described above were used to study the initial degree of mixing and the extent of mixing, or demixing, that occurred during film formation of oil/alkyd-acrylic hybrid latexes.

Hybrid latexes, containing vegetable oil, alkyd, and acrylic components, present the potential for more complicated fluorescence phenomena than do most of the systems studied to date. Previous research on oil/alkyd-acrylic hybrid latexes, described in Chapter 3 and Chapter 4 of this thesis, had shown that morphology of the latex particles was dependent on the type of monomer and the type of initiation process used. Atomic force microscopy of individual hybrid particles indicated phase separation between the alkyd phase and the acrylic phase. The study presented in this chapter is aimed at demonstrating the feasibility of using fluorescence decay measurements in the analysis of the film formation process for oil/alkyd-acrylic hybrid latexes, and at analysis of the extent of phase separation during film formation and aging. For this purpose the oil/alkyd phase was labeled with a phenanthrene dye (**1**) and the acrylic phase with an anthracene dye (**2**) (Figure 5.1).



1 9-Phenanthrylmethyl linoleate (Phe-Lin)



2 9-Anthryl methacrylate (An-Ma)

Figure 5.1. Fluorescent labels used to tag the oil/alkyd phase (Phe-Lin) and the acrylic phase (An-Ma) of the oil/alkyd-acrylic hybrid latexes.

5.2 Experimental

5.2.1 Materials

Rhenus B.V. (Dodewaard, The Netherlands) kindly provided the sunflower oil (SFO). Before use the sunflower oil was purified by filtration over a florisil ($\text{MgO}:\text{SiO}_2$, 100-200 mesh, Aldrich) column. Hydroperoxide-modified sunflower oil (SFO-HP, HPV = 730 $\mu\text{mole O}_2$ / kg of oil [11]) was prepared according to procedures described in Chapter 2. The alkyd resin was kindly supplied by DSM Resins (AH98, Zwolle, The Netherlands). The alkyd resin was based on mixed fatty acids, isophthalic acid and pentaerythritol with an oil length of 83%, an acid value of 9.3 mg KOH/g of resin and a hydroxyl number of 29.2 mg KOH/g of resin. The reagents sodium hydrogencarbonate (NaHCO_3 , 99.5%, Merck), sodium dodecyl sulfate (SDS, 99+%, Aldrich), ethylene diaminetetraacetic acid disodium salt (EDTA, 99+% Fluka), sodium formaldehyde-sulfoxylate (SFS, 97%, Fluka), ferrous sulfate hexahydrate ($\text{FeSO}_4 \cdot 6\text{H}_2\text{O}$, Fluka), hexadecane (HD, 99%, Aldrich), anhydrous *tert*-butyl hydroperoxide (*t*-BHP 70% in *tert*-butanol, Aldrich), 9-phenanthracene carboxyaldehyde (Aldrich), anthrone (Aldrich), methacryloyl chloride (MACl, Aldrich), dicyclohexyl carbodiimide (DCC, Aldrich) and linoleic acid (LA, Aldrich) were used as received. Dry 4-dimethyl-aminopyridine (DMAP) and *para*-toluene-sulphonic acid (*p*-TsOH) were obtained after recrystallization and stored in a dessicator.

Fatty acids with high content of conjugated double bonds were obtained from Akzo Nobel (Nouracid[®] 656, Germany). The fatty acid composition of Nouracid 656 determined by gas chromatographic analysis of their methyl esters was 1.6% C16:0, 7.1% C18:0, 33.6% C18:2, 47.5% C18:2 conjugated, 10.2% C18:1. The monomer ethyl methacrylate (EMA, 99%, Merck) was purified over an inhibitor-removal column (Aldrich) prior to use. Water was purified using a Waters Millipore purifying system (MilliQ).

5.2.2 Labeled Alkyd-Acrylic Hybrid Preparation

Synthesis of Components with Fluorescent Labels

9-Anthryl methacrylate (An-Ma) was prepared according to the method described by Zhao *et al.* [4].

9-Phenanthryl-modified conjugated fatty acid (Phe-Ric) and non-conjugated fatty acid (Phe-Lin) were prepared by reacting phenanthracene-9-methanol with nouracid[®] and with linoleic acid, respectively. To this end, phenanthracene-9-carboxyaldehyde was reduced to phenanthracene-9-methanol according to the method described by Ng and Guillet [12]. Phenanthracene-9-methanol (3.65 g, 17.5 mmol) was dissolved in anhydrous dichloromethane (85 mL). DCC (3.82 g, 18.5 mmol), DMAP (0.20 g, 1.6 mmol), *p*-TsOH (0.32 g, 1.8 mmol) and linoleic acid (4.95 g, 17.65 mmol) were added to the solution. The reaction mixture was stirred at room temperature for 10 h. After evaporation of the dichloromethane the crude product was purified by flash column chromatography (silica Kieselgel 60, Merck) using a gradient mixture of petroleum ether (40-60) and diethyl ether (20 to 80 volume ratio) as eluent. After evaporation of the eluent Phe-Lin was obtained as colorless oil (85%). 400 MHz ¹H-NMR (Bruker AM 400 at 295 K) in CDCl₃: δ = 0.9 (t, 3 H), 1.22-1.42 (m, 14 H), 1.65 (m, 2 H), 2.02 (m, 4 H), 2.42 (t, 2 H), 2.78 (t, 2 H), 5.32-5.40 (m, 4 H), 5.63 (s, 2 H, CH₂O), 7.58-7.72 (m, 4 H), 7.83 (s, 1 H), 7.90, 8.06, 8.68 and 8.76 (each dd, 1 H)

The synthesis of Phe-Ric was carried out according to the same procedure using nouracid 656 instead of linoleic acid. Yield of the Phe-Ric coupling was 75%. 400 MHz ¹H-NMR in CDCl₃ revealed the presence of one of the two possible *cis,trans* isomers of (Δ⁹, Δ¹¹) conjugated fatty-acid esters (as evidenced by the occurrence of four non-equivalent vinylic hydrogen atoms at δ ca. 5.35, 5.65, 5.95 and 6.28 ppm) and two (Δ⁹, Δ¹²) non-conjugated dienic fatty acid esters (as evidenced by the occurrence of two triplets at 2.72 and 2.78 (ratio approx. 2:1 for the pentadienylic hydrogen atoms) as the major isomers. This was in accordance with the composition of the Nouracid used. Shifts for all the other protons were essentially similar as those reported for the Phe-Lin (see above).

Hybrid Preparation

The oil-acrylic hybrid latexes were prepared in a batch mini-emulsion polymerization under a nitrogen blanket at 30 °C according to procedures described in Chapter 3. The hybrids were prepared to give approximately 40% solids at complete conversion, with 1% label content in each phase (molar basis). The composition of the different hybrids prepared, H1-H5, and of a blend composed of anthracene-labeled acrylic latex and a phenanthrene-labeled SFO mini-emulsion (B1) are presented in Table 5.1. Emulsification was carried out by ultrasonification (UP400s, Hielscher GmbH, 20% ampl. and 50% duty cycle), followed by homogenization (Niro-Soavi 150 MPa, primary pressure 500 bar

secondary pressure 50 bar, 5 circulations). The polymerization was started by the subsequent addition of SFS (15 mM) and complexed Fe^{2+} (0.25 mM) from concentrated aqueous solutions as described in Chapter 3. After 10 hours at 30 °C the particle size and final conversion were determined, and molecular weight of the hybrids was analyzed by GPC. The hybrid latexes were stored under nitrogen until use for further studies.

Table 5.1. Composition of Hybrid Latexes Prepared

| | EMA (w%) | SFO (w%) | SFO-HP ^a (w%) | An-MA (w%) | (mol%) ^b | Phe-Lin (w%) | (mol%) ^c |
|----|-------------|-------------|-----------------------------|---------------|---------------------|-----------------|---------------------|
| H1 | 48.8 | 49.8 | - | 1.1 | 1.0 | 0.3 | 1.0 |
| H2 | 49.2 | 35.7 | 13.7 | 1.1 | 1.0 | 0.3 | 1.0 |
| H3 | 50.0 | 49.7 | - | - | - | 0.3 | 1.0 |
| H4 | 49.2 | 50.8 | - | - | - | - | - |
| H5 | 50.0 | 36.4 | 13.6 | - | - | - | - |
| B1 | 54.6 | 43.9 | | 1.3 | 1.0 | 0.2 | 1.0 |

a) When SFO-HP was not used as initiator the polymerization was initiated by *t*-BHP (10 mol/L)

b) Concentrations based on EMA added

c) Concentrations based on SFO added

Blend Preparation

A blend of anthracene-labeled EMA latex and phenanthrene-labeled SFO mini-emulsion was prepared for comparison with the hybrids. The Phe-labeled SFO mini-emulsion (Phe-SFO) was prepared according to the recipe described in Table 5.2. The mini-emulsion was prepared by ultrasonification (UP400s, Hielscher GmbH, 20% ampl. and 50% duty cycle), followed by homogenization (Niro-Soavi 150 MPa, primary pressure 500 bar, secondary pressure 50 bar, 5 circulations). The An-EMA latex was prepared using the same conditions as used for hybrid H1. After preparation of the An-EMA latex 0.12 g of non-ionic surfactant (Berol 048, 3% wt. of solids) was added to the latex. The latex was allowed to equilibrate overnight and was combined with the Phe-SFO emulsion to form the blend (B1, see composition in Table 5.1).

Table 5.2. Recipe for An-EMA Latex and Phe-SFO Emulsion used for the Preparation of Blends

| | An-EMA | Phe-SFO |
|--------------------|---------|---------|
| Water | 25.0 g | 60.0 g |
| SDS | 0.21 g | 0.33 g |
| NaHCO ₃ | 0.04 g | 0.10 g |
| Hexadecane | 0.63 g | 1.0 g |
| Berol 048 | | 1.30 g |
| EMA | 24.46 g | |
| An-Ma | 0.57 g | |
| SFO | | 39.77 g |
| Phe-Lin | | 0.30 g |

5.2.3 Analysis

Particle Size

Particle size analysis was carried out by dynamic light scattering at a scattering angle of 90° using a Malvern 4700 System (RR98 stepper motor controller, PSC7 photomultiplier and 7032 multi-8 correlator). The Z-average particle size and the polydispersity of the particles were calculated on a personal computer with Malvern PCS software (version v1.26) using the cumulant method [13]. Prior to measurement the sample was diluted 100-500 times with water to obtain the desired translucence. All particle size measurements were carried out at 25 °C and in duplicate.

Gel Permeation Chromatography

Gel permeation chromatography (Waters modular GPC instrument, pump model 510, injector WISP 712) was used for determination of the molecular weight of the polymers. Tetrahydrofuran (AR stabilized from Biosolve), at 1 mL/min was used as eluent. Detection was carried out by refractive index (Waters 410 differential refractive index detector) and UV detection (Waters 486 UV detector at 254 nm) in conjunction with fluorescence detection (Waters 470 fluorescence detector, excitation at 300 nm, emission at 385 nm) at 40 °C. The latter served as a means of monitoring the incorporation of the donor molecules, as well as indication if any grafting of acrylic to oil had taken place. The system was calibrated using polystyrene standards (Polymer Laboratories). The data was

analyzed using Millennium HPLC software including GPC option. 4 Columns in series were used: mixed B (300*7.5 mm each) from Polymer Millipore.

Bulk latex samples were submitted to analysis by GPC as solutions in THF (~3 mg/mL). The acrylic and oil phases were also analyzed separately by GPC. A 1 mL portion of the latex was dissolved in 2-3 mL of THF. The acrylic polymer was precipitated from this solution in heptane (5-10 mL). The heptane was evaporated to concentrate the oil phase. The precipitated phase and the oil phase were dissolved in THF for analysis (1 mg/mL)

Static Fluorescence

Static fluorescence spectra were obtained using a Perkin-Elmer LS50B luminescence spectrometer. The samples were dissolved in freshly distilled and degassed THF. The static fluorescence results were used to determine the optimum excitation and emission wavelengths for the fluorescence decay measurements that are described in the next section. The following samples were analyzed: sunflower oil (SFO), Phe-Lin, Phe-Ric, An-MA and alkyd resin (AH98). For Phe-Lin, Phe-Ric and An-Ma, the excitation and emission spectra were obtained using the "pre-scan" mode. For the other samples the emission spectrum was obtained with excitation at 300 nm.

Time-Resolved Fluorescence Measurements

Time-resolved fluorescence measurements were carried out using mode-locked continuous wave (CW) lasers and time-correlated photon counting for detection. A mode-locked CW Yttrium Lithium Fluoride (YLF) laser (Coherent model Antares 76-YLF [14]), that was equipped with an LBO frequency doubler to obtain output at 527 nm wavelength, was used for the synchronously pumping of a cavity-dumped Rhodamine 6G dye laser (Coherent model 701-2 CD). The light output of the dye laser at 600 nm wavelength was frequency doubled using a BBO crystal (Gsänger, 3x4x7 mm³). A variable waveplate (New Focus model 5540) was used to rotate the polarization of the vertically polarized output light of the dye laser to horizontally polarized light to have again vertically polarized (UV) light available for excitation after the type I frequency doubling in the BBO crystal. The repetition rate of excitation pulses was 951 kHz, the wavelength 300 nm, the duration about 4 ps full width at half maximum (FWHM) and the pulse energy in the tens of pJ range.

Film samples for fluorescence decay analysis were prepared by depositing a few drops of latex on a clean quartz plate (Suprasil, 0.1 x 2 x 8 cm) and air drying. To reduce cracking and turbidity in each film, the latex film (thickness 100-200 μm) was spread around the plate surface to wet it evenly, and excess latex was drawn off using a pipette. In addition, a watch glass was placed over each plate to slow down the rate of water evaporation during drying. Solvent-cast films were prepared from freeze dried latexes by dissolving the powder in THF to give a concentrated solution. A few drops were deposited on quartz plates and allowed to dry. Once the films were formed, they were subjected to various ageing and temperature treatments as presented in Table 5.3. All films were formed and aged at room temperature unless noted otherwise. All heat treatments were carried out at 100 °C and at ca. 500 mbar vacuum.

Table 5.3. Ageing and Temperature Treatment Applied on Hybrid Films on Quartz Plates prior to Fluorescence Decay Measurements.

| Ageing: | Fresh (3 hrs.) | 1 Day | 2 Days | 4 Days | 20 Days |
|--------------|-----------------------------|-------|-----------------------------|--------|---------|
| H1 | X | X | X | X | X |
| H2 | X | X | X | X | X |
| H3 | | | | X | |
| H4 | | | | X | |
| B1 | | X | | | |
| Temperature: | 0.5 Day R.T. + 12 h. 100 °C | | 3.5 Days R.T.+ 12 h. 100 °C | | |
| H1 | X | | | X | |
| H2 | X | | | X | |
| H3 | | | | X | |

For measurements the samples were fixed on a spring-loaded holder at an angle of 15° with respect to the direction of excitation. Highly absorbing black solids were used to prevent multiple excitation with the laser pulses, the reflection on the substrate and the remainders of the excitation beam. The sample holder was placed in housing also containing the detection optics. Extreme care was taken to avoid artifacts from depolarization effects. For selection of the wavelength of detection (385 nm) a CVI model CM 112 monochromator was used with the two gratings in a subtractive dispersion configuration. By using a rotating-sheet polarizer, the parallel and perpendicular intensities could be measured separately. The time-correlated single photon counting method was used, with the data being fed to a 1024-channel analyzer (Nuclear Data, model AccuspecB). By reducing the energy of the excitation pulses with neutral density

filters, a maximum fluorescence photon frequency of 30 kHz (~5% of 594 kHz) was chosen [15] to prevent pile-up distortion. Also other instrumental sources for distortion of data were minimized to below the noise level of normal photon statistics [16]. Measurements consisted of repeated sequences of measuring during 10 s parallel and 10 s perpendicular polarized emission. The number of sequences was chosen to yield a peak content in the data files of up to 100.000 counts. After measuring the fluorescence of the sample, the background emission of a sample without added fluorophores was measured and used for background subtraction. Extreme care was taken to prevent background luminescence. The G-factor of the detection part of the setup (at the wavelength of detection) was determined by performing a tail matching operation with the fluorescence decays of parallelly and perpendicularly polarized fluorescence of a small probe molecule in solution (*p*-terphenyl in ethanol). The calculations were carried out by determining the value of G that minimized the residual sum:

$$\sum_{i, \max}^{1024} (I_{\text{par}} - G I_{\text{perp}})^2 \quad (5.6)$$

where *i,max* is the point at which the total fluorescence ($I_{\text{par}} + 2I_{\text{perp}}$) reaches its peak. This value of G was used for curve fitting of all sample data.

Data analysis was carried out using the Fluorescence Data Processor, a program recently developed by the Scientific Software Technologies Center at Belarusian State University (Minsk, Belarus). A sum of first-order exponential terms was used as a model. Optimization was performed by finding the lowest number of exponential terms that minimized χ^2 .

5.3 Results and Discussion

5.3.1 Determination of the Optimum Excitation and Detection Wavelengths

In the research described by others [4,6-9] fluorescence decay measurements were carried out using 298 nm as the excitation wavelength and 366 nm for detection when the system phenanthrene-anthracene was used. The labeled species in these studies involved polymers of acrylic esters that did not interfere with the fluorescent label at these wavelengths.

In the oil/alkyd-acrylic hybrid system sunflower oil and alkyd resin are present. These components may have fluorescent properties that interfere with the intended measurements. After application films prepared from the hybrid latexes cross-link by autoxidative drying. The formation and decomposition of fatty acid hydroperoxides in the autoxidative drying process yields fatty acid esters with conjugated double bonds. These may give rise to background fluorescence. To test this, fatty acid with conjugated double bonds (Nouracid 656, with approx. 47% of conjugated and approx. 33% of non-conjugated double bonds), esterified to phenanthrene, was prepared (Phe-Ric).

The excitation and emission spectra of the phenanthrene-modified linoleic acid (Phe-Lin) and the phenanthrene-modified Nouracid 656 (Phe-Ric) are presented in Figure 5.2a and Figure 5.2b. Except for minor differences the excitation and emission spectra of Phe-Lin and Phe-Ric are similar. This indicates that the conjugated double bonds in the fatty-acid chains of Phe-Ric have no influence on the fluorescence of the attached phenanthrene group, or that the influence is similar as that resulting from non-conjugated double bonds. At the selected excitation wavelength of 300 nm the excitation spectra of Phe-Lin and Phe-Ric show a small peak. At the selected emission wavelength of 366 nm the emission for both compounds was strong. From these results it was concluded that both Phe-Lin and Phe-Ric could be used in this study and that the formation of conjugated double bonds would not interfere. In addition they show that an excitation wavelength of 300 nm and detection wavelength of 366 nm could be

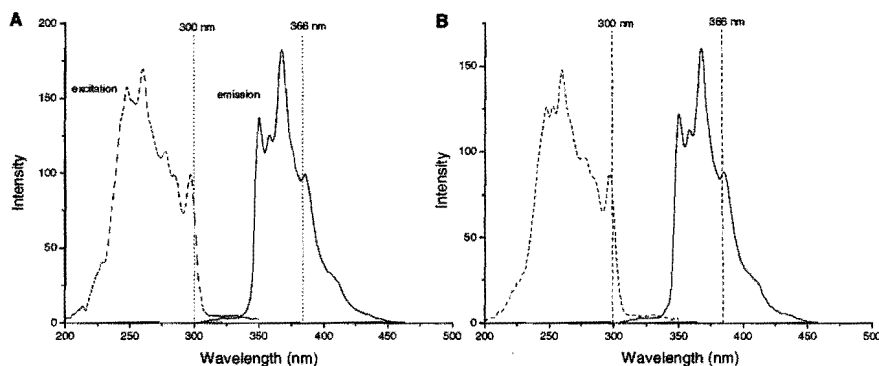


Figure 5.2. Static fluorescence excitation (----) and emission (—) spectra of Phe-Lin (A) and Phe-Ric (B).

used. Phe-Lin was used in the preparation of the hybrid system, because of the resemblance of its fatty-acid chains with the fatty acids in SFO and alkyd resin (AH98).

The emission and excitation spectra of the alkyd resin and the SFO are presented in Figure 5.3 and in Figure 5.4. Figure 5.3 shows that the alkyd is sensitive to excitation in the area from 280 nm to 400 nm. Thus, alkyd resins cannot be included in the hybrids and blends used for film formation when the analysis is carried out using phenanthrene as donor. Most likely, the strong excitation and emission result from the presence of isophthalic acid groups in the alkyd.

The excitation and emission of the SFO were weaker at the detection wavelength of 366 nm, as shown in the spectra in Figure 5.4. However, when the SFO is excited at 300 nm, then at 366 nm there was still significant emission. Therefore, detection was carried out at 385 nm because the emission of the SFO could be neglected at that wavelength. A possible cause for the observed emission of the SFO could be the presence of residual tocopherols. The use of more rigorously purified SFO may reduce this content.

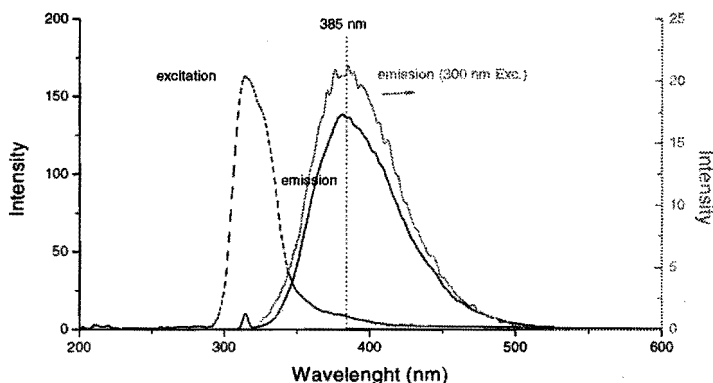


Figure 5.3. Static fluorescence spectra of alkyd resin AH98; (----) excitation, (—) emission, (—) emission from excitation at 300 nm.

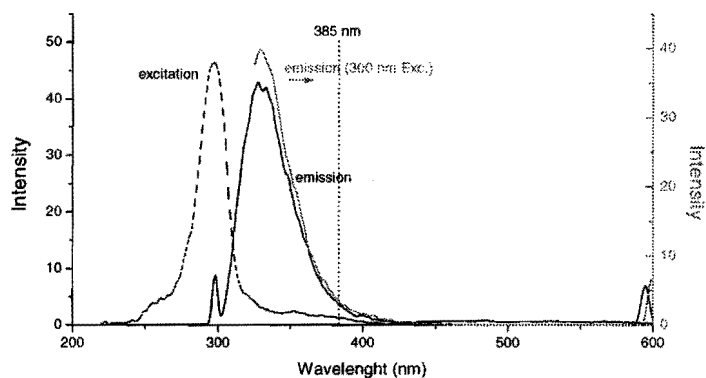


Figure 5.4. Static fluorescence spectra of SFO; (----) excitation, (—) emission, (.....) emission from excitation at 300 nm.

5.3.2 Hybrid Latex Characteristics

The characteristics of the oil-acrylic hybrids H1 to H5 and the all-acrylic An-Ma latex are presented in Table 5.4. The results presented in Table 5.4 were similar to those found for the oil-acrylic and alkyd/oil-acrylic hybrids described in Chapters 3 and 4. However, the final conversion of the acrylic monomer to polymer was lower than previously observed. Conversions ranged from 66% to 74%, whereas in Chapter 3 and Chapter 4 typically conversions of 90% were obtained for hybrids composed of 50% (wt.) of oil and/or alkyd and 50% (wt.) of acrylic. A possible explanation for the apparently low final conversions could be that evaporation of the monomer had occurred during homogenization, which was generally carried out in an open system. Since in these cases labeled monomer and fatty acid esters were used, the polymerizations were carried out in smaller batches. Therefore, loss of a small amount of monomer during homogenization due to evaporation could have a noticeable effect on the apparent final conversion.

GPC and $^1\text{H-NMR}$ analysis of the precipitated polymer at final conversion showed the incorporation of the An-MA monomer in the acrylic polymer. Quantification of the incorporation of An-MA from the NMR spectra was not possible because of the small peaks in the NMR spectrum resulting from the

anthracene group. Exact quantification of the amount of An-MA built into the polymer was not considered to be of importance for the validation of the fluorescence decay method for determination of diffusion and phase separation of oil-acrylic hybrid latexes during film formation and ageing. However, for further elaboration of this method it should be included. Also, determination of the distribution of An-MA over the polymer chains should be included in future investigations. In the papers previously published the labeled latex particles were prepared by semicontinuous emulsions polymerization under starved conditions [3-9]. When this process is applied, the effects of difference in solubility of the labeled monomer and the non-labeled monomer in the aqueous medium, as well as of the difference in reactivity between the two monomers on the composition drift of the polymer are strongly reduced. This results in a homogeneous copolymer composition. The mini-emulsion polymerization process is expected to strongly reduce the drift resulting from the solubility difference. To our knowledge reactivity ratios for labeled and non-labeled monomers have not been reported thus far.

Table 5.4. Characteristics of the Hybrids Prepared.

| | H1 | H2 | H3 | H4 | H5 | An-MA |
|--|-------|-------|-------|-------|-------|-------|
| Part. Size (Z_{av} nm) | 219 | 187 | 178 | 195 | 172 | 140 |
| Mol. Weight ^a ($M_n \cdot 10^{-3}$) | 71.7 | 58.9 | 54.0 | 43.6 | 53.4 | 138.3 |
| Mol. Weight ^a ($M_w \cdot 10^{-3}$) | 440.1 | 231.9 | 406.5 | 176.2 | 374.5 | 597.5 |
| Solids (%) | 34.9 | 34.4 | 34.5 | 34.2 | 33.4 | - |
| Conversion (%) | 74.2 | 72.3 | 72.7 | 69.3 | 66.3 | - |

a) Determined from the polymer fraction

5.3.3 Fluorescence Resonance Energy Transfer Measurements

For reasons described in the previous section the time-resolved fluorescence resonance energy transfer measurements were performed on films prepared from hybrid latexes composed of SFO and acrylic polymer. The composition of the hybrids and the blend used for the preparation of the films are given in Table 5.1, and the ageing and temperature treatment applied is presented in Table 5.3. Figure 5.5 shows a typical fluorescence-time profile of a Phe-Lin-labeled oil-acrylic hybrid (H3). Hybrid H3 contains only the donor Phe-Lin. No acceptor molecules were present in this system. The fluorescence lifetime (τ_0 , Eqn. 5.1) was determined to be 39.1 ns. This value is close to the τ_0 value of 45.4 ns found for a Phe-MMA-labeled pBMA [4]. Also, the fluorescence profile showed a first

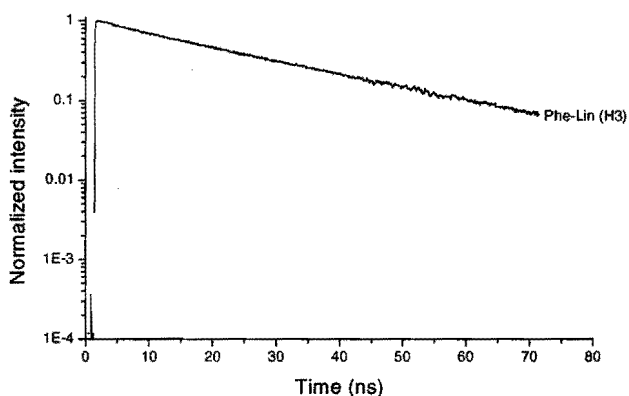


Figure 5.5. Fluorescence decay profile of hybrid H3 (Phe-Lin labeled SFO-EMA hybrid) after 4 days of drying/ageing at R.T.; $\tau_0 = 39.1$ ns. Excitation 300 nm, detection 385 nm.

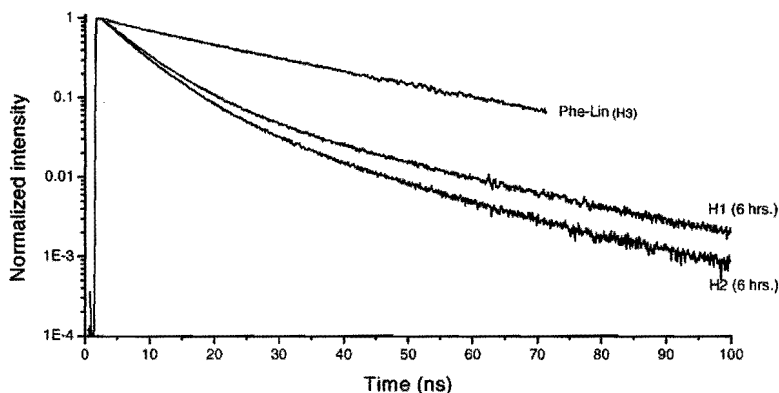


Figure 5.6. Fluorescence decay profile of Phe-Lin labeled SFO/An-Ma-labeled pEMA hybrids H1 and H2 after 6 h of drying/ageing compared to hybrid H3 (only Phe-Lin labeled). Hybrid H1 was initiated externally by *t*-BHP and H2 internally by SFO-HP. Excitation 300 nm, detection 385 nm.

order decay. This is an indication that no fast relaxation due to quenching had taken place. Hence, it was concluded that the presence of the double bonds of the SFO had little influence on the fluorescence characteristics of Phe-Lin. The

small difference in τ_0 with the one reported in literature could be caused by a difference in backbone attached to the chromophore. Also, this could have been caused by a difference in excitation pulse width. For this study the instrumental response function had a width of ca. 40 ps, as opposed to ca. 30 ns used by Zhao *et al.* [4].

Typical fluorescence decay profiles of the Phe-Lin-labeled SFO/An-MA-labeled pEMA hybrid latexes initiated externally by *t*-BHP (H1) and hybrid latexes initiated internally by SFO-HP are given in Figure 5.6. These fluorescence decay profiles clearly showed a difference in the initial degree of mixing between the SFO-acrylic system initiated externally by *t*-BHP and the SFO-acrylic system initiated internally by SFO-HP using the ROOH/Fe²⁺-EDTA/SFS redox initiation system. The sharper decrease of the fluorescence decay profile of H2 after 6 hours of drying/ageing indicated that the quenching of Phe-Lin by An-MA was stronger in the SFO-HP-initiated system. Hence, it was concluded that in films prepared from the SFO-HP-initiated latexes the initial degree of mixing was higher. This initially higher degree of mixing may result from the compatibilization effect of oil-acrylic copolymer resulting from initiation by the fatty-acid hydroperoxides.

For determination of the effect of time (and cross-linking by autoxidation) on films prepared from hybrids H1 and H2 the films were aged for longer periods (up to 20 days). The two analytical models described in the introductory section of this chapter were used for the analysis of the fluorescence decay results. The fluorescence decay profiles of films prepared from the blend (B1) and of films prepared from solvent-borne hybrids were used to compare the results with a totally phase-separated system and a fully mixed system. These results are discussed in the next section.

Methods of Analysis

A first approach for analysis of fluorescence decay data was carried out by fitting the experimental data to a sum of exponential terms. In this approach the pre-exponential factors were normalized by dividing the sum of the raw values for that particular sample. This was carried out as a first attempt to correct for thickness variations from one sample to the next. Attempts to fit a linear combination of stretched exponential and first-order decay models were unsuccessful. The failure of this approach is prove for the complex nature of the energy-transfer processes taking place in the films prepared from the hybrid latexes.

The use of a sum of first order exponential terms resulted in good fits when four time constants were used, τ_1 to τ_4 . These four time constants can be considered as resulting from different modes of energy transfer of the chromophore.

The results of the analysis of the films by fitting with a sum of first-order exponential terms for the films prepared from H1 in time and of H3 and the blend are presented in Figure 5.7. The results of the analysis of the films prepared from H2 are presented in Figure 5.8.

The τ_1 value of 39.1 ns was obtained using the data of the film prepared from H3 (only Phe-labeled) and was kept fixed for all other runs. This value represents the lifetime of the excited, unquenched donor groups. A shorter lifetime (τ_2 , ca. 14 ns) was also observed for all films. This value most likely represents the lifetime of Phe when it transfers energy to oil molecules. The third lifetime (τ_3 , ca. 5 ns) was not observed when acceptor groups were absent. Therefore, this value most likely characterizes the energy transfer from the excited Phe group to An. Finally, low τ_4 values (0.1 – 1.5 ns) were observed. This value appeared only in films that were aged for 20 days and in films that were aged at elevated temperatures. This parameter suggests the formation of fast quenching species under conditions that promote autoxidation and crosslinking of the oil.

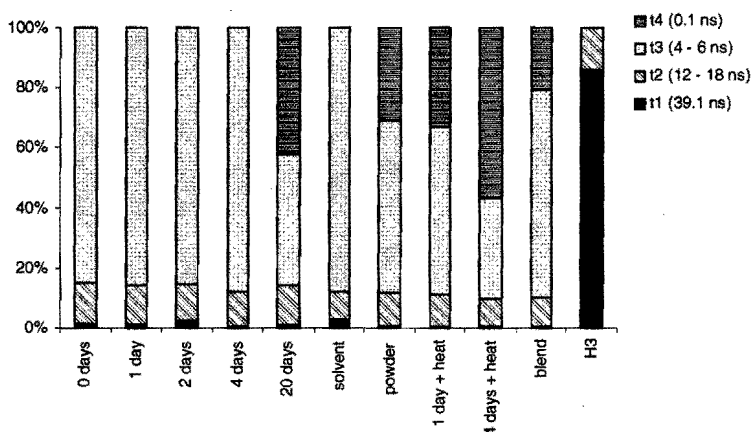


Figure 5.7. Relative values of lifetime values (τ_1 to τ_4) of films prepared from hybrid H1, aged for different periods of time, and of films prepared from the blend and from hybrid H3.

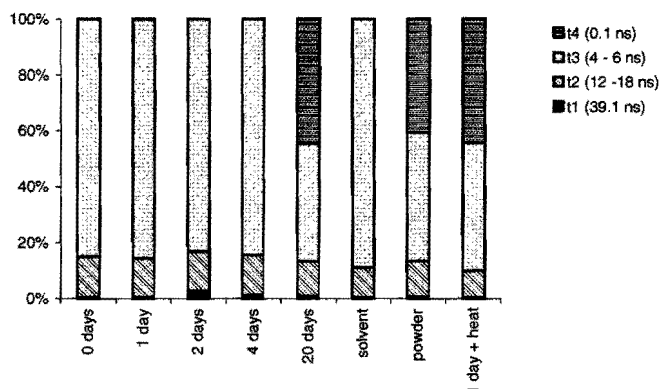


Figure 5.8. Relative values of lifetime values (τ_1 to τ_4) of films prepared from hybrid H2, aged for different periods of time.

For all samples, except for the H3 film, low values for the contribution of τ_1 were observed. This suggests that the amount of unquenched Phe-Lin in the films was low and therefore that the films were highly mixed (including the blend). Also, the normalized value corresponding to τ_2 (resulting from the quenching of Phe by the oil) was approx. constant over time and the same for the different films. Hence, it was concluded that the energy transfer by this mechanism was of little influence between the H1 and H2 system and remained small over time.

The normalized value corresponding to τ_3 was of greatest interest. This value contains information on the quenching of Phe by An and therefore on the mixing of the donor and acceptor. It was observed that the value corresponding to this time constant was approx. similar between the H1 and the H2 films and also similar to the films prepared from the solvent-borne hybrids.

One could argue that these results indicate that there is little difference between the different systems and that time has no effect on the degree of mixing (except after 20 days or after heat treatment when a considerable amount of cross-linked material has formed). However, the fluorescence decay profiles of H1 and H2 after 6 hours given in Figure 5.6 showed a considerable difference. This suggests that the normalized values obtained from fitting the decay curve do not give optimal results. A possible reason for this could be the normalization that was performed in order to exclude the effect of differences in film thickness was not correct.

From these results it was concluded that analysis of fluorescence decay profiles by fitting to a the sum of exponential terms method could be used for a first

evaluation of the different mechanisms of quenching that occur. For quantitative evaluation of the films by this analysis method a better control of the film, in particular of film thickness, is required.

Area Integration Method

In 1998 Feng *et al.* [6] introduced an alternative approach for determination of the efficiency of energy transfer. In this approach the efficiency of energy transfer (or the volume fraction of mixing) was determined from the area under the donor fluorescence decay profile $I(t)$ from samples containing both D and A using Eqn. 5.5. Calculation of the volume fraction of mixing f'_A requires A_D , the area under the profile of the donor only, A_{∞} , the area under the profile from a completely mixed system and A , the area under the profile of the decay from the hybrid film. The value of A_D could be determined from the decay profile of the film prepared from H3. It was expected that films prepared from solvent-borne systems of freeze dried H1 and H2 would supply the values of A_{∞} . However, the films prepared from the solvent-borne systems appeared to reflect incomplete mixing of A and D. Possibly this was caused by phase separation between the acrylic polymer and the Phe-Lin resin during drying. Therefore, a value of normalized area was used to determine the efficiency of mixing of the H1 and H2 hybrid films.

Figure 5.9 shows the values of normalized area determined from the area under the fluorescence decay profiles of films prepared from hybrids H1 and H2 in time. As was observed in Figure 5.6 the initial mixing of H2 is stronger than that of H1. However, it was observed that the efficiency of mixing of films prepared from H2 decreased in the first days to a value that was higher than the value obtained for H1. This behavior suggests that the phase behavior of H2 films is governed by two processes. In the initial film the acrylic and oil are mixed to a certain extent on a molecular level, but as the oil begins to polymerize by autoxidative polymerization the mobility of the Phe-labeled molecules is strongly reduced. In addition, the compatibility between the two phases is expected to decrease because of this polymerization. The result is a short mixing of the two phases, followed by demixing. The film prepared from hybrid H1 does not show this demixing. The most likely reason for this is that the initial degree of mixing is lower and that the onset of crosslinking is slower. In hybrid H2 residual hydroperoxides will result in faster crosslinking. Surprisingly, after 20 days the efficiency of mixing is similar for both H1 and H2 films. This value suggests that

at longer time the efficiency of mixing has increased upon cross-linking, compared to the initial degree of mixing and, more importantly, that the type of initiation, externally or internally, has no effect on the final degree of mixing.

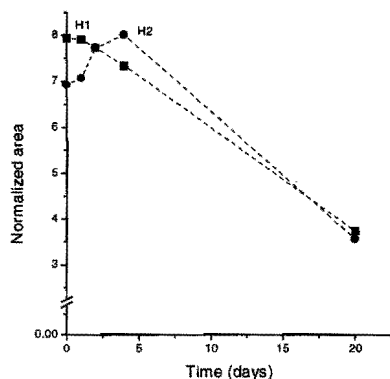


Figure 5.9. Normalized area of films prepared from H1 and H2 in times. Area determined from integration of fluorescence decay profiles.

5.4 Conclusions

The results described in this study show that valuable information on the degree of mixing of oil-acrylic hybrids and on the processes that take place during film formation and ageing of these complex systems can be obtained by fluorescence decay measurements. In oil-acrylic hybrids phenanthrene-labeled fatty acid esters can be used as donor and anthracene-labeled acrylate as acceptor. The use of this donor-acceptor couple excludes the use of commercially interesting alkyd resins in the hybrid formulation, because of background fluorescence by the resin. At the wavelengths used for excitation of the phenanthrene and detection of the fluorescence, 300 nm and 385 nm, respectively, SFO gives no significant background fluorescence.

By using the fluorescence decay profile it was shown that internal initiation by SFO-HP (H2) results in an initially more homogeneous film than by using external initiation by *t*-BHP (H1). However, these films partially phase separate

during the first days of drying. After 20 days of drying the degree of mixing of the films prepared from H1 and from H2 is equal.

5.5 References

1. P. Vink, T.L. Bots, *Verfkroniek*, 7/8, (1995) 15.
2. K. Hahn, G. Ley, H. Schuller, R. Oberthür, *Coll. Polym. Sci.*, 264, (1986) 1092.
3. O. Pekcan, L.S. Egan, M.A. Winnik, M.D. Croucher, *Macromolecules*, 23, (1990) 2673.
4. C.-L. Zhao, Y. Wang, Z. Hruska, M.A. Winnik, *Macromolecules*, 23, (1990) 4082.
5. M.A. Winnik, Y. Wang, F. Haley, *J. Coat. Tech.*, 64, (1992) 51.
6. J. Feng, H. Pham, V. Stoeva, M.A. Winnik, *J. Polym. Sci., Polym. Phys.*, 36, (1998) 1129.
7. P. Marion, J. Lang, D. Juhué, *23th Fatipac Congr. Proc.*, Vol. 1, Brussels, (1996) A-71.
8. P. Marion, G. Beinert, D. Juhué, J. Lang, *J. Appl. Polym. Sci.*, 64, (1997), 2409.
9. E. Perez, J. Lang, *Langmuir*, 12, (1996) 3180.
10. J. Vogelsang, M. Hauser, *J. Phys. Chem.*, 19, (1990) 7489.
11. R.D. Mair, R.T. Hall, in *"Organic Peroxides"*, Vol. 2, D. Swern (Ed.), Wiley, New York, (1971).
12. D. Ng, J.E. Guillet, *Macromolecules*, 15, (1982) 724.
13. R. Pecora, *"Dynamic Light Scattering"*, Plenum Press, New York, (1985) 50.
14. E. Reed, G. Frangineas, *"SPIE Proc."* Vol. 1223: Solid State Lasers (1990).
15. E.H.W. Pap, P.I.H. Bastiaens, J.W. Borst, P.A.W. van den Berg, A. van Hoek, K.W.A. Wirtz, A.J.W.G. Visser, *Biochemistry*, 32, (1993) 13310.
16. A. van Hoek, A.J.W.G. Visser, *Analytical Instrumentation* 14, (1985) 359.

CHAPTER 6: PRELIMINARY INVESTIGATIONS ON THE PERFORMANCE OF OIL/ALKYD-ACRYLIC HYBRID COATINGS

Abstract

This chapter describes the preliminary investigations carried out to determine the performance characteristics of oil/alkyd-acrylic hybrid latexes as binders for waterborne coatings. The coating performance of non-pigmented oil/alkyd-acrylic latexes was compared to that of a blend of alkyd emulsion and acrylic latex with similar chemical composition and to that of an alkyd emulsion binder.

The film morphology of the blend system was studied using transparency measurements and atomic force microscopy. It was found that a minimum volume fraction of 45% of alkyd emulsion was required for the preparation of transparent blend films. AFM imaging showed that in films prepared from blend systems the alkyd resin acted as the binder and the acrylic latex was randomly dispersed in this matrix.

The oil/alkyd acrylic hybrid latex showed a decreased drying time when compared to the blend system and the alkyd emulsion. The gloss of films prepared from the hybrid systems was similar to that of the blend system but lower than that of the film prepared from the alkyd emulsion. The hardness of the various systems was similar with the exception of the fatty-acid hydroperoxide-initiated hybrid, which initially showed a slightly higher hardness.

6.1 Introduction

The ultimate objective of the research carried out on paints and coatings is the development of new systems that give better performance than existing systems. The performance of these new, or improved, systems is generally evaluated according to specific requirements emanating from the application they were designed for. For instance, for outdoors wood coatings a system is required that shows short drying time, ease of application, does not emit volatile organic components, gives good and durable protection to the wood and has good weatherability properties. The performance properties of the coating systems are for a great part determined by the properties of the main components of the coating system, *i.e.*, the binder, the pigments and the carrier (or solvent).

This chapter describes the preliminary investigation on the performance of coatings prepared from alkyd-acrylic hybrid latexes. These latexes were designed for use as binders in VOC-free waterborne decorative coatings. In our previous studies, described in Chapters 2 to 5 of this thesis, the preparation of alkyd-acrylic hybrid latexes with varying compositions was investigated. Also, the morphology of these hybrid latexes and of films prepared from them was analyzed. In the current study the developed alkyd-acrylic hybrid latexes were formulated to a non-pigmented coating system using a minimal amount of additives. Only additional surfactant, primary driers and, if necessary for film application, thickener were added. Secondary driers, pigments and other additives were not added.

The performance of the hybrid coating system, *i.e.*, drying time, cross-linking, hardness and gloss, was compared to that of a blend system and of an alkyd emulsion. The blend system was composed of an alkyd emulsion and an all-acrylic latex with the same chemical composition as the alkyd-acrylic hybrid and was formulated in a similar manner. The comparison of the various systems and the evaluation of the coating performance are described in the final part of this chapter.

First results on the morphology study of films prepared from the blend system are described, as it was expected that this study would be beneficial for the comparison of the coating properties of the blend and hybrid systems. Furthermore, several new binders based on blends of waterborne systems have been developed in recent years [1-6]. For these reasons the morphology of films prepared from blend systems was analyzed using atomic force microscopy (AFM) and transparency measurements. This is described in the first part of this chapter.

6.2 Experimental

6.2.1 Materials

Sunflower oil (SFO, Rhenus B.V. The Netherlands) was purified by filtration over a florisil (Merck) column. The alkyd resin was kindly supplied by DSM Resins (AH98, Zwolle, The Netherlands). Sodium dodecyl sulfate (SDS, Fluka BioChemica., very pure), ethylene-diaminetetraacetic acid (EDTA, Merck), sodium formaldehyde-sulfoxylate (SFS, Merck), sodium hydrogencarbonate (NaHCO_3 , Merck), ferrous sulfate hexahydrate ($\text{FeSO}_4 \cdot 6\text{H}_2\text{O}$, Merck), hexadecane (HD, Merck), *tert*-butyl hydroperoxide (*t*-BHP, Merck), nonionic surfactant (Berol-048, Akzo-Nobel, Sweden), Co-siccative (WEB-Co, 8% Co, Servo Delden), associative thickener (Acrysol 2020, Zeneca resins), as well as the solvents iso-octane (Aldrich), methyl ethyl ketone (MEK, Aldrich) and tetrahydrofuran (THF, Aldrich) were all used as received.

6.2.2 Preparation and Formulation of the Systems

Alkyd-Acrylic Hybrids

Alkyd-acrylic hybrid latexes with various ratios of oil/alkyd to acrylic were prepared by mini-emulsion polymerization according to the procedures described in Chapter 4 (Section 4.3.2). The polymerization of the acrylic monomer, ethyl methacrylate (EMA), was initiated by *t*-BHP or by sunflower-oil hydroperoxide (SFO-HP) in an $\text{ROOH}/\text{Fe}^{2+}$ -EDTA/SFS redox initiation system. The hybrids were composed of various proportions of sunflower oil (SFO), or oxidized sunflower oil (SFO-HP), and alkyd resin, to monomer (EMA). The composition and the properties of the hybrids prepared are presented in Chapter 4 (Table 4.3).

After preparation of the alkyd-acrylic hybrids non-ionic surfactant (Berol-048, 3 w% of solids) and drier (WEB-Co, 0.1 w% on oil/alkyd) were added and the system was allowed to equilibrate for 48 h and 24 h, respectively. After equilibration associative thickener (0.1 w% to 0.5 w% on total emulsion) was added for control of viscosity during film application.

Alkyd-Acrylic Blends

Blends of alkyd emulsion and all acrylic latex with various ratios of alkyd emulsion to acrylic latex were prepared for analysis of the film structure and for comparison with the hybrids. The alkyd emulsion (Ak1) was prepared by direct emulsification of the alkyd resin AH98 in water according to the procedure described in Chapter 4 (Section 4.3.2). The surfactants SDS and Berol-048 were used for stabilization. The all acrylic latex (Ac1) was prepared by mini-emulsion polymerization using EMA as monomer according to the procedure described in Chapter 4 (Section 4.3.2). SDS was used as surfactant and hexadecane as the hydrophobe for the preparation of the all acrylic latex. The composition and properties of Ak1 and Ac1 are presented in Table 6.1. After preparation of the Ac1 latex additional non-ionic surfactant (Berol 048, 3 w% on solids) was added. The latex was allowed to equilibrate for 3 days under gentle shaking and was combined with various amounts of alkyd emulsion Ak1 to form the blends. The blends were mixed by gently shaking for 24 h. After mixing and equilibration of the blends drier was added (WEB-Co, 0.1 w% Co on oil/alkyd) and the formulated blend systems were vigorously shaken for 1 min. The compositions of the blends prepared are presented in Table 6.2. The formulated blends were stored under nitrogen while shaking gently until further use.

Film Preparation

Film samples were prepared on polypropylene sheet (Moplefan CD442) and on glass plates. Because of ease of removal of the dried films polypropylene sheet was used as substrate for the preparation of free films. These films were used for analysis of the chemical composition (gel content). Films of alkyd-acrylic hybrid

Table 6.1. Composition and Properties of Alkyd Emulsion and Acrylic Latex used for Preparation of Blend Systems

| | SFO (w%) | AH-98 (w%) | EMA (w%) | Solids (w%) | D _{av} (nm) | Mn ($\times 10^{-3}$) | Mw ($\times 10^{-3}$) |
|-----|-------------|---------------|-------------|----------------|-------------------------|----------------------------|----------------------------|
| Ak1 | 33.7 | 66.3 | - | 50 | 230 ^a | - | - |
| Ac1 | - | - | 100 | 50 | 180 | 139.1 | 876.5 |

a) Measured using Malvern Mastersizer

Table 6.2. Composition of the Formulated Blend Systems Used

| | Φ_A^a | Ak1 (g) | Ac1 (g) | WEB-Co (μL) ^b |
|------|------------|------------|------------|--|
| B-40 | 0.4 | 40 | 60 | 25 |
| B-45 | 0.45 | 45 | 55 | 28.2 |
| B-50 | 0.5 | 50 | 50 | 31.3 |
| B-55 | 0.55 | 55 | 45 | 34.4 |
| B-60 | 0.6 | 60 | 40 | 37.5 |

a) Volume fraction of alkyd emulsion

b) Amount (μL) of WEB-Co (8% Co) added to 10 mL of blend

latex, alkyd-acrylic blends and alkyd emulsion were applied on polypropylene sheet using a doctor blade (wet film thickness of 300 μm). After 48 h the films were carefully removed from the substrate and the free film was aged in the air until further analysis.

Film samples for hardness and gloss measurements were prepared on glass plates using a doctor blade (wet film thickness 120 μm).

6.2.3 Analysis

Atomic Force Microscopy (AFM)

AFM experiments were carried out using a Nanoscope III Multimode microscope (Digital Instruments, Santa Barbara, U.S.A.). AFM height and phase images were obtained simultaneously at ambient conditions while operating the instrument in tapping mode. Force modulation images were obtained in contact mode. Commercial etched silicon nitride cantilevers of 125 μm (spring constant 20-100 N/m, resonance freq. 298-369 kHz) and of 400 μm (spring constant 5-10 N/m, resonance freq. 6-8 kHz) were used for imaging in tapping mode and for force modulation imaging, respectively (Nanoprobe™ TESP, Digital Instruments, Santa Barbara U.S.A.). Images were obtained at a scan rate of 1 Hz, with 512 lines. The image size ranged from 1 x 1 μm^2 to 15 x 15 μm^2 .

Films to be imaged were prepared by placing a drop of blend emulsion onto freshly cleaved muscovite mica (EMS, USA). The emulsion was spread out on the mica using the top of a pipette. The films were allowed to dry at ambient temperature for 2 days prior to imaging.

Hardness

The hardness of the films on glass was determined using a König pendulum hardness measurement (Braive instruments). The hardness measurements were carried out at indoors atmospheric conditions (temperature varying from 18 to 25 °C, R.H. varying from 20% to 45%). The hardness was calculated as the average value from three measurements on different locations on the film.

Gloss

The gloss of the films on glass was measured at angles of 20°, 60° and 85°. The gloss was calculated as the average value of five measurements on different locations on the film.

Transparency

Film transparency was measured using a UV-Vis spectrometer (Shimadzu UV-160 A), and recorded as transmittance at 550 nm. Films were prepared by spreading blends of pEMA latex and alkyd emulsion onto cleaved pMMA cuvettes and air-drying at room temperature for 1 h prior to the measurement.

Chemical Composition

The chemical composition of films prepared from alkyd-acrylic hybrid latexes, from alkyd-acrylic blends and from alkyd emulsions was determined by soxhlet extraction. After a predetermined time of drying the free films were cut into small pieces and subsequently extracted for 48 h each by iso-octane, methyl ethyl ketone (MEK) and tetrahydrofuran (THF). The iso-octane was used for selective extraction of non-cross-linked oil and -alkyd resin and the pEMA was extracted using the MEK and THF. The composition of the films, *i.e.*, non cross-linked oil/alkyd, pEMA and gel content, was calculated from the weight of selectively extracted material and residual material after removal of the solvent and drying in vacuum for 24 h (at 30 °C).

Drying Time

Drying time was recorded using a Bekker-Koller (BK) drying time analyzer (Braive Instruments). Films were prepared on long glass bars using a film applicator (120 µm wet film thickness). The drying time was visualized as

consisting of four phases resulting from the trace pattern of the needle in the film (schematically shown in Figure 6.1).

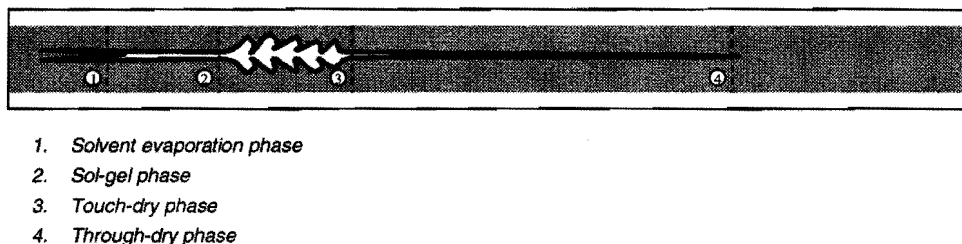


Figure 6.1. Trace pattern of the needle in a drying film

6.3 Results and Discussion

6.3.1 Morphology of Films Prepared from Blend Systems

The surface morphology of films prepared from blends of alkyd emulsion (Ak1) and acrylic latex (Ac1) was studied using Atomic Force Microscopy. In addition, the bulk morphology of films prepared from blends of various compositions was studied using transparency measurements. The use of transparency measurements as a method for evaluation of films prepared from blend systems was described by Feng *et al.* [6]. The films were prepared on the inside of vertically cut pMMA cuvettes. Once dried, they were visually evaluated and the percent transmittance was measured by UV-Vis spectroscopy. The transparency phase diagram, describing the transparency of films prepared from alkyd-acrylic blends with various fractions of alkyd emulsion, is presented in Figure 6.2. Figure 6.2 shows that the transmittance of films prepared from blends with a fraction of alkyd emulsion in excess of 0.45 was in the order of 70% to 85% at 550 nm. These films were optically clear. At lower fractions of alkyd emulsion non-transparent films were observed with a transmittance of 0% to 1%. The critical volume fraction of alkyd emulsion (Φ_c), at which a clear film could be obtained, was approximately 0.45. This critical volume fraction of soft material was in agreement with the value reported by Feng *et al.* [7,8] for films prepared from blends of hard and soft acrylic latexes.

Transparent films can be obtained when there are negligible voids remaining in the film, which can scatter light [9]. This requires complete coalescence of the

particles in the film. Other criteria for transparency in a blend film are a close match of the refractive indexes (RI) of the components (typically the RI mismatch should be smaller than 0.01 [10]) and a good dispersion of the 'hard' particles [11]. The optical clarity of the films observed at a Φ_A of 0.45, and higher, suggests a good coalescence of the alkyd emulsion droplets and the acrylic particles and a good match of the refractive indexes of the alkyd resin, the sunflower oil and the acrylic polymer. Most likely, the soft alkyd resin forms the continuous phase, with the hard acrylic particles evenly dispersed in this phase. The difference in refractive index of the alkyd resin/sunflower oil and the pEMA is larger than 0.01. This should result in opaque films. A possible explanation of the observed transparency at Φ_A of 0.45 and higher could be that the sunflower oil or the alkyd resin partly dissolves in the pEMA and thereby decreases the mismatch in refractive index.

The non-transparency observed at alkyd fractions lower than 0.45 was most probably caused by air voids between acrylic particles that were created when not enough oil and alkyd resin was present to completely 'wet' the hard acrylic particles.

Atomic force measurements were carried out for analysis of the morphology of the surface of films prepared from blends of alkyd emulsion and of acrylic latex. A typical topographic image of a surface corresponding to a clear film ($\Phi_A = 0.6$) is presented in Figure 6.3. This image shows a smooth surface with a small number of spherical structures protruding from the surface. These spherical

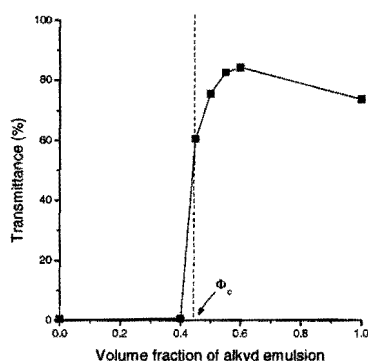


Figure 6.2. Plot of percent transmittance vs. volume fraction of alkyd emulsion in the blend.

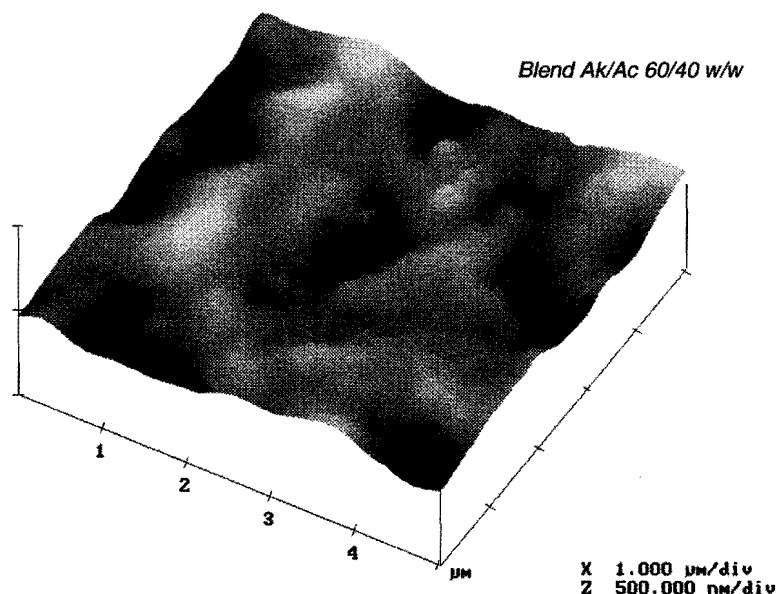


Figure 6.3. Side-view image of film prepared from alkyd-acrylic blend with 60 w% of alkyd emulsion and 40 w% of acrylic latex

structures most likely are the dispersed acrylic particles. The image shows that the acrylic particles were randomly dispersed in the film. A typical topographic image corresponding to an opaque film ($\Phi_A = 0.40$) is presented in Figure 6.4. This image shows a large number of particles and generally a relatively rough surface (z-axis is expanded in the image). The particles were spherically shaped and showed no deformation. Smooth areas corresponding to alkyd resin (as observed in Figure 6.3) were not observed. These observations confirm the results of the transparency measurements, which suggested that below $\Phi_A = 0.45$ not enough alkyd resin was present to 'wet' the acrylic particles. The effect of lower concentrations of acrylic latex on the number of particles visible at the surface of the films is shown in Figure 6.5. The images presented in Figure 6.5 showed that a decreased concentration of acrylic particles in the formulation of the blend resulted in a decreased number of particles at the surface. These images are presented in the phase mode for increased contrast between alkyd resin and acrylic particle. This result indicates that the acrylic particles are randomly distributed in the alkyd resin matrix. Information on the distribution

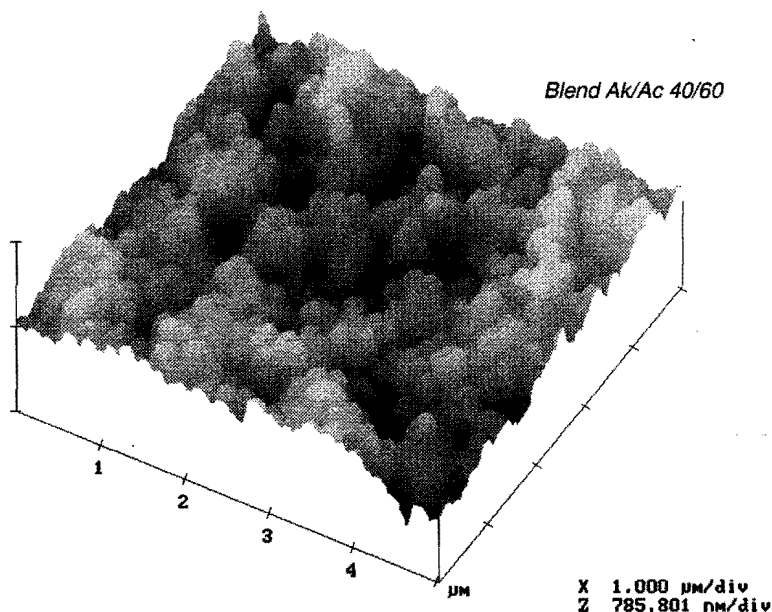


Figure 6.4. Side-view image of film prepared from alkyd-acrylic blend composed of 40 w% of alkyd emulsion and 60 w% of acrylic latex

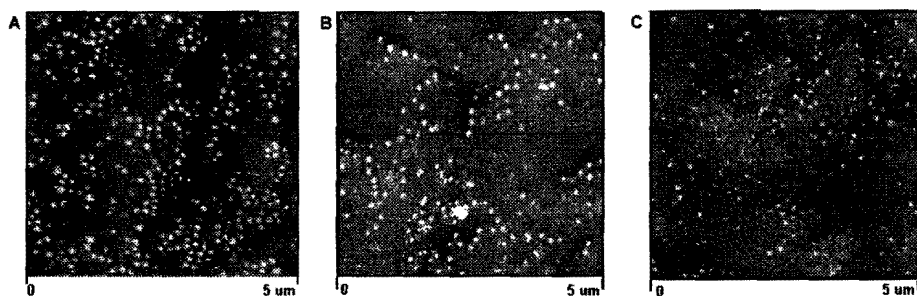


Figure 6.5. AFM images (phase mode) of surfaces of films prepared from blends with various alkyd-acrylic compositions. Volume fraction alkyd (Φ_A) is 0.50 (A), is 0.55 (B) and is 0.60 (C).

of the acrylic particles was considered to be of importance because a non-random distribution was expected to be of influence on the final coating performance. For instance, because of 'floating' or 'sinking' of the acrylic

particles in the alkyd resin matrix films with a certain degree of stratification could be formed. This stratification could result in differences in properties of the films. The images presented in the Figures 6.3–6.5 indicate that the acrylic particles are dispersed in the alkyd resin matrix. These images do not show the, partial, mixing between the acrylic polymer and the alkyd resin that was suggested as a possible reason for the observed transparency. Force modulation imaging was used in order to determine if mixing between the alkyd resin and the acrylic polymer particle had occurred. Force modulation imaging is a contact mode technique that provides mechanical information to complement topographic data. With the use of force modulation local stiffness can be mapped and this stiffness can be correlated to topographic features on the surface [12,13].

Figure 6.6a and Figure 6.6b represent the topographic and force modulation images of a typical film prepared from a blend system (alkyd volume fraction $\Phi_A = 0.8$). The film was imaged at low fraction of acrylic particles in order to be able to optimally visualize the acrylic particles in the force modulation image. In correspondence with topographic images obtained in tapping mode Figure 6.6a showed spherical structures protruding from the surface, reminiscent of acrylic particles. At the same locations the force modulation image in Figure 6.6b showed dark spherical structures. This dark color is the result of a higher stiffness. The resolution of the force modulation image was not high enough to show whether softening at the edge of the particles had occurred because of

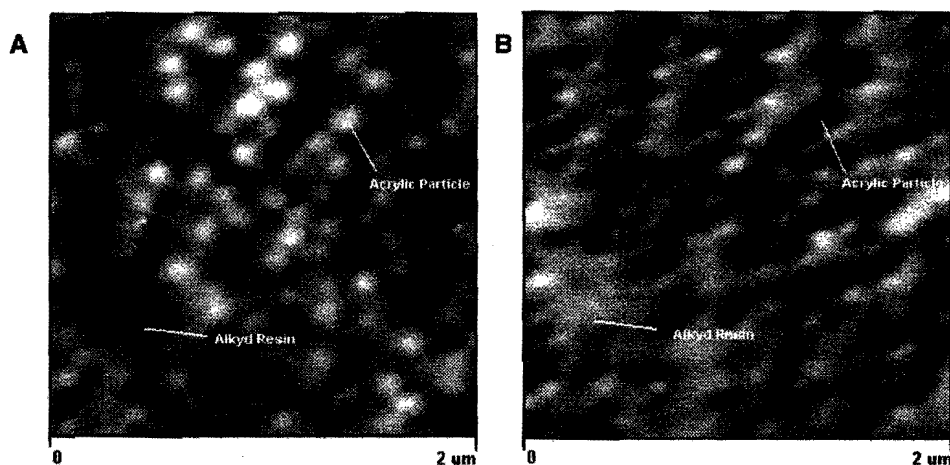


Figure 6.6. AFM Image of blend of alkyd emulsion and acrylic latex (ratio Ak/Ac 80/20). (A) Top-view of height image, (B) Top-view image of force-modulation.

diffusion of oil, but the strong difference in stiffness indicted that this was not the case.

From the transparency measurements and the AFM analysis it was concluded that clear films could be prepared from blends of alkyd emulsion and acrylic latex. In these films the alkyd resin forms the matrix and the acrylic particles are randomly dispersed in this matrix.

6.3.2 Coating Performance of Hybrids vs. Blends

The results of the drying time, gloss and hardness measurements and the appearance evaluation of films prepared from the various formulated systems are presented in Table 6.3. For good comparison between the various systems the chemical composition of the systems was designed to be similar and the same types of additives were added in similar amounts (except for the single component systems Ak1 and Ac1).

The results presented in Table 6.3 showed interesting differences between an alkyd-acrylic blend binder and the alkyd-acrylic hybrid binders. The most significant difference between the two systems was observed with the drying time of the films. Films prepared from the hybrid latexes typically showed a drying time of approx. 3 h. This drying time was not only observed for hybrids containing 50 w% of acrylic polymer but also at lower acrylic polymer content (to 25 w%). The drying time of films prepared from the blend systems was 16 h. These results indicated a difference in drying process between the hybrid system and the blend system.

Table 6.3. Properties of Coatings Investigated

| | Ak1 | Ac1 | H3-50 | H4-50 | B-50 |
|------------------------------|-------|---------------------|-------|-------|------|
| Hardness after 3 days (s.) | 19 | .. ^b | 22 | 17.4 | 22.4 |
| Gloss (60°) | 146 | .. ^b | 70 | 63 | 69 |
| Drying Time ^a (h) | 13 | < 1 | 3 | 3 | 16 |
| Film Appearance | clear | opaque ^b | clear | clear | hazy |

a) Time to reach stage 4 of drying

b) Film was cracked

The difference in drying process between the blend system and the hybrid system was also observed in the structure of the trace resulting from the needle in the film during drying. The trace in the films prepared from the blend system showed the four phases as described in Section 6.2.3. However, the trace in the films prepared from the hybrid systems did not show phase 3, the touch-dry phase. The occurrence of phase 3 in a drying time measurement is typical for autoxidatively drying systems, like alkyd emulsions. In autoxidatively drying systems the rate of crosslinking at the air-surface is higher than in the layer underneath. This results in the formation of a 'skin' layer at the surface of the film. With the movement of the needle through the film in time this 'skin' results in the film appearance typically described as phase 3 of drying in a BK drying time measurement.

More detailed visual observations of the films on glass plates during drying confirmed the observed difference between the blend system and the hybrid system. In the initial stages of drying, during the water evaporation, films prepared from the hybrid systems showed a single drying front (from transparent to white) moving from the outside of the film to the center. The occurrence of this front was also reported by Winnik [5] and was described to result from the transition of non-coalesced particles in water to a film of coalesced particles. The front was described to move from the outmost region of the film to the center because of differences in film thickness. Upon time this drying front moved to the center of the film. A schematic representation of the observed drying front is presented in Figure 6.7.

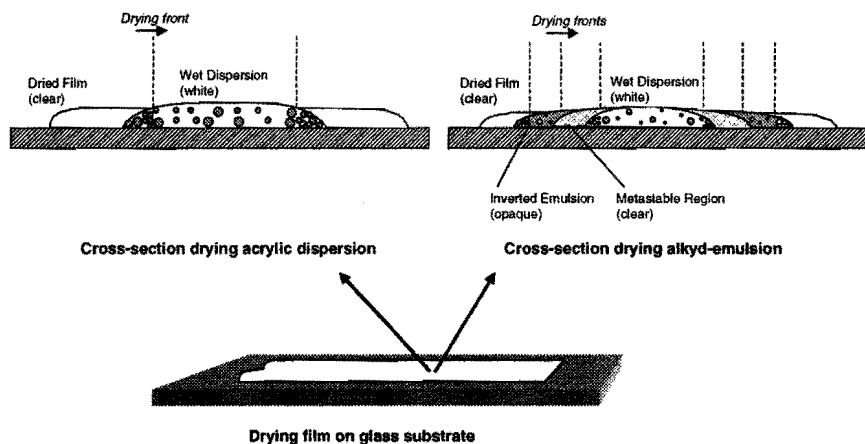


Figure 6.7. Schematic representation of drying fronts observed during drying of acrylic dispersion and of alkyd emulsion.

During drying of the alkyd-acrylic blend binder a different pattern was observed. From the center of the film to the outermost region three fronts were observed. A schematic representation of the observed fronts is given in Figure 6.7. This pattern of drying was also observed during drying of the alkyd emulsion.

In Chapter 4 (Section 4.3) the drying of alkyd emulsions was described as taking place in four stages. It is suggested that these four stages were visualized by the three drying fronts, going from the outside of the film to the center. During drying of the alkyd emulsion or the blend system a phase inversion from an oil-in-water emulsion (white) to a water-in-oil emulsion (opaque) takes place. This phase transition involves a meta-stable (clear) transition stage. After phase separation further evaporation of the water results in a clear film. Most likely the drying fronts observed during drying of the alkyd emulsion and the blend system are the resultant of these transitions.

The drying time results and the visual observations during drying of the films prepared from the various systems suggest that the hybrid latexes dry in a similar manner as acrylic latexes. The drying process of the blend system, on the other hand, is similar to that of an alkyd emulsion.

The results presented in Table 6.3 also showed small differences in hardness and gloss between the various coating systems. The gloss of the alkyd emulsion film was high compared to the blend system. The gloss is strongly related to the surface roughness. As observed with the AFM analysis, the surface of the films becomes rougher with the blending of acrylic particles into the alkyd emulsion. This explains the decrease in gloss. The relation between the acrylic latex content and the gloss is presented in Figure 6.8. Figure 6.8 shows a strong drop in gloss in the region around the critical volume fraction of alkyd ($\Phi_c = 0.45$). At 20° and 85° the same trend was observed. Although less pronounced, a similar relation between the gloss and the chemical composition was observed for the hybrid systems in the region of 75% of alkyd to 25% of alkyd. In the hybrid systems this effect is probably the result of stronger deformation at higher alkyd resin contents.

The hardness of the various systems after 3 days of drying did not show large differences. After 28 days of drying all three systems showed a small increase in hardness. It was expected that the presence of acrylic resin in both the blend system and the hybrid systems would result in an increase in hardness. However, this was not observed. Because of cracks in the films the hardness of the all acrylic films could not be measured. Therefore, comparison of the hardness of this system with the other systems was not possible.

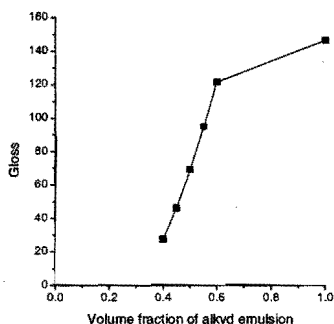


Figure 6.8. Gloss values at 60° of films prepared from blends with varying volume fractions of alkyd emulsion.

A small difference in hardness was observed between the two hybrid systems. After 3 days of drying the film prepared from hybrid H3-50 showed a higher hardness than the film prepared from H4-50. Since both hybrids had a similar chemical composition this difference is most probably caused by the more homogeneous particles structure of the sunflower oil hydroperoxide-initiated system. In addition, the difference in hardness could have resulted from an enhanced level of crosslinking in the case of H3-50 because of residual hydroperoxides.

The chemical composition of films prepared from the various systems after varying periods of drying were determined by soxhlet extraction. The films were cut into small pieces and extracted subsequently by iso-octane, MEK and THF. Iso-octane is a good solvent for non cross-linked alkyd resin and a non-solvent for the acrylic polymer. MEK and THF both are good solvents for the acrylic polymer. With the use of this sequential extraction information on the chemical composition, *i.e.*, the content of non-cross linked oil/alkyd, the content acrylic polymer and the gel content, was obtained.

The evolution of the chemical composition of films of the various systems in time are presented in Figure 6.9a to Figure 6.9d. After 4 days the alkyd emulsion showed a gel content of 35%. This gel content increased to approx. 70% after 8 days and remained constant thereafter (Figure 6.9a). In the blend system a gel content of 40%, an acrylic polymer content of 40% and an alkyd content of 20% was observed after 4 days. In time (up to 28 days) the content of alkyd resin decreased and the gel content increased (Figure 6.9b). The content of acrylic polymer remained approximately constant in time.

The chemical composition of the hybrids H4-50 and H3-50 showed a similar crosslinking pattern in time as the blend system. For determination of the chemical composition after mixing the hybrid latexes were freeze-dried immediately after addition and equilibration of the drier. The gel content after freeze-drying was approx. 20% for the H4-50 hybrid and approx. 35% for the H3-50 hybrid. Analysis of the chemical composition of freeze dried hybrid latexes prior to the addition of the drier showed approx. 50% of alkyd resin and 50% of acrylic polymer for both systems.

These results show that a considerable amount of cross-linking occurred during the equilibration of the drier. The continuous shaking of the hybrids in the presence of air may have caused this. Also, these results confirm that the increased hardness observed for the H3-50 film was the result of increased crosslinking in the first three days. After 10 days the gel content of both systems was approx. 40%. The acrylic polymer content remained constant in time for both

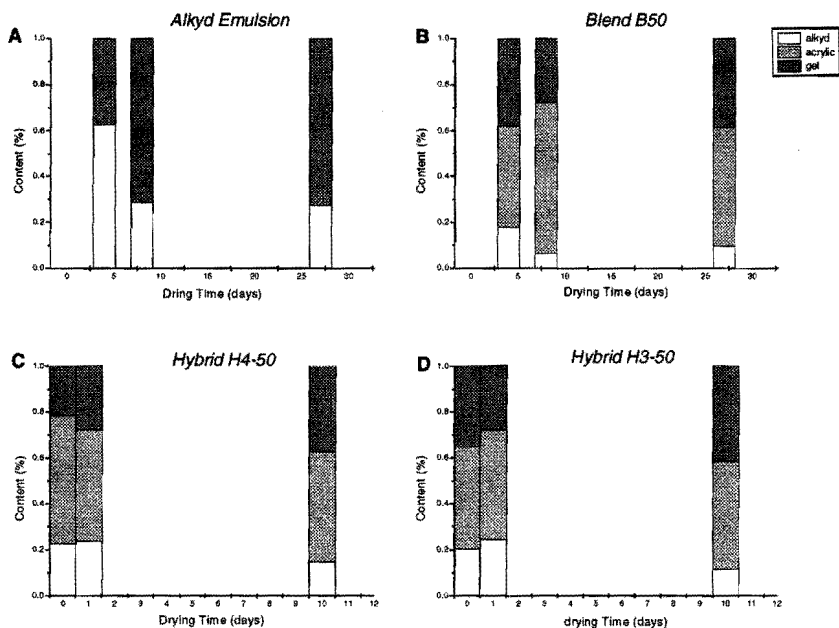


Figure 6.9. Chemical composition, alkyd resin content, acrylic content and gel content, in time of films prepared from various binder systems; alkyd emulsion (A), blend B-50 (B), hybrid H4-50 (C) and hybrid H3-50 (D).

systems. This indicates that for both hybrid systems the amount of acrylic polymer trapped (via semi-IPN) in the cross-linked network of the alkyd resin was small. However, this method was not considered to be accurate enough to analyze the incorporation of small amounts (1 to 2%) of oil-poly acrylate copolymer that was expected to result from initiation by fatty-acid hydroperoxides.

6.4 Conclusions

The results presented in this chapter are twofold. First, analysis of the morphology of films prepared from blends of alkyd emulsion and acrylic latex showed that transparent films can be obtained when the fraction of alkyd emulsion is 45% or higher. In the blend films the alkyd resin forms the continuous matrix. The acrylic particles are randomly dispersed in this matrix.

The function of the alkyd resin as the binder, or continuous matrix, is also observed in the coating performance analysis. The drying time and drying process of the blend system is similar to that of an alkyd emulsion. The hybrid system, on the other hand, shows a short drying time over a wide composition range. Other properties, like gloss and hardness are approx. similar to those found for the blend and alkyd emulsion system. The initial hardness of films prepared from hybrids initiated by fatty-acid hydroperoxides is higher because of increased crosslinking in the first time-period.

From this preliminary investigation on the coating performance of alkyd-acrylic hybrids latexes as compared to alkyd-acrylic blends and alkyd emulsions, it is concluded that alkyd-acrylic hybrid latexes offer promising properties as binders for VOC-free waterborne coatings, unparticular because of their short drying time and clear film appearance. These results justify future research on the complete formulation and application of oil-acrylic hybrid latexes.

6.5 References

1. C.R. Hegedus, K.A. Klotz, *J. Coat. Tech.*, 86 (860), (1996) 39.
2. A. Hoffland, R. van der Linde, R.A. Bayards, Eur. Patent 0551942 A2, (1993).

3. M.P.J. Heuts, R.A. le Fèvre, J.L.M. van Hilst, G.C. Overbeek, *Polym. Mat. Sci. Eng.*, 73, (1995) 140.
4. A.J. Fream, S. Magnet, *Färg och Lack Scand.*, 1, (1998) 4.
5. M.A. Winnik, J. Feng, *J. Coat. Tech.*, 68 (852), (1996) 39.
6. J. Feng, M.A. Winnik, R.R. Shivers, B. Cubb, *Macromolecules*, 28, (1995) 7671.
7. J. Feng, M.A. Winnik, *Polym. Mater. Sci. Eng.*, 73, (1995) 252.
8. J. Feng, M.A. Winnik, A. Siemiarczuk, *J. Polym. Sci., Polym. Phys.*, 36, (1998) 1115.
9. D.R. Karsa, in *"Additives for Water-based Coatings"*, Royal Chem. Soc., London, (1990).
10. L. Bohn, in *"Polymer Handbook"*, 2nd Ed., J. Brandrup, E.H. Immergut (Eds.), Wiley, New York, (1975) 111.
11. S.L. Rosen, *Polym. Eng. Sci.*, 7 (2), (1967) 115.
12. A.G. Gilcinski, C.R. Hegedus, in *"Film Formation in Waterborne Coatings"*, M.A. Winnik, T. Provder, M. Urban (Eds.), ACS Symp. Ser. 648, (1996) 286.
13. A.A. Galuska, R.R. Poulter, K.O McElrath, *Surf. Int. Anal.*, 25, (1997) 418.

CHAPTER 7: GENERAL DISCUSSION & PROSPECTS FOR FURTHER RESEARCH

7.1 Introduction

The investigations described in this thesis were aimed at the development of oil-acrylic hybrid latexes for binders of high performance waterborne coatings. Mini-emulsion polymerization of the acrylic monomer in the presence of vegetable oil or alkyd resin was applied for the preparation of the hybrid latexes. For optimal performance of these hybrid systems, control of the morphology of the latex particles and knowledge on the translation of particle morphology and film formation to coating properties was considered to be of utmost importance. Therefore, the research was focused at the preparation and characterization of the hybrid latexes and at characterization of the films prepared from these hybrids.

In general the results obtained belong to two categories. On the one hand, the preparation of oil-acrylic hybrid binders was investigated. On the other hand, a number of recently developed techniques for analysis of particle morphology and film structure, *i.e.*, Atomic Force Microscopy (AFM), Cryogenic TEM and fluorescence resonance energy transfer, were used for the analysis of the oil/alkyd-acrylic hybrid system. Their use for analysis of the complex oil-acrylic hybrid system has resulted in new application methods of these techniques and in increased understanding of the process. In the next sections of this chapter these results are discussed in more detail.

7.2 Oil-Acrylic Hybrid Latexes by Mini-Emulsion Polymerization

The preparation of oil-acrylic hybrid latexes was carried out using a mini-emulsion polymerization process. With the use of this emulsion polymerization technique, nucleation is directed towards the oil-monomer droplets and the occurrence of secondary nucleation is strongly suppressed. This makes mini-emulsion polymerization particularly well suited for the preparation of oil-acrylic hybrid latexes. In general, mini-emulsion polymerization can be considered as an excellent method for the preparation of hybrids of polyester-type of resins and addition-polymerization type of polymers. Examples of other hybrid systems prepared by mini-emulsion polymerization are polyester-acrylate and polyurethane-acrylate hybrids [1]. An additional advantage for the preparation of hybrids of polyesters and addition-polymerization type of polymers is that the monomer can act as solvent for the polyester. The resultant reduction in viscosity increases the efficiency of direct emulsification.

Although not discussed in this thesis, the process of mini-emulsion polymerization could in principle also be used for the preparation of oil-acrylic hybrid latexes using acrylic monomers functionalized with unsaturated fatty-acid chains (fourth approach described in Chapter 1). In a mini-emulsion polymerization, diffusion of such monomers through the aqueous phase is not required, in contrast to conventional emulsion polymerization.

From the results presented in this thesis it is concluded that the limitation in conversion is at present the major drawback of the use of mini-emulsion polymerization for the preparation of oil-acrylic hybrid latexes. Others also reported that 100% conversion was not obtained when using mini-emulsion polymerization [1,2]. The reasons for this limitation are not clear yet. It is obvious that this issue needs to be addressed for the successful practical application of mini-emulsion polymerization.

The compatibility between the vegetable oil phase and the acrylic polymer phase is increased with the use of initiation by fatty-acid hydroperoxides in an ROOH/ Fe^{2+} -EDTA/SFS redox initiation system. When compared to the use of an external hydroperoxide initiator, this type of initiation can be expected to result in the formation of a higher amount of copolymer of oil resin and acrylic polymer. The presence of oil-acrylic copolymer could not be experimentally determined. However, the cryo-TEM analysis of sunflower oil-acrylic (MMA) hybrids indicates increased homogeneity of the resultant particles for the SFO-HP initiated system. Phase separation between the oil phase and the acrylic phase was not observed when using EMA as monomer. These results suggest that the incompatibility

between acrylic polymer and alkyd or oil resin is reduced when the chain length of the ester group of the acrylic polymer increases. This is in agreement with the results reported by Schork *et al.* [3], who did not find indication for phase separation when an MMA-BMA copolymer was used. Therefore, it is questionable whether initiation by fatty-acid hydroperoxides is necessary for the preparation of a film-forming oil-acrylic hybrid latex or not. The cryo-TEM analysis of hybrids prepared with EMA suggests that initiation by *t*-BHP gives a similar particle morphology as initiation by SFO-HP. However, analysis of the degree of mixing on micro-scale by fluorescence microscopy of films prepared from the different hybrids indicates that initiation by SFO-HP results in an initially higher degree of mixing. In addition, the results on the analysis of gel content and film hardness indicate higher values for films prepared from the SFO-HP-initiated latex. From these results it is concluded that a difference exists in particle morphology and in reactivity during oxidative crosslinking between hybrid latexes initiated by SFO-HP vs. those initiated by *t*-BHP. Whether this difference is of practical importance depends on the specific application requirements of the hybrid binder.

7.3 Experimental Techniques

A number of experimental techniques were used for the analysis of the particle morphology of oil-acrylic hybrid latexes and of the structure of films prepared from these latexes. Because of the complexity of the oil-acrylic system these techniques in most cases could not be used in a standard way. Therefore, new practical methods were developed that may also be useful in other investigations.

Cryogenic Transmission Electron Microscopy (Cryo-TEM)

The use of cryo-TEM for the analysis of monomer droplets of alkyd resin and acrylic monomer was reported previously by Nabuurs *et al.* [4,5]. We have used this technique for the analysis of monomer-oil droplets (sunflower oil-acrylic monomer). In addition, the technique has been used for the analysis of the morphology of oil-acrylic hybrid latexes. It was shown that it is possible to visualize the presence of two distinct phases without staining.

The most surprising observation from the use cryo-TEM analysis was obtained during the analysis of thin films of highly concentrated oil/alkyd-acrylic hybrid latexes. These films show areas of hexagonally deformed particles and areas of

spherical particles. These results indicate that cryo-TEM imaging can be used for the analysis of the processes that take place in the Stages I and II of the latex film formation process. Traditionally, characterization of the processes that take place during these stages has been very difficult. It is expected that the use of this technique can give new insights into these stages of the film formation process. However, before cryo-TEM analysis can be used for this purpose, control of evaporation during sample preparation needs to be improved.

Atomic Force Microscopy (AFM)

Since its invention in 1989 [6] atomic force microscopy has developed as a strong tool for the analysis of surfaces. One of the strong points of AFM is the ease of sample preparation and of utilization of the technique. However, one should be very careful with respect to the chemical interpretation of the images observed when using new modes of analysis of the technique (like phase mode), because the exact forces represented are still subject of discussion [7]. Hence, in this thesis the images obtained were treated in a qualitative way.

In this study, a method of adsorption of individual particles was presented. This method was based on the work described by Johnson [8,9]. It is shown that interesting information on the morphology of singularly adsorbed particles and monolayers of clustered particles can be obtained when using this technique.

In addition, with the use of force modulation it is shown that the difference in stiffness in alkyd resin and acrylic particles can be visualized in the blend system. Thus, force modulation imaging is a very powerful tool for determination of the surface morphology of blends of rubbery material and stiffer material. Analysis of the surface of films prepared from the hybrid system by force modulation does not give additional information. It is expected that AFM will continue to develop in the future and that the information when using the different modes can be quantitatively explained.

Fluorescence Resonance Energy Transfer

Fluorescence resonance energy transfer measurements were used for the analysis of the degree of mixing of films prepared from hybrid latexes. The preliminary results presented in Chapter 5 show that this technique is capable of analyzing the initial degree of mixing at atomic level of a complex system like an oil-acrylic hybrid film and the changes taking place in this mixing in time.

However, these preliminary results only show the potential of the system.

7.4 References

1. S.T. Wang, F.J. Schork, G.W. Phoehlein, J.W. Gooch, *J. Appl. Polym. Sci.*, 60, (1996) 2069.
2. C.C. Wang, N.S. Yu, C.Y. Chen, J.F. Kuo, *Polymer*, 37 (12), (1996) 2509.
3. F.J. Schork, personal communication, 1999.
4. T. Nabuurs, "Alkyd-Acrylic Composite Emulsions. Polymerization and Morphology", Ph.D. Dissertation, Eindhoven University of Technology (1997).
5. T. Nabuurs, R.A. Bayards, A.L. German, *Prog. Org. Coat.*, 27, (1996) 163.
6. G. Binnig, C. Quate, G. Gerber, *Phys Rev. Lett.*, 56, (1986) 930.
7. See for instance discussion in the SPM Digest in the period from 12-1997 to 02-1998 (SPM Digest is discussion forum related to AFM on the site of DI at the internet)
8. C.A. Johnson, "Adsorption Behavior of Proteins and Colloidal Particles Studied Using Atomic Force Microscopy", Ph.D. Dissertation, University of Delaware (1997).
9. C.A. Johnson, A.M. Lenhoff, *J. Coll. Interf. Sci.*, 179, (1996) 587.

SUMMARY

The objective of the investigations described in this thesis was the development of systems that enable use of vegetable oils as binders for VOC-free waterborne coatings. For this purpose research was directed towards the preparation and characterization of oil-acrylic hybrid latexes and towards the analysis of the film formation behavior of these oil-acrylic hybrid latexes.

The first part of the thesis describes the study on the preparation of oil-acrylic hybrid latexes using mini-emulsion polymerization. The mini-emulsion polymerizations were initiated by fatty-acid hydroperoxides (SFO-HP) or by *tert*-butyl hydroperoxide (*t*-BHP) in an ROOH/Fe²⁺-EDTA/sodium formaldehyde-sulfoxylate (SFS) redox initiation system. In this part MMA was used as the monomer. It was shown that the formation of a second generation of all-acrylic particles was strongly reduced with the use of the mini-emulsion polymerization process. The mini-emulsion system was established using *n*-hexadecane as hydrophobe.

Oxidized sunflower oil was used as initiator in the SFO-HP initiated system and the process was compared with that initiated by *tert*-butyl hydroperoxide (*t*-BHP). Cryogenic transmission electron microscopic analysis (cryo-TEM) of the particle morphology of hybrid latexes prepared from the two different types of initiators showed that initiation by SFO-HP resulted in a more homogeneous particle morphology.

The kinetics of the SFO-HP initiated mini-emulsion polymerization were studied by analysis of the polymerization rate of MMA at various conditions. It was shown that the rate of MMA polymerization depended on the concentration of hydroperoxide groups, represented by the hydroperoxide value (HPV) of the oxidized sunflower oil, and on the polymerization temperature. The concentration of SFS and of Fe²⁺ did not influence the rate of polymerization. This suggested that the availability of fatty-acid hydroperoxides was the rate-limiting step during initiation.

The preparation of emulsions of sunflower oil with different levels of hydroperoxides was studied by oxidation of emulsions of sunflower oil at high partial oxygen pressure and by bulk oxidation of sunflower oil followed by emulsification. At high oxygen pressure the rate of formation and concurrent decomposition of hydroperoxides was found to increase with increasing oxygen pressure. In the bulk the oxidation temperature was of major influence. As the bulk method appeared to be the most flexible oxidation method that yielded the highest HPVs, it was used throughout the rest of the work described in this thesis for the preparation of SFO-HP initiated oil-acrylic hybrid latexes.

The preparation of high-solids oil/alkyd-acrylic hybrid latexes with film forming properties and the analysis of the film formation of these hybrid latexes is described in the second part of the thesis. Ethyl methacrylate was used as monomer in the preparation of the film forming hybrids. The hybrid latexes could be prepared with a solids content of 45 w% in various compositions of oil/alkyd to acrylate. The studied compositions varied from 25 w% to 75 w% of oil/alkyd.

Cryo-TEM analysis of the oil/alkyd-acrylic hybrid particles, initiated either by SFO-HP or *t*-BHP, indicated that the particles had a homogeneous particle structure. Analysis by atomic force microscopy (AFM) of individually adsorbed and dried particles suggested that (partial) phase separation had occurred between the oil/alkyd phase and the acrylic phase. Contact angle measurements and ESCA analysis of surfaces of films prepared on substrates of various degrees of hydrophobicity showed that this phase separation was not very prominent in bulk films.

Analysis of films prepared from the hybrid latexes time resolved fluorescence microscopy showed an initial difference in the degree of micro-scale mixing between films prepared from latexes initiated by SFO-HP or from by *t*-BHP.

In the final part of the thesis the coating performance of the developed oil/acrylic hybrid system is compared in a non-pigmented formulation with that of a blend system of alkyd emulsion and an all-acrylic latex with similar composition and with that of an alkyd emulsion. It was shown that the drying time of films prepared from the hybrid systems were shorter than those prepared from the blend system and the alkyd emulsion. The hardness and gloss of the films were related to the chemical composition of the systems. Higher contents of oil/alkyd in the hybrid system and in the blend system resulted in an increase in the gloss of the film and in a decrease in the film hardness. This effect was more pronounced in the blend system.

AFM analysis of the morphology of films prepared from blend systems with different compositions showed that the oil/alkyd phase forms the continuous matrix, in which the acrylic particles were randomly distributed. At higher acrylic contents (higher than ~55 w%) not all of the acrylic particles could be enclosed by the oil/alkyd. This resulted in non-transparent films.

The developed oil-acrylic hybrid latexes show interesting opportunities for use of vegetable oils in waterborne coatings.

SAMENVATTING

De doelstelling van het werk dat beschreven is in dit proefschrift was onderzoek naar de toepassing van natuurlijke oliën als bindmiddel voor oplosmiddelvrije verven. Hiertoe was het onderzoek gericht op het bereiden en karakteriseren van olie-acrylaat hybride-latexen en op de analyse van hun filmvormingsgedrag.

Het eerste gedeelte van het proefschrift beschrijft de studie naar het bereiden van de olie-acrylaat hybride-latex met behulp van mini-emulsie-polymerisatie technologie. De mini-emulsie-polymerisaties werden geïnitieerd door middel van een ROOH/ Fe^{2+} -EDTA/natriumformaldehydesulfoxylaat (SFS) redox-initiatiesysteem. De ROOH in dit systeem was ofwel vetzuurhydroperoxide (SFO-HP), ofwel *tert*-butylhydroperoxide (*t*-BHP). Methylmethacrylaat (MMA) is gebruikt als monomeer in dit gedeelte. Door gebruik te maken van het mini-emulsie-polymerisatieproces bleek het mogelijk de vorming van een tweede generatie van deeltjes, welke geheel bestaan uit acrylaat, sterk te verminderen. Het mini-emulsie-polymerisatiesysteem werd verkregen door toepassing van hexadecaan als hydrofoob.

In het SFO-HP geïnitieerde systeem is geoxideerde zonnebloemolie gebruikt als initiator. De eigenschappen van dit systeem zijn vergeleken met die van het systeem waarin initiatie door *t*-BHP plaatsvond. Analyse, met behulp van cryogene-transmissie-elektronenmicroscopie (cryo-TEM) van de deeltjes-morfologie van hybride-latexen, die gevormd waren via initiatie door de twee verschillende initiortypen, toonde aan dat initiatie door SFO-HP resulteerde in een meer homogene deeltjes-morfologie.

De kinetiek van SFO-HP geïnitieerde mini-emulsie-polymerisatie is bestudeerd door middel van analyse van de snelheid van polymerisatie van MMA onder verschillende condities. Het is aangetoond dat de polymerisatiesnelheid van MMA afhangt van de concentratie van aanwezige hydroperoxide-groepen, weergegeven door het hydroperoxidegetal (HPV) van de zonnebloemolie, en van de polymerisatie-temperatuur. De SFS-concentratie en Fe^{2+} -concentratie hadden geen invloed op de polymerisatiesnelheid. Dit gaf aan dat bij een constante temperatuur de beschikbaarheid van vetzuur-hydroperoxides de

snelheidsbepalende stap was in de cascade van reacties die plaatsvindt gedurende initiatie.

Het vormen van emulsies van zonnebloemolie met verschillende concentraties aan hydroperoxides is onderzocht via oxidatie van emulsies van zonnebloemolie bij hoge partiële zuurstofdruk en via bulkoxidatie van zonnebloemolie gevolgd door emulsificatie. De resultaten gaven aan dat bij oxidatie van emulsies van zonnebloemolie bij hoge zuurstofdruk de snelheid van vorming, en van de daaropvolgende afbraak van hydroperoxiden toeneemt met een toenemende temperatuur. Voor de bulkoxidatie van zonnebloemolie is bepaald dat de oxidatietemperatuur de grootste invloed op de vorming van hydroperoxiden had. Vanwege de hogere flexibiliteit van bulkoxidatie en de hogere maximale hydroperoxide-waarden die verkregen konden worden is gedurende de rest van het in dit proefschrift beschreven onderzoek gebruik gemaakt van deze methode voor het vormen van door SFO-HP-geïnitieerde olie-acrylaat hybride latexen.

De bereiding van olie/alkyd-acrylaat hybride latex met een hoog vaste-stof-gehalte en met filmvormende eigenschappen, en de analyse van de filmvorming van deze hybride-latexen, wordt beschreven in het tweede gedeelte van het proefschrift. Ethylmethacrylaat (EMA) is gebruikt als monomeer in de bereiding van deze filmvormende hybriden. De hybriden zijn bereid met een vaste-stof-gehalte van 45 w% in verschillende samenstellingen van olie/alkyd en acrylaat. De samenstellingen varieerden van 25 w% tot 75 w% olie/alkyd.

Cryo-TEM-analyse van olie/alkyd-acrylaat hybride deeltjes, geïnitieerd door ofwel SFO-HP ofwel *t*-BHP, gaf aan dat de deeltjes een homogene morfologie hadden. Analyse van individuele geadsorbeerde en gedroogde deeltjes, met behulp van 'atomic force microscopy' (AFM), wees op gedeeltelijke fase-scheiding tussen de olie-fase en acrylaat-fase. Contacthoek-metingen en ESCA-analyse van oppervlakten van filmen die gevormd waren op substraten van verschillende hydrofobiciteit duiden op een minder nadrukkelijke fasescheiding in dikkere filmen (meerdere lagen deeltjes).

Analyse van filmen van hybride-latexen door middel van fluorescentie-microscopie toonde een initieel verschil in de mate van menging op microschaal van de olie-alkyd-fase en de acrylaat-fase aan tussen het SFO-HP en het *t*-BHP geïnitieerde systeem. Filmene die gevormd waren uit latex geïnitieerd door SFO-HP waren meer gemengd.

In het laatste gedeelte van het proefschrift worden de coatingeigenschappen van het ontwikkelde olie/alkyd-acrylaat hybride in een niet-gepigmenteerde

formulering vergeleken met de eigenschappen van een mengsel van een alkyd-emulsie en acrylaat-latex, en van een alkyd-emulsie. De chemische samenstelling van het gemengde systeem was gelijk aan die van het hybride systeem. De resultaten gaven aan dat de droogtijd van films gevormd met het hybride systeem aanzienlijk korter waren dan die van films van het gemengde systeem en van de alkyd-emulsie. De hardheid en glans van de films van de verschillende systemen waren gerelateerd aan de chemische samenstelling. Hogere hoeveelheden olie/alkyd in het hybride systeem en in het gemengde systeem resulteerden in een toename in glans en in een verlaging van de hardheid. Dit effect werd in sterkere mate waargenomen voor het gemengde systeem.

AFM analyse van de morfologie van de filmoppervlakken gevormd uit gemengde systemen (blends) gaf aan dat de olie/alkyd fase de continue fase van de film vormde. De acrylaatdeeltjes waren willekeurig verspreid in deze fase. Bij hogere hoeveelheden acrylaat (meer dan ~55 w%) was er niet voldoende olie/alkyd aanwezig om alle acrylaat-deeltjes te omsluiten. Dit resulteerde in niet transparante films.

Het ontwikkelde olie/alkyd-acrylaat hybride-systeem lijkt interessante mogelijkheden te bieden voor toepassing van natuurlijke oliën in bindmiddelen voor oplosmiddelvrije watergedragen verven.

DANKWOORD/ ACKNOWLEDGEMENT

Hoewel de titelpagina meestal maar één naam aangeeft, komt een proefschrift nooit tot stand zonder de bijdrage van vele personen. Bij deze wil ik een aantal daarvan met name bedanken.

In de eerste plaats wil ik Ton German en Hans Derksen bedanken voor het creëren van dit project en voor de vrijheid die zij mij geboden hebben in de invulling en uitvoering ervan.

Steven van Es en Petrus Cuperus wil ik bedanken voor hun creatieve input tijdens het onderzoek en voor hun bijdrage aan het manuscript. De combinatie van Limburgse academische wetenschap met de projectmatige directheid uit het noorden is voor mij in vele opzichten zeer interessant, en zeker leerzaam, geweest. Ik wens jullie beiden veel succes in je nieuwe functies.

De medewerkers van het ATO-DLO, waar ik in de loop van tijd met veel plezier kennis gemaakt heb met vele richtingen van onderzoek, wil ik bedanken voor de fijne en gezellige samenwerking. Met name mijn kamergenoten, Sjoukje, Anne-Marie, Gerard, Godfried, Harmen en Arjanne.

De studenten met wie ik de afgelopen jaren gewerkt heb; Onno, Dickie, Dennis, Arjanne en Dayanand, bedankt voor jullie inzet en bijdrage.

Ook mijn collegae in Eindhoven wil ik bedanken. Tijdens mijn wekelijkse 'bezoeken' heb ik genoten van de goede onderlinge sfeer en behulpzaamheid en van de taart die er iedere keer als ik er was toevallig bleek te zijn.

I would like to thank the people of Ytkemiska Institutet for their extraordinary hospitality. Up to two times, you have hosted me and showed me how the summers are spent in Stockholm. Special thanks go to Peter Weissenborn, Ann-Charlotte Hellgrenn and Krister Holmberg. Your enthusiastic support has been a strong motivation. You have given me an example of how pleasant it can be to work in a well-organized international oriented organization.

"Jag har hade ett mycket bra tid med ni."

Arie van de Hoek en Ton Visser wil ik bedanken voor hun bijdrage aan de fluorescentie metingen. Tevens gaat mijn dank uit naar Wim Frederik en Paul Bomans voor hun bijdrage aan de cryo-electronen microscopy.

Verder wil ik Wieb Kinga, Alfons Franken, en Anne Spoelstra bedanken voor hun technische ondersteuning en Helly voor het doorspelen van de nodige informatie. Tot slot, de meest belangrijke personen, mijn ouders en familie. Pa, ma, Simone en Pascale, hoewel jullie waarschijnlijk niet altijd begrepen hebben waar ik mee bezig was, en nog minder waar ik naar toe wilde, heeft jullie interesse en vertrouwen mij altijd enorm gesteund. De totstandkoming van dit proefschrift is daarom een prestatie die jullie ook aan jezelf mogen toekennen.

Yvette, zoveel onderzoek naar coatings en het tuinhak is nog steeds niet geverfd. Met name dankzij jou liefde, begrip en ondersteuning heb ik de afgelopen jaren een schitterende tijd gehad. Ik heb nog steeds vertrouwen in het heden...en de toekomst.

Eelco



CURRICULUM VITAE

Eelco van Hamersveld was born in Hoogland, on January 9th, 1969.

After graduation from secondary school in 1988, he started his study in Economics at Tilburg University. In 1989 he switched to study Chemistry at Nijmegen University. As part of this study he worked in the group of Prof.dr. B. Zwanenburg on the project: "Stereospecific Synthesis of Conduritol". In addition, he spent 9 months at the Eindhoven University of Technology in the group of Prof.dr. P.J. Lemstra on the project: "In Vitro Synthesis of Poly Hydroxy Alkanoates (PHAs)". He obtained his masters degree in chemistry in 1994.

In 1994 he started his Ph.D. project at the Eindhoven University of Technology in the group of Prof.dr.ir. A.L. German, which resulted in the research presented in this thesis. The Ph.D. project was performed in cooperation with the group of Dr. F.P. Cuperus of the Agricultural Research Institute (ATO-DLO). In 1997 he spent 6 months at the Institute of Surface Chemistry, Stockholm, Sweden, in the Group of Dr. Lars Jarnstrom.

As from February 1999, he has joined General Electric Plastics in the Edison Leadership Program.

Stellingen

behorende bij het proefschrift

Oil-Acrylic Hybrid Latexes

van

Eelco van Hamersveld

1. De toekomstige waardering van een wetenschappelijk artikel zal niet meer worden weergegeven door de 'Citation Index' maar door de 'Internet Download Index'.
2. When you stand still, you have a chance to look around.
3. De berekening door Wang et al. van de omzetting van dubbele bindingen van alkyd moleculen gedurende de mini-emulsie polymerisatie van acrylaat met behulp van ^{13}C -NMR, gaat voorbij aan de omleggingreacties die plaats kunnen vinden aan pentadienylgroepen en is daarom niet correct.
S.T. Wang, F.J. Schork, G.W. Poehlein, J.W. Gooch, J. Appl. Polym. Sci., 60 (1996), 2069.
4. Vervorming van ronde latexdeeltjes naar hexagonale deeltjes kan reeds plaatsvinden gedurende de verdampingsfase van het filmvormingsproces.
Hoofdstuk 4 van dit proefschrift
5. Analyse van individuele latexdeeltjes met behulp van 'Atomic Force Microscopy' biedt unieke mogelijkheden voor het bestuderen van morfologie en vervormingsgedrag van deze deeltjes.
Hoofdstuk 4 van dit proefschrift

6. Het definiëren van mini-emulsies op basis van druppelgrootte en stabiliteit door Sudol *et al.* gaat voorbij aan de verschillen die ontstaan tussen het conventionele emulsiopolymerisatie proces en het mini-emulsiopolymerisatie proces als gevolg van het toevoegen van een hydrofoob bij het vormen van een mini-emulsie.

E.D. Sudol, M.S. El-Aasser, in "Emulsion Polymerization and Emulsion Polymers", P.A. Lovell, M.S. El-Aasser (Eds.), Wiley, New York (1997), 700.

7. Kennis was macht

8. Met de huidige snelheid van verandering van spelregels van volleybal valt het te betwijfelen of er over 25 jaar nog wel een net tussen de twee speelhelften zal zitten.

9. Het gebruik van olie-acrylaat hybride latexen voor het vormen van poedercoatings geeft nieuwe mogelijkheden voor de ontwikkeling van groene verven.

E.M.S. van Hamersveld, F.P. Cuperus, J.T.P. Derksen, J.G.G.S. van Es en A.L. German, Patent Application no. 1009254 (1998).

10. Bloedeiwitaddukten van nitro-polycyclische aromatische koolwaterstoffen, met name 1-nitropyreen, kunnen dienen als een 'early warning system' voor blootstelling aan de verdacht kankerverwekkende emissies van dieselmotoren.

Proefschrift van Y.M. van Bekkum, K.U. Nijmegen, 1999.

11. "Being a researcher is like being a detective; you have to prove your point beyond any doubt by excluding all possible suspects"

Peter Weissenborn, Ytkemiska Institutet, 1998